UNCLASSIFIED

AD NUMBER:	AD0373614
CLASSIFICATION CHANGES	
TO:	Unclassified
FROM:	Confidential
LIMITATION CHANGES	
TO:	Approved for public release; distribution is unlimited.
FROM:	Distribution authorized to U.S. Gov't. agencies and their contractors; Export Control; 30 Jun 1966. Other requests shall be referred to the Air Force Rocket Propulsion Lab, Research and Technology Division, Attn: RPPR/STINFO, Edwards, CA 93523
AUTHORITY	
31 Dec 1972 per document marking; AFRPL ltr 7 May 1973	

THIS PAGE IS UNCLASSIFIED

GENERAL DECLASSIFICATION SCHEDULE

IN ACCORDANCE WITH
DOD 5200.1-R & EXECUTIVE ORDER 11652

THIS DOCUMENT IS:

Subject to General Declassification Schedule of
Executive Order 11652-Automatically Downgraded at
2 Years Intervals- DECLASSIFIED ON DECEMBER 31, 1972

BY

Defense Docum Center
Defense Agency
Cameron Station
Alexandria, Virginia 22314

SECURITY MARKING

The classified or limited status of this report applies to each page, unless otherwise marked.
Separate page printouts MUST be marked accordingly.

373614

CONFIDENTIAL

AFRPL-TR-66-138

(Unclassified Title)

QUARTERLY PROGRESS REPORT

ADVANCED CRYOGENIC ROCKET ENGINE PROGRAM,

AEROSPIKE NOZZLE CONCEPT

Rocketdyne, A Division of
North American Aviation, Inc.
6633 Canoga Ave.
Canoga Park, California

Technical Report AFRPL-TR-66-138

June 1966

Group 4
Downgraded at 3-Year Intervals
Declassified After 12 Years

THIS MATERIAL CONTAINS INFORMATION AFFECTING THE NATIONAL DEFENSE OF THE UNITED STATES WITHIN THE MEANING OF THE ESPIONAGE LAWS, TITLE 18 U.S.C., SECTIONS 793 AND 794, THE TRANSMISSION OR REVELATION OF WHICH IN ANY MANNER TO AN UNAUTHORIZED PERSON IS PROHIBITED BY LAW

"In addition to security requirements which must be met, this document is subject to special export controls and each transmittal to foreign governments or foreign nationals may be made only with prior approval of AFRPL (RPPR/STINFO), Edwards, California, 93523."

Air Force Rocket Propulsion Laboratory
Research and Technology Division
Edwards Air Force Base, California
Air Force Systems Command
United States Air Force

CONFIDENTIAL

CONFIDENTIAL

AFRPL-TR-66-138

(Unclassified Title)

Quarterly Progress Report

Advanced Cryogenic Rocket Engine Program,

Aerospike Nozzle Concept

Rocketdyne, A Division of
North American Aviation, Inc.
6633 Canoga Ave.
Canoga Park, California

June 1966

Group 4
Downgraded at 3-Year Intervals
Declassified After 12 Years

THIS MATERIAL CONTAINS INFORMATION AFFECTING THE NATIONAL DEFENSE OF THE UNITED STATES WITHIN THE MEANING OF THE ESPIONAGE LAWS, TITLE 18 U.S.C., SECTIONS 793 AND 794, THE TRANSMISSION OR REVELATION OF WHICH IN ANY MANNER TO AN UNAUTHORIZED PERSON IS PROHIBITED BY LAW.

In addition to security requirements which must be met, this document is subject to special export controls and each transmittal to foreign governments or foreign nationals may be made only with prior approval of AFRPL (RPPR/STINFO), Edwards, California, 93523."

Air Force Rocket Propulsion Laboratory
Research and Technology Division
Edwards Air Force Base, California
Air Force Systems Command
United States Air Force

CONFIDENTIAL

FOREWORD

(U) The first quarterly progress report of the work accomplished under the Advanced Development Program, Aerospike, Air Force Contract AF04(611)-11399 is presented. Covered is the period from 1 March 1966 to 1 June 1966. A portion of the design and tooling effort in Task II represents a joint effort with the Advanced Engineering Program, Systems and Dynamics Investigation (Aerospike), Contract NAS8-19. This report has been assigned Rocketdyne report No. R-6537-1.

(U) Publication of this report does not constitute Air Force approval of the report's findings or conclusions. It is published only for the exchange and stimulation of new ideas.

VERNON L. MAHUGH, 1/Lt, USAF
Project Engineer

ABSTRACT

(U) Program status and technical results obtained at the end of the first 3 months are described for the Advanced Development Program, Aerospike. This program includes analysis and preliminary design of an advanced rocket engine using an aerospike nozzle and analysis, test hardware design, and test evaluation of thrust chamber performance and thrust chamber durability.

CONTENTS

ILLUSTRATIONS

TABLES

SUMMARY

(U) This report presents the program status, progress, and problem areas and solutions at the end of the first quarter of the Advanced Development Program (ADP), Aerospike and a brief summary of planned effort for the next quarter. The total effort is comprised of three tasks, namely Demonstrator Module Design (Task I), Thrust Chamber Performance Evaluation (Task II), and Thrust Chamber Durability Evaluation (Task III).

(U) In the design of the Demonstrator Module (Task I), major effort was directed toward defining system and component requirements and features, and establishing flight module characteristics. A functional analysis was brought through its first cycle, establishing initial component design requirements. A major trade study on turbine arrangement was completed, confirming the choice of parallel turbines for LO_2 and LH_2 pumps and defining some control requirements. System and component layouts were started. Studies are in progress on the throttling and mixture ratio control arrangement, LH_2 turbopump configuration and RPM, turbine driven preinducer operation, light-weight thrust chamber structures, and ignition controls.

(C) In the Thrust Chamber Performance Evaluation (Task II), progress was made in injector performance investigation with 2.5K hot-fired test segments and in design and fabrication of the 250K thrust chamber nozzle demonstration hardware. Segment testing started from a base of similar testing on other programs at lower chamber pressure and somewhat different combustor shapes. Water-cooled, drilled-copper segments were used successfully and combustion (c*) efficiencies of over 97 percent were obtained. A solid-wall 250K thrust chamber with water-film cooling at the throat was released and started in fabrication for use in injector checkout, ignition evaluation, and stability testing. A tube-wall 250K thrust chamber for full-scale chamber and nozzle performance demonstration was designed up to

the release point. Tube tapering and tooling was initiated, and other large rough machining was started. The 250K injector body was released and machining commenced.

(C) Thrust Chamber Durability Evaluation (Task III) consists of the 2.5K segment cooling investigation and a 20K segment structural evaluation, in addition to tube material analysis and laboratory work. The 2.5K segment cooling evaluation and tube material selection from nickel, copper, or stainless steel started from a base of segment testing on other programs. Hot-fire testing had shown that regenerative cooling limits were not reached at 1500 psi for stainless steel and 1900 psi for nickel. The 2.5K segments of all three materials were designed and partially released on this program in this period, and tube fabrication was started. An analytical approach to comparing various materials in resistance to thermal stress fatigue and predicting their life has been defined. Laboratory tests of materials and simulations of thrust chamber conditions in a tube tester were started.

(U) Program milestones scheduled in the first quarter were completed by the end of the quarter with two exceptions as presented in the schedules on pages 3 through 5. Task I milestone No. 2, scheduled for June 1 will be completed in the first week of June. Task II milestone No. 4 has been rescheduled from May 15 to June 15, which can be done without effect on the tube-wall fabrication and test. Several milestones have been added since the original program plan was issued, to better measure progress.

(U) There are no program-level conclusions to be drawn at the end of the first quarter. No program redirection is warranted, and no recommendations are made at this time.

Air Force ADP Aerospike Engine Program Plan Milestones

⇧ Current Schedule
◇ Expected Completion
⬆ Actual Completion

NO.	DEMONSTRATOR MODULE DESIGN MILESTONES	1966 J	F	M	A	M	J	J	A	S	O	N	D	1967 J	F	M	A	M	J	J
				1	2	3	4	5	6	7	8	9	10	11	12	13	14	15	16	17
	Task I: Demonstrator Module Design (1XXX, 6XXX, 7XXX, 9XXX)																			
1	System Requirements and Functions Defined			⬆																
2	Component Requirements Defined					⇧														
3	Component Preliminary Weight and Interface Established								⇧											
4	Thrust Chamber Design Requirement Specification								⇧											
5	Turbopump Design Requirement Specification								⇧											
6	Controls Design Requirement Specification								⇧											
7	Gimbal System Study Completed										⇧									
8	Flight Module Layouts Completed											⇧								
9	Thrust Chamber Design Freeze													⇧						
10	Turbopump Design Freeze													⇧						
11	Controls Design Freeze													⇧						
12	Demonstrator Module Design Freeze														⇧					
13	Final Design Review Completed														⇧					
14	Engine Performance and Functional Data Completed														⇧					
15	Applications Study Completed															⇧				
16	Demonstrator Module Design Completed																			⇧
17	Final Turbopump Layout and Analysis Completed																			⇧
18	Demonstrator Module Thrust Chamber Design Completed																			⇧

Air Force ADP Aerospike Engine Program Plan Milestones
(Continued)

Current Schedule

Expected Completion

Actual Completion

NO.	DEMONSTRATION MODULE DESIGN MILESTONE
	Task II Performance Evaluation (SDW 3000,4000)
1	2.5K Injector Segment Development Test Started
2	Parts List Released
3	No. 1 250K Experimental Thrust Chamber Released (solid wall)
4	No. 2 250K Experimental Thrust Chamber Released (tube wall)
5	No. 1 250K Injector Released
6	No. 2 250K Injector Released
7	Tapered Tubes Received
8	250K Solid Wall T/C Facility Completed
9	250K Solid Wall Tests Completed
10	No. 3 250K Injector Released
11	Segment Design and Fabrication Completed
12	First 250K Tube Wall Fabrication Completed
13	2.5K Solid Wall Segment Tests Completed
14	2.5K Solid Wall Segment Tests of Advanced Injector Completed
15	Injector Fabrication Completed
16	250K Tube Wall Testing Completed

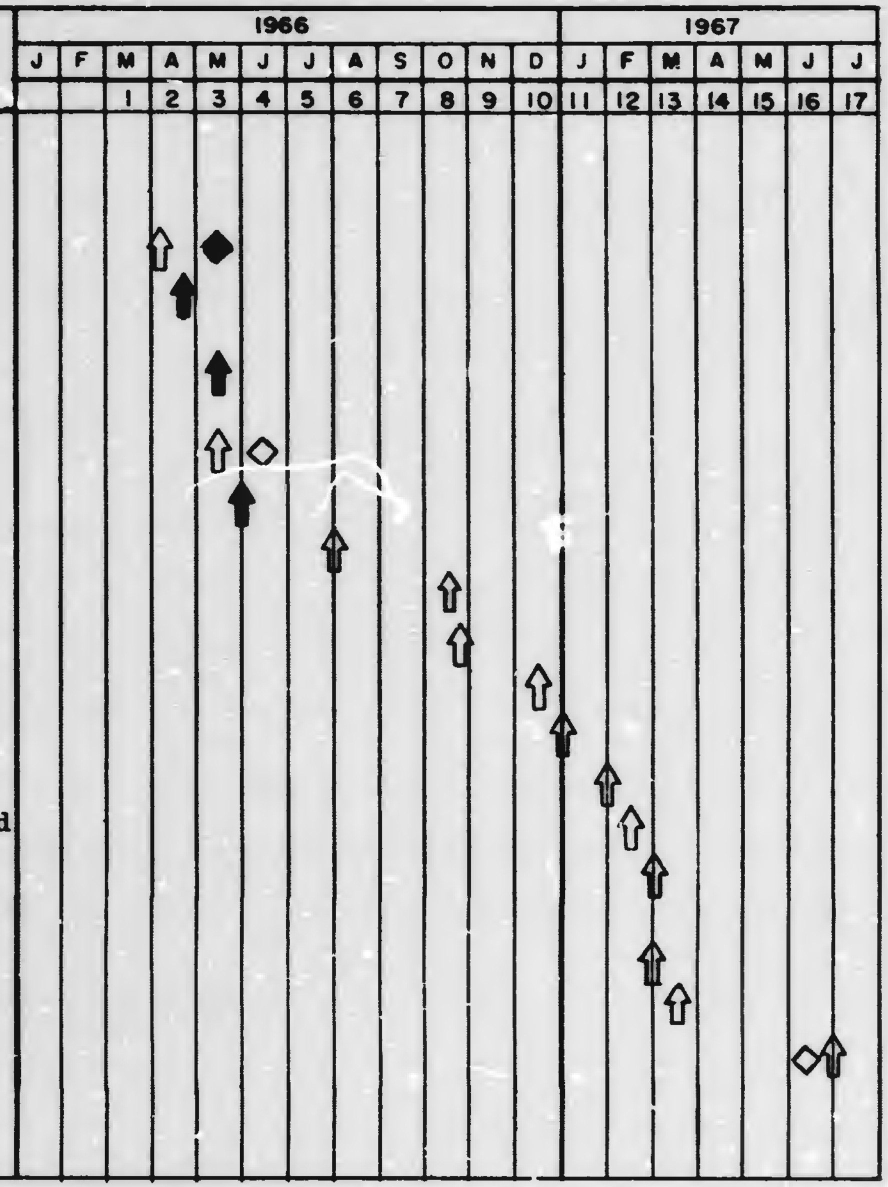

Air Force ADP Aerospike Engine Program Plan Milestones
(Concluded)

⇧ Current Schedule
◇ Expected Completion
⬆ Actual Completion

NO.	PERFORMANCE EVALUATION MILESTONES
	Task III: Thrust Chamber Cooled Structure Evaluation (2000, 5000, 8000)
1	Tube Tester Tests Initiated
2	2.5K Tube Wall Segments Released
3	Initial Material Selection for 20K Segment
4	20K Segment Released
5	2.5K Tube Wall Segment Cooling Tests Started
6	Laboratory and Tube Tester Evaluation Completed
7	2.5K Tube Wall Segment Design and Fabrication Completed
8	2.5K Tube Wall Segment Evaluation Tests Completed
9	2.5K Tube Wall Segment Test and Analysis Completed
10	20K Segment Cooling and Structural Tests Started
11	20K Segment Design and Fabrication Completed
12	20K Segment Test and Analysis Completed

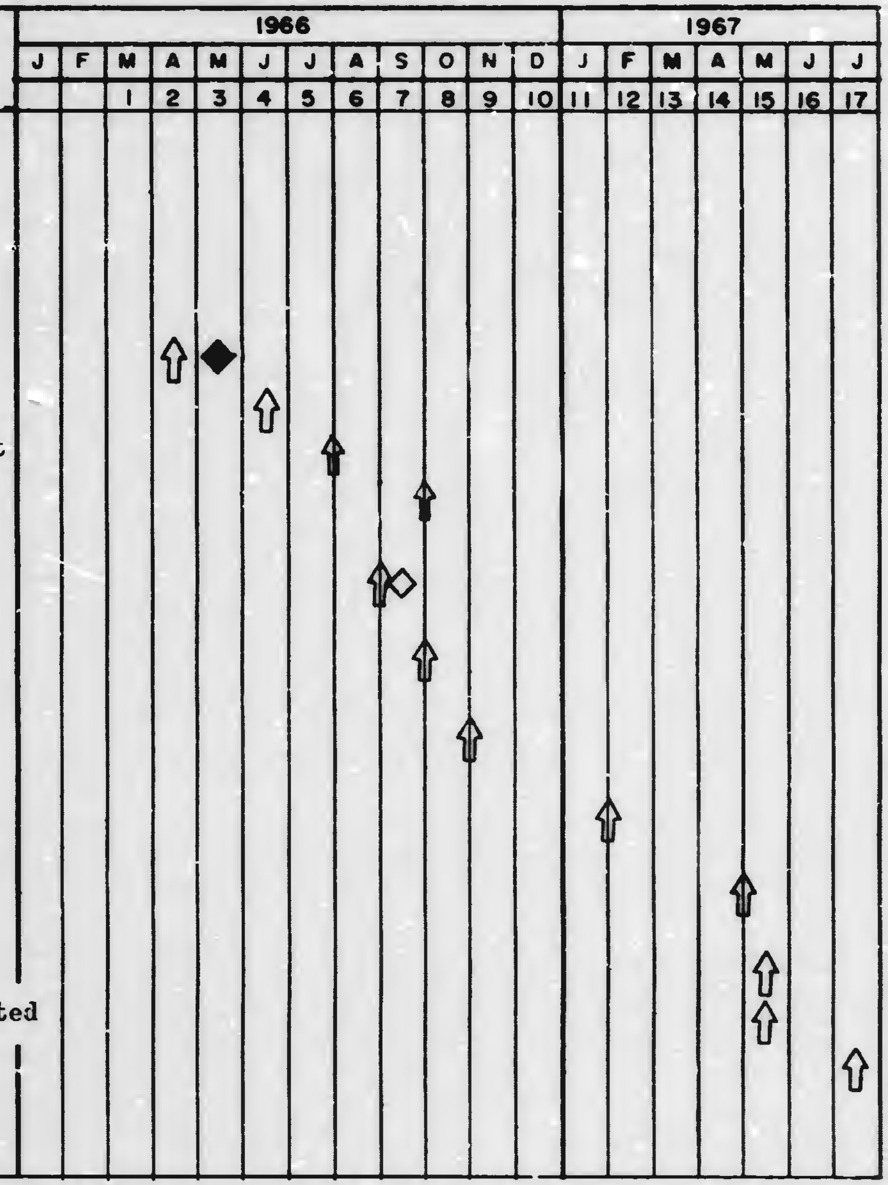

MODULE DESIGN

Functional Analysis

(U) The System Engineering technique being implemented on this program provides a standardized method for conducting functional analyses of mission and program requirements, defining all elements of the engine system, and documenting the technical information and decisions which lead to the final configuration. It serves to ensure that all functions and interfaces are satisfied by the end product. Proper implementation of the technique also provides standardized data to support the decision-making process, and thus established total integrated design criteria.

(U) An analysis of the functional requirements of the Demonstrator Module was initiated early in this report period as part of the systems engineering effort. Preliminary Functional Flow Diagrams (FFD'S) were completed and the initial Requirements Allocation Sheets (RAS's) and major subsystem Design Sheets (DS's) written. Typical samples of the FFD's are presented in Fig. 1 through 3 and typical RAS and DS follow (Fig. 4 through 6). Figure 1 is a second-level FFD defining the three major sequences of a rocket engine, start, mainstage, and cutoff. Figure 2 is the third-level FFD which expands the mainstage function shown in Fig. 1. Fig. 3 then expands the "Provide Thrust Chamber Propellant" function shown on Fig. 2. A RAS exists for every function shown on every FFD. On the upper levels, the RAS's reflect only the primary contract constraints such as shown in the second-level RAS for "Produce Thrust" (Fig. 4, function 1.1.2). The lower levels become more detailed as shown in the RAS for "Provide Propellant Head and Flow" (Fig. 5, function 1.1.1.2.1.2). At this level, a Design Sheet can be written. Figure 6 is the Oxidizer Turbopump Design Sheet.

(U) Trade study requirements are listed in the RAS's, and the results of higher level studies become reflected in the lower level RAS's. For

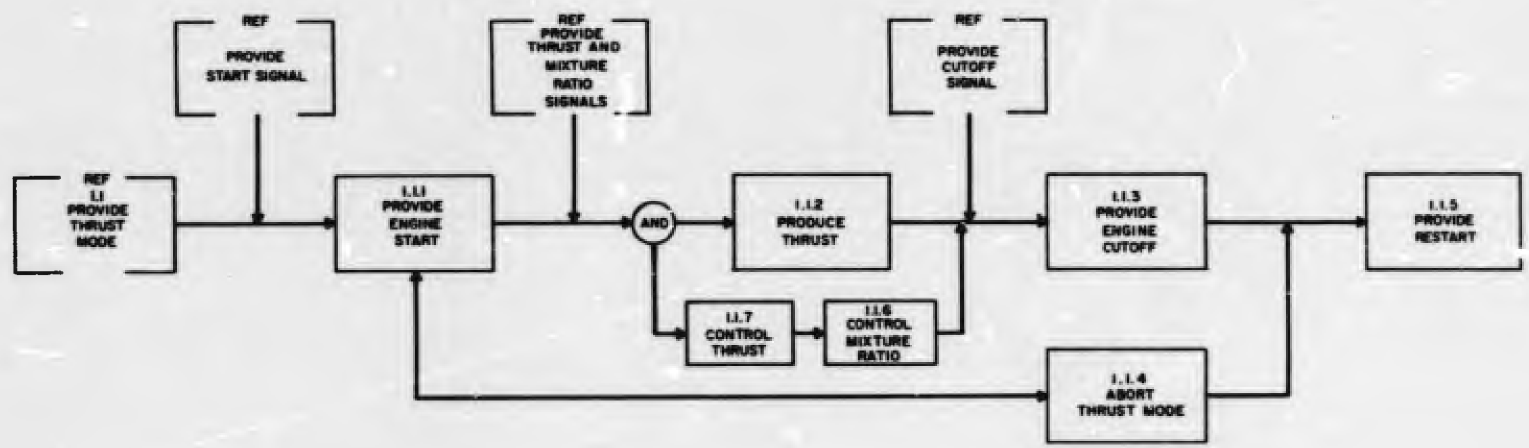

Figure 1. Second-Level Functional Flow Diagram, Provide Thrust Mode

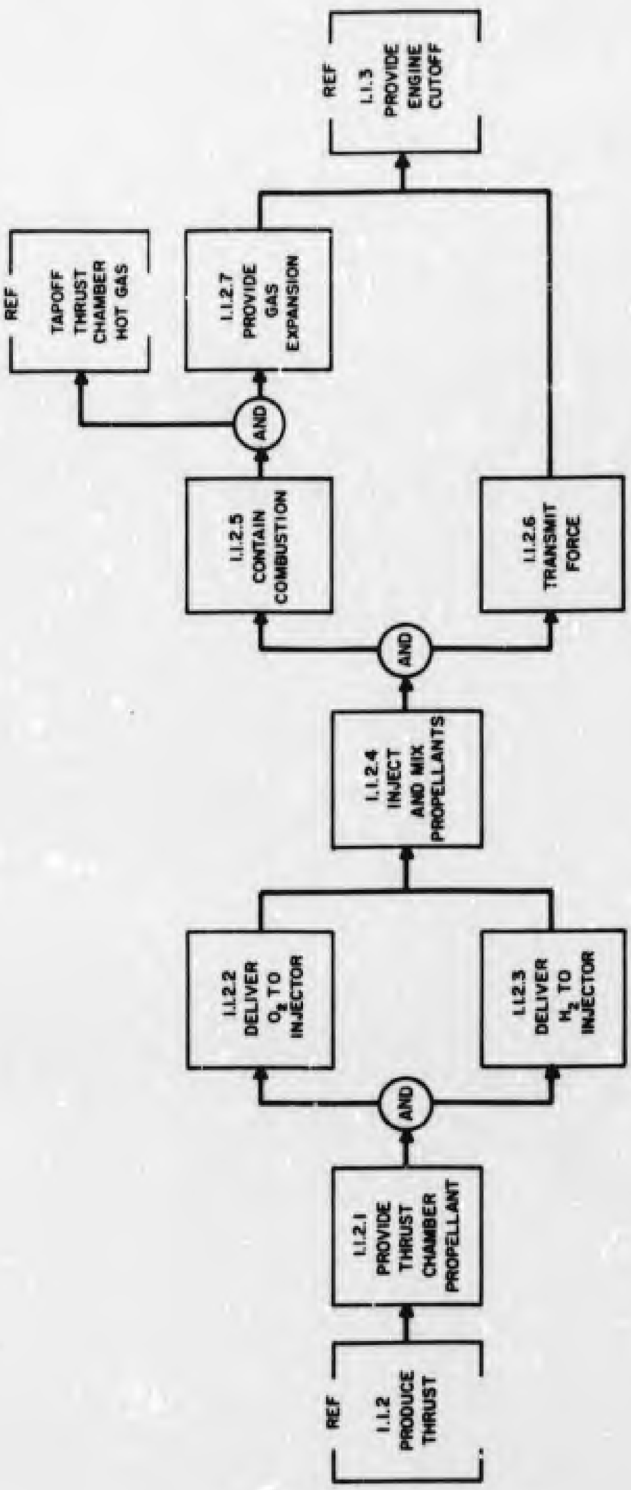

Figure 2. Third-Level Functional Flow Diagram, Produce Thrust

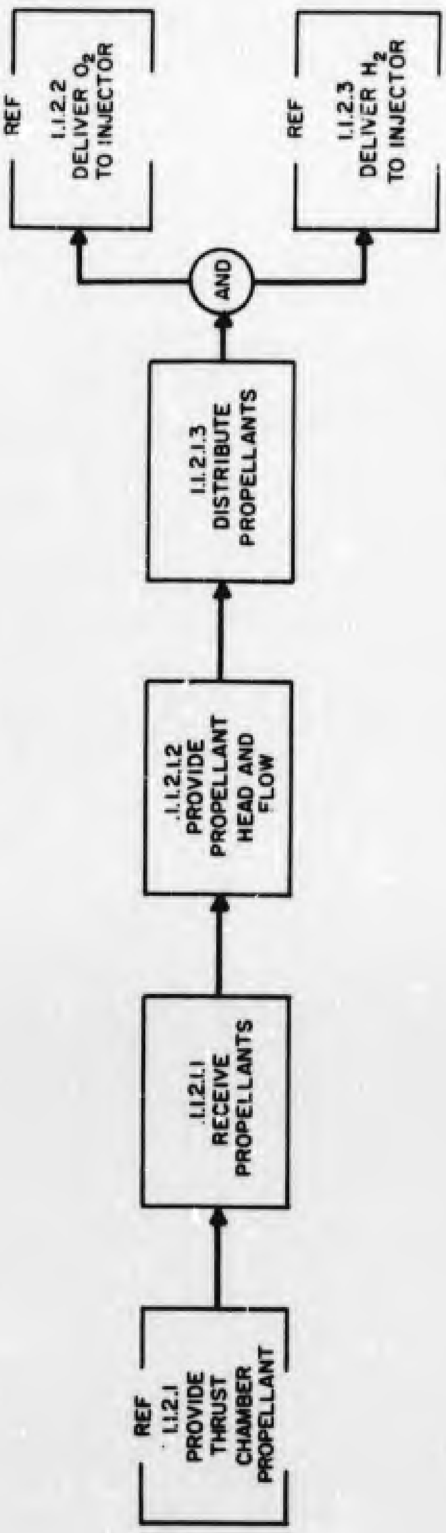

Figure 3. Fourth-Level Functional Flow Diagram, Provide Thrust Chamber Propellant

REQUIREMENTS ALLOCATION SHEET	FUNCTIONAL DIAGRAM TITLE AND NO.
CODE IDENT NO 02602 ROCKETDYNE A DIVISION OF NORTH AMERICAN AVIATION INC 6633 CANOGA AVENUE CANOGA PARK CALIFORNIA	OR NOMENCLATURE AND NO. OF CEI

FUNCTION NAME & NUMBER	DESIGN REQUIREMENTS
1.1.2 Produce Thrust	The demonstrator module shall be capable of (1) Operation at all vacuum thrust levels from 50,000 lbs to 250,000 lbs, (2) Operation at all engine mixture ratios from 5 to 7 over the entire thrust range, (3) A change from one extreme to the other extreme in the engine operating range for either thrust or mixture ratio will be achieved in ≤ 5 seconds. (4) A delivered vacuum specific impulse equal to or greater than 96 percent of theoretical shifting at 250,000 lbs thrust and an engine mixture ratio of 6. The demonstrator module shall be capable of recovery of chamber pressure from a _____ grain high explosive bomb in _______ milliseconds.

Figure 4. RAS for Produce Thrust

TEST FORM 1867

REQUIREMENTS ALLOCATION SHEET	FUNCTIONAL DIAGRAM TITLE AND NO.
CODE IDENT NO 02602 ROCKETDYNE A DIVISION OF NORTH AMERICAN AVIATION INC 6633 CANOGA AVENUE CANOGA PARK CALIFORNIA	OR NOMENCLATURE AND NO. OF CEI

FUNCTION NAME & NUMBER	DESIGN REQUIREMENTS
1.1.2.1.2 Provide Propellant Head & Flow	

Turbomachinery shall be provided to accept propellants at tank head pressures and impart the necessary energy to them in order to distribute the propellants at the flowrates and pressures necessary to achieve engine start, mainstage operation and throttle mode.

Individual direct-drive fuel and oxidizer turbopumps shall be of centrifugal design (see trade study R-6360).

Hot gas from the thrust chamber shall provide the energy to drive the turbines (see trade study R-6360).

The turbines shall be arranged in parallel (see trade study "Series vs Parallel").

The turbopumps shall be designed to meet the following throttled and full thrust performance requirements (see trade study R-6360).

Requirement	Oxidizer	Fuel
Pump		
Inlet pressure (minimum), psia	40	35
Discharge pressure range, psia	2055	2634
Developed head range, feet	4220	81,650
Volumetric flowrate range, gpm		
Weight flowrate	475	80
Minimum NPSH, feet	16	60
Horsepower (maximum), bhp	4600	16,000
Speed (at rated thrust), rpm	25,000	36,000
Turbine		
Inlet total pressure range, psia	100-600	200-1200
Inlet temperature range, °F	1200-1500	1200-1500
Hot gas flowrate range, lb/sec	0.5-3.0	1.0-8.0
Hot gas mixture ratio	0.4-0.5	0.4-0.5
Exhaust pressure range, psia	5-40	5-40
Horsepower range, bhp	10-4600	40-16,000

The turbopumps shall be capable of receiving drive gas from the thrust chamber and/or hot gas igniter at pressures below 100 psia and accelerating to any pump speed which falls within the discharge pressure and flowrate in the preceding table.

Figure 5. RAS for Provide Propellant Head and Flow

CONFIDENTIAL

REQUIREMENTS ALLOCATION SHEET	FUNCTIONAL DIAGRAM TITLE AND NO.
CODE IDENT NO 02602 ROCKETDYNE A DIVISION OF NORTH AMERICAN AVIATION INC 6633 CANOGA AVENUE CANOGA PARK CALIFORNIA	OR NOMENCLATURE AND NO. OF CEI

FUNCTION NAME & NUMBER	DESIGN REQUIREMENTS
1.1.2.1.2 Provide Propellant Head & Flow (Continued)	The turbopumps shall be capable of starting and build-up to 20 percent thrust at all altitudes from sea level up with mixed-phase propellants present in the pump in a minimum of ______ seconds. A trade study shall be undertaken to determine the degree of turbopump temperature conditioning required to produce smooth starts. Means shall be provided to measure pump speeds over the following ranges: Oxidizer pump speed, rpm 0 to 30,000 Fuel pump speed, rpm 0 to 40,000 The turbopump and inlet ducting shall be designed to withstand inlet pressure surges of ______ psi above the nominal inlet pressures. The turbopumps shall be designed such that no outside lubricant is utilized, and the bearing lubrication shall be performed with the main propellants (trade study R-6360).

Figure 5. (Concluded)

DESIGN SHEET	NOMENCLATURE	CEI NO OR CRITICAL COMPONENT CODE IDENT. ______ SPEC NO. DS-ADP-08
CODE IDENT. NO. 02602 ROCKETDYNE A DIVISION OF NORTH AMERICAN AVIATION INC 6633 CANOGA AVENUE CANOGA PARK CALIFORNIA	OXIDIZER TURBOPUMP	REVISION DATE 6-10-66 APPROVAL

REQUIREMENTS FOR DESIGN & TEST

3. Requirements

3.1 Performance

3.1.1 Functional Requirements

a. The oxidizer turbopump function is to provide sufficient head and flow in the liquid oxygen feed system to meet all required modes of engine system operation.

3.1.1.1 Primary Performance Characteristics

a. The oxidizer pump shall be designed to operate with the following pump inlet conditions:

(1)	Inlet pressure	40	psia
(2)	Inlet temperature	175.6	°R
(3)	Inlet density	68.8	lb/ft^3
(4)	NPSH (min. req.)	16	ft

b. The oxidizer pump shall be designed to deliver the following performance of nominal rated thrust and mixture ratio:

Flowrate, $\dot{W}$, lb/sec	476.2
Discharge Pressure, P_D, psia	2055
Pump Efficiency, η_P	.80

c. The oxidizer turbine shall be designed to operate with the following inlet conditions at nominal thrust and MR:

(1)	Inlet pressure, P_{T_1}, psia	600
(2)	Inlet Temperature, T_{T_1}, °F	1500
(3)	Hot Gas, MR	0.5

Figure 6. Oxidizer Turbopump Design Sheet

DESIGN SHEET

DESIGN SHEET	NOMENCLATURE	CEI NO OR CRITICAL COMPONENT CODE IDENT.
		SPEC NO. DS-ADP-08
CODE IDENT. NO. 02602 ROCKETDYNE A DIVISION OF NORTH AMERICAN AVIATION INC 6633 CANOGA AVENUE CANOGA PARK CALIFORNIA	OXIDIZER TURBOPUMP	REVISION DATE 6-10-66 APPROVAL

REQUIREMENTS FOR DESIGN & TEST

(4) Hot Gas Molecular Weight 3.024

(5) Hot Gas C_p 2.471

(6) Hot Gas γ 1.362

d. The oxidizer turbine shall be designed to meet the following performance:

(1) Hot gas flowrate, lb/sec 2.59

(2) Turbine pressure ratio, PR 15.0

(3) Turbine efficiency, η_T 0.501

e. The turbopump shall be designed to have a response time from start signal to 20% of rated thrust of ______ seconds.

3.1.1.2 Secondary Performance Characteristics

a. Preliminary design studies have established the following pump specifications:

(1) Speed, N, rpm 25,011

(2) Horsepower, HP 4567

(3) Suction Specific Speed, S_s 205,500

(4) Head, H, ft 4220

(5) Pressure Rise, ΔP, psi 2015

(6) Flowrate, Q, gpm 3109

(7) NPSH (design), ft 13.3

b. Pump flowrates for throttled thrust and off design MR are given below:

Figure 6. (Continued)

MR	5	6	7
Full Thrust	459.7	476.2	496.1
Throttled Thrust, 20%	92.3	95.8	100.0

DESIGN SHEET

DESIGN SHEET	NOMENCLATURE	CEI NO OR CRITICAL COMPONENT CODE IDENT. SPEC NO. DS-ADP-08
CODE IDENT. NO. 02602 ROCKETDYNE A DIVISION OF NORTH AMERICAN AVIATION INC 6633 CANOGA AVENUE CANOGA PARK CALIFORNIA	OXIDIZER TURBOPUMP	REVISION DATE 6-10-66 APPROVAL

REQUIREMENTS FOR DESIGN & TEST

c. Preliminary design studies have established the following turbine specifications:

(1)	Speed, N, rpm	25,011
(2)	Horsepower, HP	4567
(3)	Exhaust Pressure, psia	40.1

d. Turbine flowrates for throttled thrust and off design MR are given below:

MR	5	6	7	
Full Thrust	2.59	2.59	2.65	lbs/sec
Throttled Thrust, 20%	0.20	0.20	0.21	lbs/sec

3.1.2 Operability

3.1.2.1 Reliability

3.1.2.2 Maintainability

3.1.2.3 Useful Life - The turbine shall be capable of operating for a maximum duration of 600 sec for a single thrust period and shall have a useable lifetime of 10 hours.

3.1.2.4 Environment

3.1.2.5 Transportability

3.1.2.6 Human Performance

3.1.2.7 Safety

3.2 CEI Definition

3.2.1 Interface Requirements

3.2.1.1 Schematic Arrangement

3.2.1.2 Detailed Interface Definition

Figure 6. (Continued)

DESIGN SHEET

DESIGN SHEET	NOMENCLATURE	CEI NO OR CRITICAL COMPONENT CODE IDENT SPEC NO DS-ADP-08
CODE IDENT NO 02602 ROCKETDYNE A DIVISION OF NORTH AMERICAN AVIATION INC 6633 CANOGA AVENUE CANOGA PARK CALIFORNIA	OXIDIZER TURBOPUMP	REVISION DATE 6-10-66 APPROVAL

REQUIREMENTS FOR DESIGN & TEST

3.2.2 Component Identification

3.2.2.1 Govt.-Furnished Property List

3.2.2.2 Engineering Critical Components List

3.2.2.3 Logistics Critical Components List

3.3 Design and Construction

3.3.1 General Design Features

a. The turbopump consists of a liquid oxidizer pump and a hot gas turbine designed in a common housing.

b. The oxidizer pump will consist of a single centrifugal stage with a hydraulic turbine-driven preinducer made integral with the main pump. The pump will have a single pump inlet and a single pump discharge.

c. The oxidizer turbine shall be a single-stage velocity-compounded turbine.

d. The oxidizer turbopump shall be designed to the following dimensional and weight requirements.

(1) Overall Diameter, D, in. 16.5 (max)

(2) Overall Length, L, in. 19.75 (max)

(3) Allowable T/Pump Weight, lbs

Pump

Pre-inducer

Turbine

e. All bearings and seals shall be propellant lubricated.

f. The pump shall be capable of operation with mixed phase propellants.

Figure 6. (Continued)

DESIGN SHEET

DESIGN SHEET	NOMENCLATURE	CEI NO. OR CRITICAL COMPONENT CODE IDENT. ____ SPEC NO. DS-ADP-08
CODE IDENT. NO. 02602 ROCKETDYNE A DIVISION OF NORTH AMERICAN AVIATION INC 6633 CANOGA AVENUE CANOGA PARK CALIFORNIA	OXIDIZER TURBOPUMP	REVISION DATE 6-10-66 APPROVAL

REQUIREMENTS FOR DESIGN & TEST

g. The pump shall be designed for a minimum of conditioning to produce smooth repeatable starts.

h. The pump shall be designed to operate stably despite inlet pressure surges.

i. The turbine shall be designed or insulated to achieve an external surface temperature no greater than ___

j. The turbine manifold shall be designed with a pressure loss no greater than ____ psi.

Figure 6. (Concluded)

DESIGN SHEET

(U) example, during this report period a trade study was conducted to compare a series versus a parallel turbine arrangement. The result of this study (parallel arrangement selection) can be found in the sample RAS.

(U) The final form of the FFD's, RAS's and DS's is reached only after a series of iterations. The preliminary FFD's define the engine functions. However, many of the system operating requirements cannot be determined until after design analysis has been conducted. Therefore, preliminary RAS's and DS's are issued to initiate design analysis, and these preliminary releases are revised as feedback from the design group and trade studies is received.

(U) The definition of component performance requirements will be accomplished through the release of the following preliminary design sheets early in June.

1. Demonstrator Module System
2. Thrust Subsystem
3. Turbine Drive Hot-Gas Subsystem
4. Igniter Subsystem
5. Propellant Feed Subsystem
6. Oxidizer Turbopump
7. Fuel Turbopump
8. Main Oxidizer Valve
9. Main Fuel Valve
10. Fuel Bypass Valve
11. Propellant Ducting
12. Thrust Chamber Assembly

(U) During the next quarter, effort will continue to revise, update, and extend the existing documents and delineate and conduct additional trade studies.

Trade Study, Series vs Parallel Turbine Arrangement

(U) A turbine arrangement study was conducted to reassess the selection of parallel turbines for the aerospike engine made during the initial proposal effort. Effect on performance, engine design, turbomachinery, start system throttling and mixture ratio controls, and weight of the two flow arrangements was assessed on a comparative basis. The results are presented in the following paragraphs.

(U) Performance Analysis. For turbines designed on the same basic philosophy, i.e., state-of-the-art and stress levels, etc., a series turbine design will require approximately 20 percent less turbine flowrate than the parallel arrangement. For the nominal design thrust and mixture ratio, the difference in engine specific impulse resulting from the difference in turbine flowrate gives the series configuration a performance advantage of about 0.5-second specific impulse. At other mixture ratios and thrust levels at which the engine must operate, the difference between the turbine configurations are of the same order or less.

(U) In an oxygen/hydrogen propulsion system, the disparity between densities of the propellant usually requires that the pumps operate at different speeds for an optimum design. With a speed differential between pumps, either a geared single turbine or a dual shaft configuration is possible. The two turbines of the dual shaft configuration could be arranged in series or parallel relative to the flow path of the turbine drive gases. In both of the designs, the pressure available for turbine work is approximated by chamber pressure at the inlet and base pressure at the exit less provisions for pressure drops for required ducting, manifolds, and valves. Further, in order to decouple the turbine block from the base region, an additional constraint was imposed that the pressure ratio across the base closure is above critical at all times. Thus, providing for a base pressure at sea level approximating ambient pressure, the minimum pressure at the upstream side of the base closure was 30 psia.

(U) The single turbine configuration was eliminated from consideration early in the evaluation for the following reasons. The gearing between the oxidizer and fuel pump shafts, in addition to the required lubrication system, would at best offset or exceed the weight of the oxidizer turbine it would functionally replace. To achieve mixture ratio control, a single turbine system would have to resort to a pump bypass system on the oxidizer side. Based on estimates derived from the J-2 engine which demonstrates a mixture ratio excursion of $\pm$0.3 units with an 18-percent bypass fraction (ratio of bypass flow to delivered flow), as much as 30 percent or more bypass flow fraction may be required by the engine to provide for the $\pm$1.0 mixture ratio unit excursion requirement. While the oxidizer pump power requirements are substantially less than the fuel side, nonetheless a 30-percent increase in power requirements translates directly into increased turbine flowrate with the attendant reduction in engine specific impulse.

(U) From an aerospike engine performance point of view, the primary parameter of interest is the turbine flowrate necessary to meet pump power requirements as defined by the engine thrust and mixture ratio. Because gas properties are relatively invariant over the range of temperatures suitable for turbine operation, the operating pressure ratio and corresponding efficiency of the turbine unit are the governing variables in a performance evaluation. Table 1 presents a comparison of parameters of interest for the series and parallel turbine designs used in the evaluation. The parallel turbines were identical to those proposed in R-6360P. The nominal inlet temperature was 1500 F using tapoff gas properties. It should be reemphasized that both the series and parallel turbines were designed to reflect the same state of the art.

TABLE 1

TURBINE PARAMETER COMPARISON
(THRUST 250K, MIXTURE RATIO 6.0)

Parameter	Series		Parallel	
	Fuel	Oxidizer	Fuel	Oxidizer
Number of Stages	2	2	2	2
Configuration	Pressure modified, velocity compounded	Pressure compounded	Pressure modified, velocity compounded	Velocity compounded
Speed, rpm	36,000	25,000	36,000	25,000
Inlet Pressure (total), psia	1200	95	1200	600
Exit Pressure (static), psia	95	32	40	40
Pressure Ratio	12.6	3.0	30	15
Efficiency, percent	64	70	60	50
Pitch Diameter, inches	7.9	10	8.9	12.8
Flowrate, lb/sec	7.26	5.43	6.39	2.59

(U) The series configuration utilized an overall pressure ratio of 37.8 as contrasted with the maximum pressure ratio for the parallel configuration of 30. Had the comparison been restricted to equal overall pressure ratios for both the series and parallel configurations, the results would be altered slightly by minimizing the performance differential between them but the series would still maintain its small advantage. The oxidizer turbine in the series configuration bypassed 25 percent of the available flowrate from the fuel turbine through a duct directly to the base region. The bypassing of part of the fuel turbine flow increased the operating pressure ratio of the oxidizer turbine and also provided a convenient means of controlling engine mixture ratio by a variable area device in the bypass duct.

(U) The optimum parallel configuration resulted in an unbalance in the operating pressure ratios between the oxidizer and fuel turbines, caused largely by the 3.5 to 1 ratio between the required fuel and oxidizer horsepowers. The pressure ratio of the oxidizer turbine could not be increased above the design value of 15 because of minimum blade height considerations and the prospects of requiring a partial admission design with the attendant loss in efficiency. Similarly, the fuel turbine pressure ratio should not be lowered appreciably as it would result in increased flow requirements, inasmuch as the rate of increase in efficiency does not offset the rate of decrease in the pressure ratio function. Thus, a lower fuel turbine pressure ratio would result in a small increase in the performance advantage to the series configuration.

(U) Assuming a minimum flowrate turbine design, configuration notwithstanding, increasing the flowrate by means of an alternate design affects either design pressure ratio and efficiency or both, overall engine performance is reduced for two reasons. First, as turbine flowrate is increased for a fixed engine mixture ratio, an increase in the thrust chamber mixture ratio results as a larger percentage of the fuel available to the system is used to make up the turbine drive gas. This mixture ratio shift has the effect of lowering the theoretical nozzle performance as specific impulse decreases with increasing mixture ratio in the range of interest. Second, the

(U) increased turbine flowrate reduces overall base performance. Although an increase in base pressure and correspondingly thrust is noted as base flowrate is increased, the net effect is for the "specific impulse" of the base to drop because the base pressure increases at a much slower rate than the base flowrate. Figure 7 presents the variation of engine specific impulse with the ratio of turbine flowrate to thrust chamber flowrate.

(U) The engine performance of the two candidate turbine configurations were compared and the results presented with engine mixture ratio and maximum and minimum thrust of interest in Table 2. Even at the full thrust condition where the series configuration has a 20-percent advantage in required turbine flowrate, the effect on engine specific impulse is quite small. The difference is even less at the minimum thrust condition with similar trends noted, except with the mixture ratio of 6.0 where the reversal of the performance advantage to the series is noted. However, the performance differential is much less than at full thrust and within the tolerance of the computer model. On the basis of this table it can be concluded that there is no significant performance advantage to either series or parallel over the entire operating range.

TABLE 2

ENGINE PERFORMANCE COMPARISON

Engine Mixture Ratio	5.0		6.0		7.0	
Turbine Drive Arrangement	S	P	S	P	S	P
Full Thrust (100 percent)	452.8	452.7	450.5	450.3	443.5	443.0
Minimum Thrust (20 percent)	447.9	448.1	442.0	442.1	432.1	432.1

S series turbine arrangement

P parallel turbine arrangement

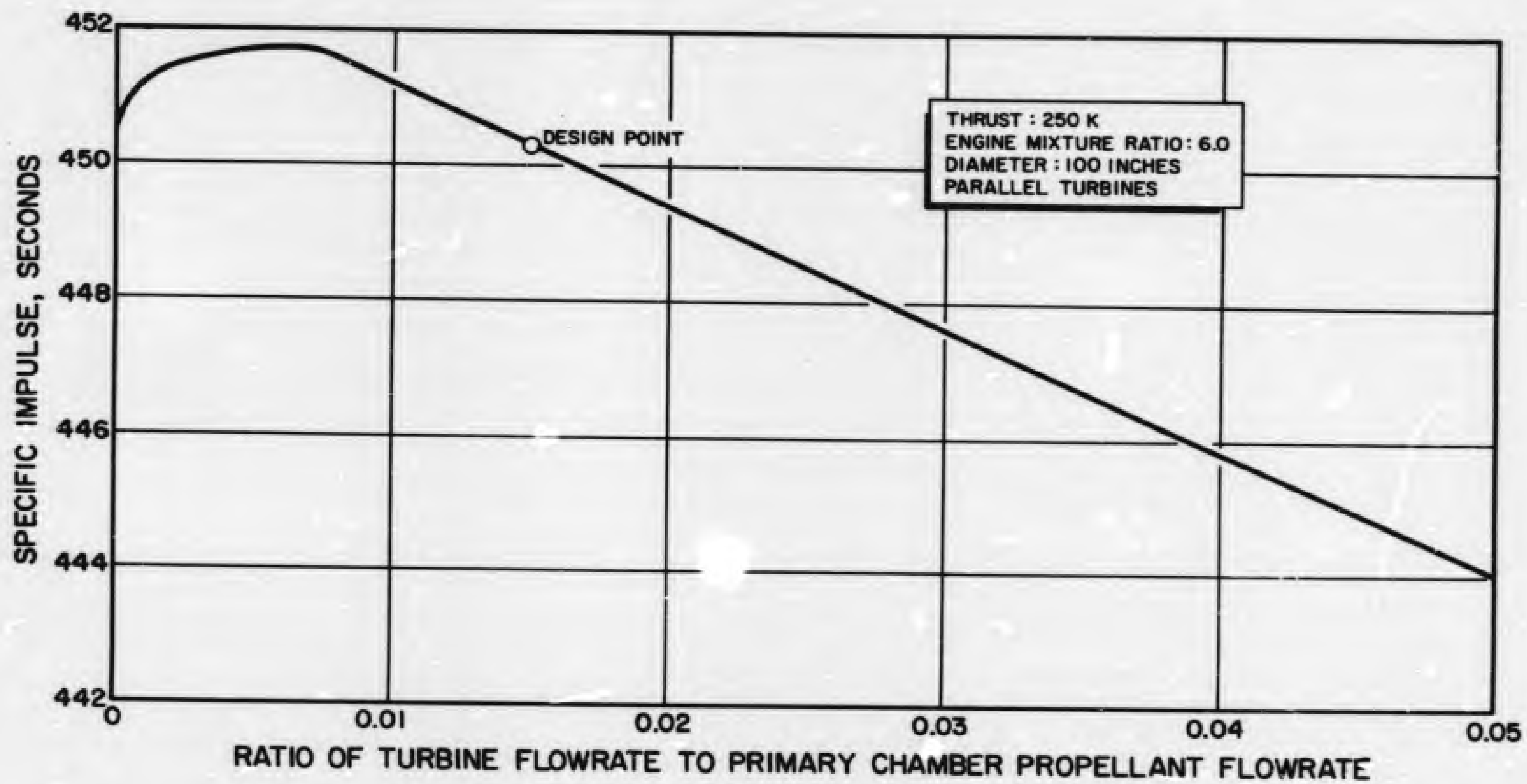

Figure 7. Variation of Engine Specific Impulse with the Ratio of Turbine Flowrate to Thrust Chamber Flowrate

(U) Late in the trade study and subsequent to completion of Tables 1 and 2, an updating of the engine balances was accomplished. A comparison of nominal engine operating characteristics is presented as Table 3 for the series and parallel configurations. The system parameters are identical to those presented previously except for an updating of the thrust chamber performance to reflect the most recent combustor shape, shroud length, and kinetic performance. A slight diffierence between the specific impulse values presented in Table 2 and 3 is noted. However, the difference does not change the conclusions derived from the earlier data.

(U) Engine Design. Design layouts were prepared for both turbine arrangements. The systems were compared on the basis of structural and weight considerations and component packaging and accessibility.

(U) The engine system with the parallel arrangement is shown in Fig. 8. The tapoff gases are collected in a common manifold and carried through two identical tapoff lines to the fuel and oxidizer turbine control valves. These two valves control the flow of tapoff gases to the fuel and oxidizer turbines. The fuel discharge from the fuel pump flows through a single line to the fuel manifold at the base of the nozzle. The oxidizer discharged from the oxidizer pump flows through the main oxidizer valve and then splits and flows through two equal length, equal diameter lines and enters the oxidizer manifold at two points 180 degrees apart. The system layout (Fig. 8) includes a hydraulic pump driven through a bevel gear arrangement by the oxidizer turbine. Detailed requirement for a hydraulic pump does not presently exist; however, this pump is being shown so that its impact on the series and parallel arrangement packaging can be noted. Lacking definitive requirements for this pump, the J-2 hydraulic pump used in the Saturn S-II stage was selected as being representative.

(U) The engine system with the series turbine arrangement is shown in Fig. 9. As can be seen by comparing Fig. 8 with Fig. 9, the major portion of the components of both systems are very similar. The thrust chamber, thrust structure, base closure and turbopump

TABLE 3

TABLE OF OPERATING CHARACTERISTICS

	Parallel	Series
ENGINE		
Oxidizer	Liquid Oxygen	
Inlet Pressure, psia	40	
Inlet Temperature, R	175.6	
Inlet Density, lb/ft^3	68.9	
Flowrate, lb/sec	475.26	474.62
Fuel	Liquid Hydrogen	
Inlet Pressure, psia	35	
Inlet Temperature, R	41.3	
Inlet Density, lb/ft^3	4.21	
Flowrate, lb/sec	79.21	79.10
Mixture Ratio, o/f	6.0	
Vacuum Performance		
Thrust, pounds	250,000	
Specific Impulse, seconds	450.9	451.5
Specific Impulse Efficiency	0.970	0.972
Sea Level Performance		
Thrust, pounds	206,080	206,240
Specific Impulse, seconds	371.68	372.48
THRUST CHAMBER		
Primary Nozzle		
Chamber Pressure (nozzle stagnation), psia	1500	
Mixture Ratio, o/f	6.45	6.36
Oxidizer Flowrate, lb/sec	472.27	472.20
Fuel Flowrate, lb/sec	73.23	74.26
Thrust Coefficient	1.9791	1.9746
Characteristic Velocity, ft/sec	7230	7252
Throat Area, cu in.	81.72	82.11
Expansion Area Ratio	76.97	76.61
Percent Length, percent of 15-degree cone	25	

TABLE 3

(Concluded)

<table>
<tr><th></th><th>Parallel</th><th>Series</th></tr>
<tr><td>FUEL TURBOPUMP</td><td></td><td></td></tr>
<tr><td>Pump</td><td></td><td></td></tr>
<tr><td>Inlet Pressure, psia</td><td colspan="2">35</td></tr>
<tr><td>Inlet Temperature, R</td><td colspan="2">41.3</td></tr>
<tr><td>NPSH (minimum required), feet</td><td colspan="2">60</td></tr>
<tr><td>Discharge Pressure, psia</td><td colspan="2">2635</td></tr>
<tr><td>Head, feet</td><td>81,650</td><td>81,650</td></tr>
<tr><td>Flowrate, lb/sec</td><td>79.21</td><td>79.10</td></tr>
<tr><td>Speed, rpm</td><td colspan="2">36,000</td></tr>
<tr><td>Shaft Horsepower, bhp</td><td>15,690</td><td>15,670</td></tr>
<tr><td>Efficiency, percent</td><td colspan="2">75</td></tr>
<tr><td>Turbine</td><td></td><td></td></tr>
<tr><td>Inlet Pressure (total), psia</td><td>1200</td><td>1200</td></tr>
<tr><td>Inlet Temperature, R</td><td>1960</td><td>1960</td></tr>
<tr><td>Exit Pressure (static), psia</td><td>40</td><td>95.2</td></tr>
<tr><td>Flowrate, lb/sec</td><td>6.39</td><td>7.26</td></tr>
<tr><td>Speed, rpm</td><td colspan="2">36,000</td></tr>
<tr><td>Shaft Horsepower, bhp</td><td>15,690</td><td>15,670</td></tr>
<tr><td>Efficiency, percent</td><td>60</td><td>64</td></tr>
<tr><td>OXIDIZER TURBOPUMP</td><td></td><td></td></tr>
<tr><td>Pump</td><td></td><td></td></tr>
<tr><td>Inlet Pressure, psia</td><td colspan="2">40</td></tr>
<tr><td>Inlet Temperature, R</td><td colspan="2">175.6</td></tr>
<tr><td>NPSH (minimum required), feet</td><td colspan="2">16</td></tr>
<tr><td>Discharge Pressure, psia</td><td colspan="2">2055</td></tr>
<tr><td>Head, feet</td><td colspan="2">4225</td></tr>
<tr><td>Flowrate, lb/sec</td><td>475.26</td><td>474.62</td></tr>
<tr><td>Speed, rpm</td><td colspan="2">25,000</td></tr>
<tr><td>Shaft Horsepower, bhp</td><td>4560</td><td>4560</td></tr>
<tr><td>Efficiency, percent</td><td colspan="2">80</td></tr>
<tr><td>Turbine</td><td></td><td></td></tr>
<tr><td>Inlet Pressure (total), psia</td><td>600</td><td>95.2</td></tr>
<tr><td>Inlet Temperature, R</td><td>1960</td><td>1345</td></tr>
<tr><td>Exit Pressure (static), psia</td><td>40</td><td>31.7</td></tr>
<tr><td>Flowrate, lb/sec</td><td>2.59</td><td>5.43</td></tr>
<tr><td>Speed, rpm</td><td colspan="2">2500</td></tr>
<tr><td>Shaft Horsepower, bhp</td><td>4560</td><td>4560</td></tr>
<tr><td>Efficiency, percent</td><td>50</td><td>70</td></tr>
</table>

CONFIDENTIAL

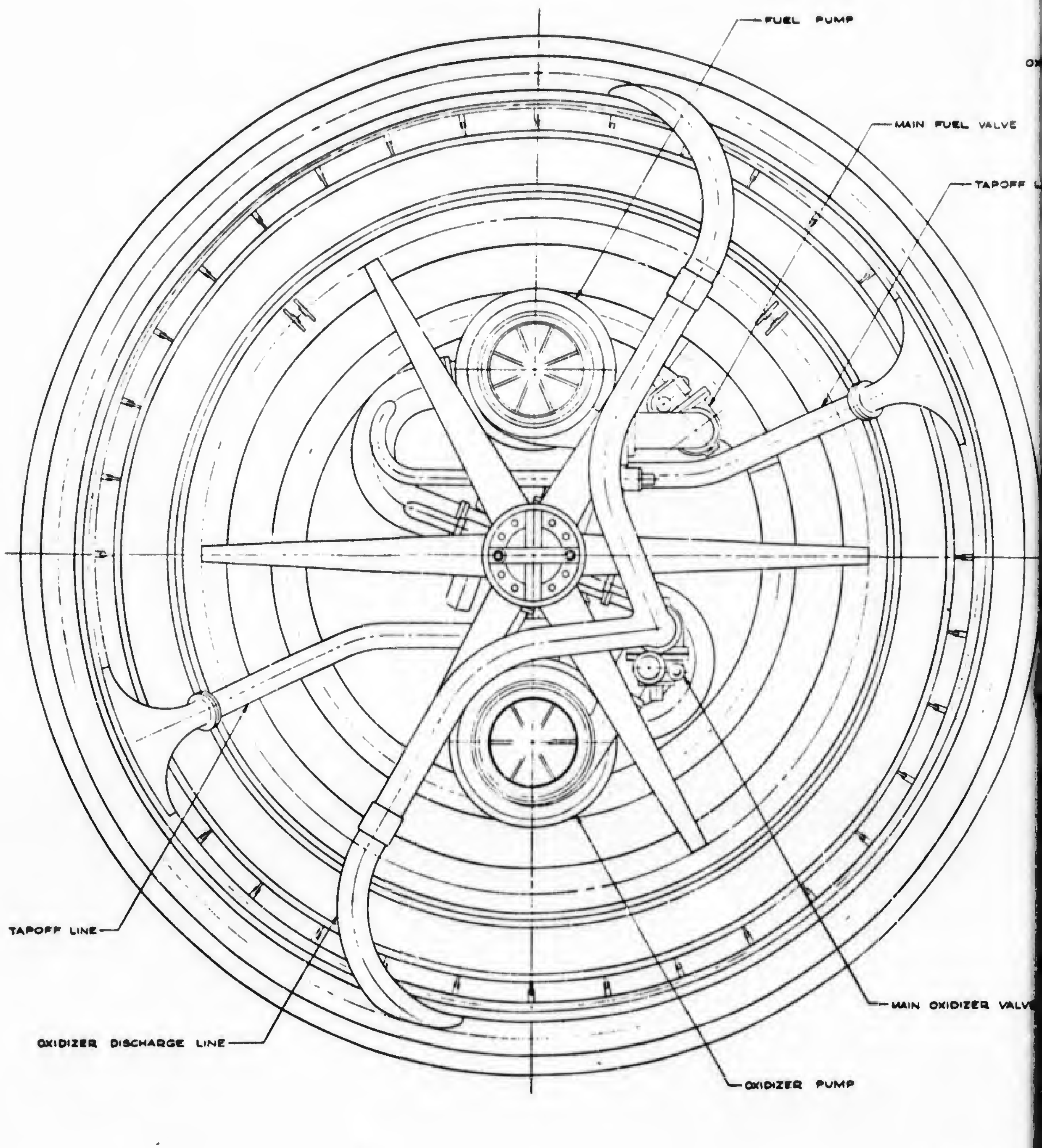

1

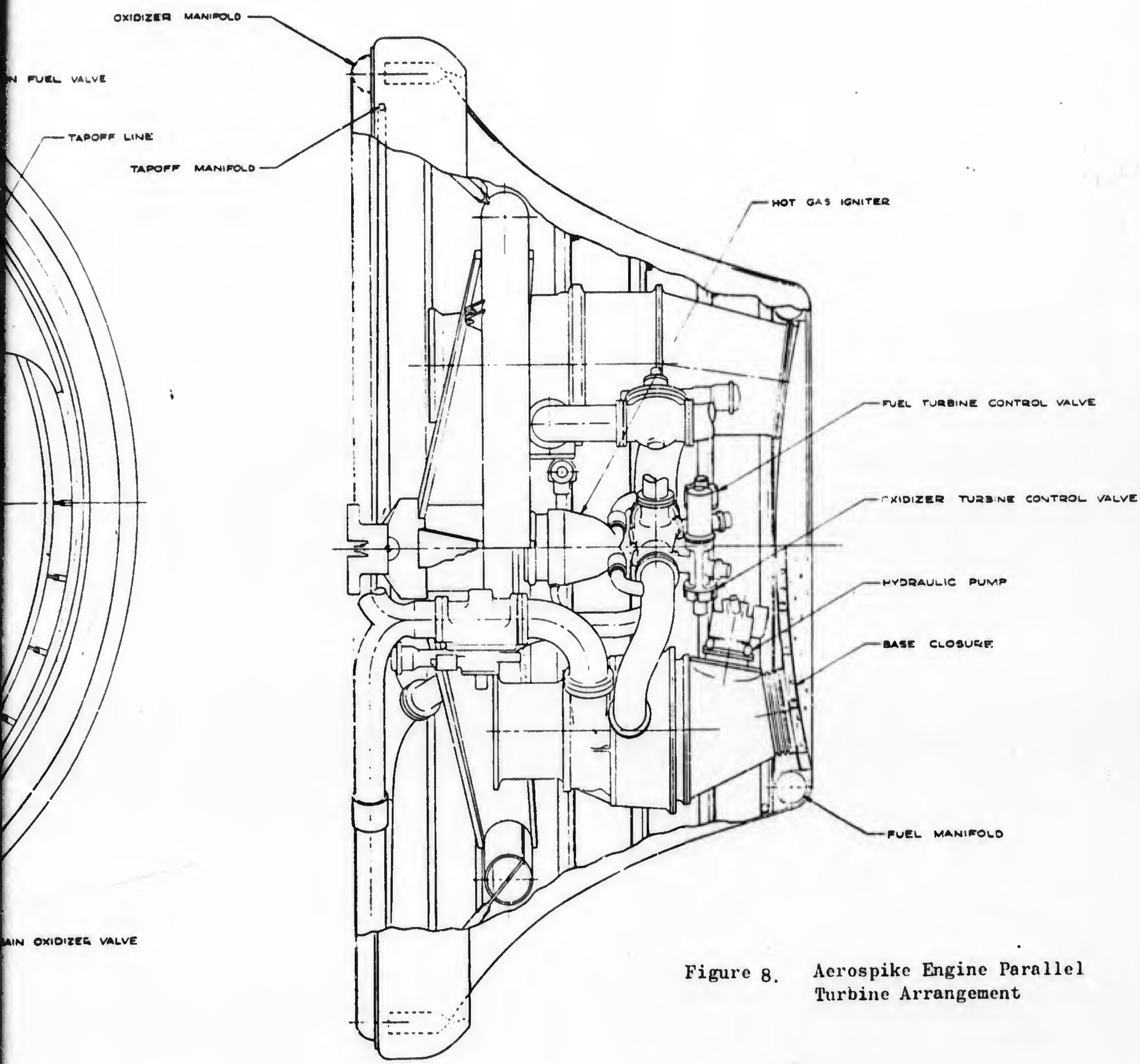

Figure 8. Aerospike Engine Parallel Turbine Arrangement

2

CONFIDENTIAL

CONFIDENTIAL

PREVIOUS PAGE WAS BLANK THEREFORE WAS NOT FILMED

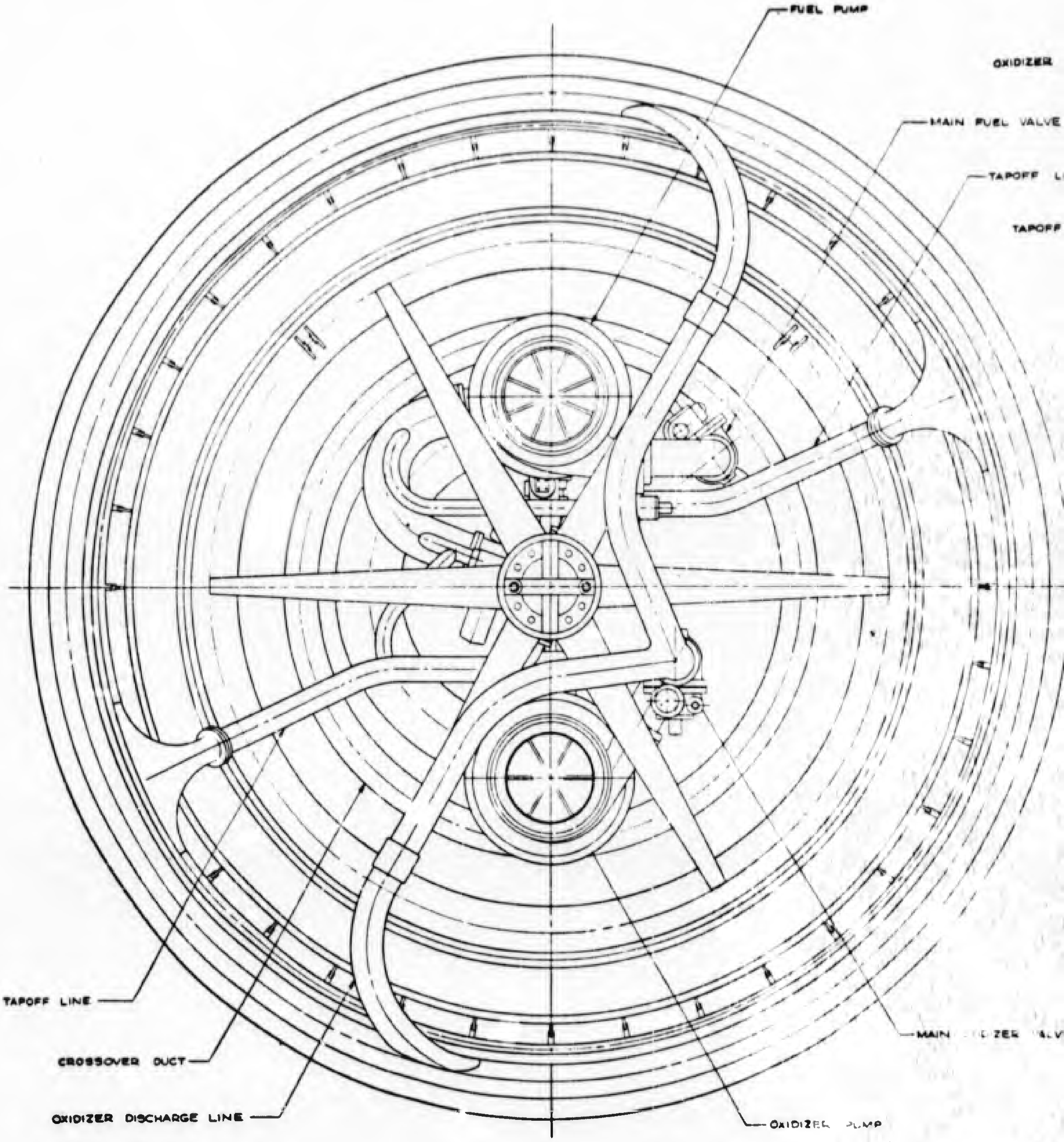

1

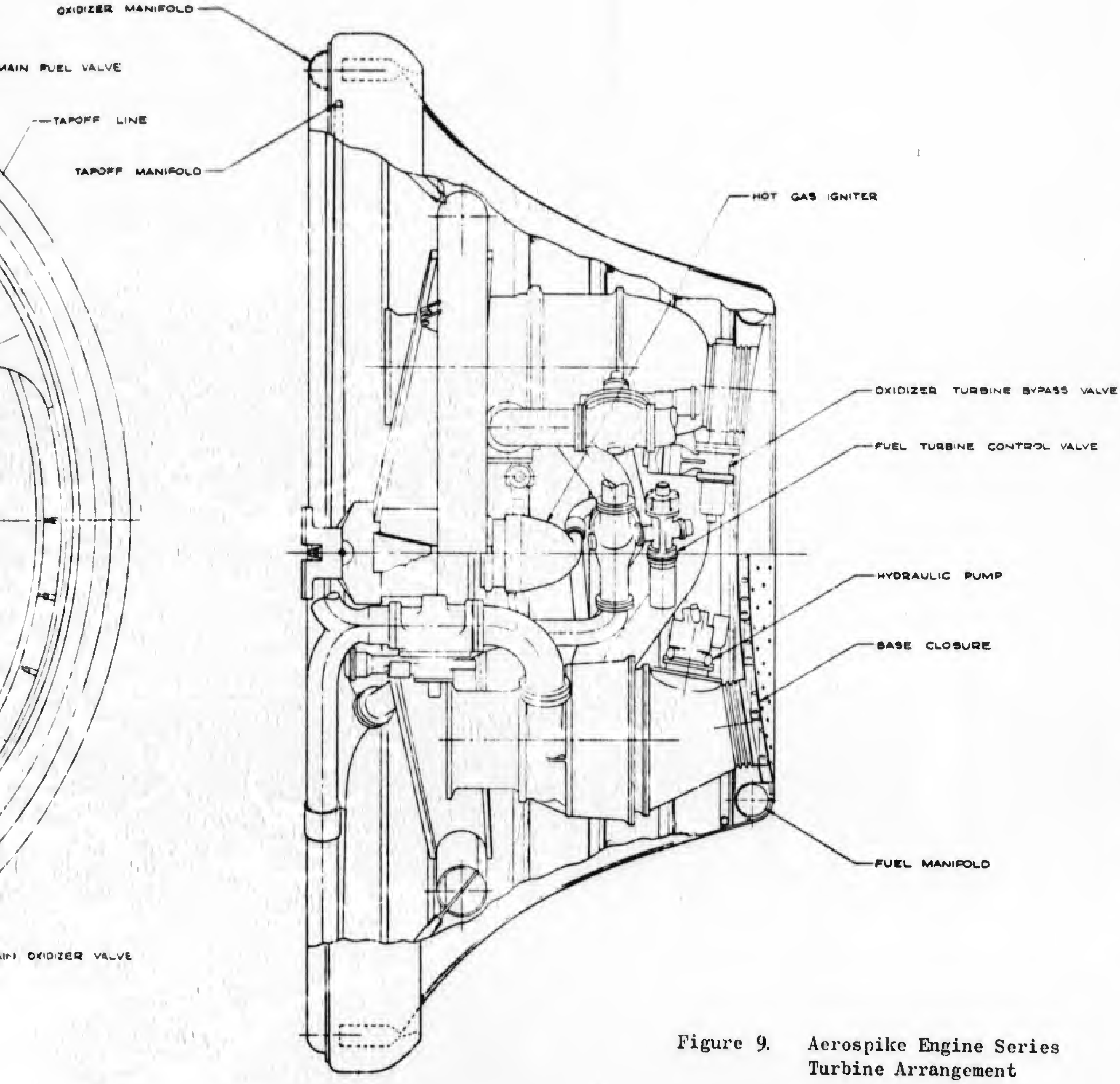

Figure 9. Aerospike Engine Series Turbine Arrangement

(U) locations, and high-pressure propellant lines and manifolds are identical. The major difference is in the hot-gas system. The oxidizer turbine control valve and oxidizer turbine hot-gas line have been deleted and a cross-over duct between the fuel and oxidizer turbines added. An oxidizer turbine bypass and valve have also been added to the system.

(U) Both turbine arrangements were examined to determine if one arrangement had a structural advantage over the other. Only those components which are affected by the turbine arrangement were investigated. The structural investigation determined that there is no significant structural problem associated with the parallel arrangement that would be eliminated by using the series turbine arrangement. However, it was determined that the series arrangement introduced structural problems that do not exist with the parallel system.

(U) The cross-over duct used in the series arrangement will experience thermal growth as its temperature rises during operation. Because the duct is restrained by the two turbopumps, side loads will be placed on the turbopumps. If the duct was allowed to operate in the yield or plastic region, the side load would be reduced. However, this is not desirable because the duct would have a limited life because of the thermal cycles and subsequent fatigue failure. The thickness of the cross-over duct can be increased so that it will not yield, but the stresses will increase as the side load on the pumps are increased and the pump mounts will have to be strengthened. It was determined that three restrained bellows should be used in the cross-over duct. These bellows would allow for thermal growth without yielding the cross-over duct or placing large side loads into the turbopumps.

(U) The fuel turbine exhaust duct in the series arrangement must be heavier than the fuel turbine exhaust duct in the parallel system because it operates at a higher pressure, and it must be able to take side load from the cross-over duct and separating load from the oxidizer turbine bypass valve.

(U) From the standpoint of assembly and component packaging, the parallel arrangement has an advantage in engine assembly and component packaging. The series arrangement was found to be 37 pounds heavier than the parallel arrangement. It was also found that the series arrangement occupies more volume.

(U) The parallel system weighs less, occupies less volume and has fewer design problems. On the basis of these factors, the parallel system is the most favorable from the standpoint of design integration.

(U). Start System. The analog model was used to compute starting torques for both turbines in parallel and series flow. Variations in central igniter pressure and ambient pressure were explored.

(U) Successful starting techniques were developed for both the parallel and the series system up to main LOX valve opening. Starting torque capability of the series system appears to be about 700 in-lb for both turbines. In the parallel configuration, the starting torque capability appears to be about 500 in-lb. Starting time to main LOX valve opening for both turbine arrangements is about 3.5 seconds.

(U) In the parallel configuration, the hot-gas valve was moved to the turbine side of the central igniter (the original proposal had it on the thrust chamber side) and used to control LOX pump speed during the start. With this system, hot gas always flows to the thrust chamber as long as the central igniter is running.

(U) In series flow, a fuel turbine bypass is necessary to provide the flowrate required to start the LOX turbine. A turbine bypass equal to fuel turbine flow (LOX turbine flow is twice fuel turbine flow) was required to bring torque up to 700 in-lb. Excessive LOX pump speed occuring later in the transient was eliminated by closing the fuel turbine bypass.

(U) With system modifications as described above, either system will start adequately. Neither appears to have a significant advantage over the other considering starting torque and time as criteria.

(U) Throttling and Mixture Ratio Controls. The series and parallel turbine arrangements were compared on the basis of meeting the specified throttling and mixture ratio requirements; thrust range from 100 to 20 percent, mixture ratios from 5 to 7, and response to a 2-cps sinusoidal disturbance with a ±0.5 mixture ratio unit magnitude. For the comparison, a 10 percent per second ramp rate was assumed for both mixture ratio and chamber pressure.

(U) Both systems, when properly compensated, responded well to thrust and mixture ratio commands over the required range. There was essentially no difference in the transient response of the two systems (Fig. 10). The frequency response on mixture ratio of both systems is shown for the 100-percent thrust level in Fig. 11. It can be seen that at the 2-cps point, the parallel system has an attenuation of 2.5 db, while the series system attenuation is 1 db. This was an effect of the control system and could be adjusted if it were determined to be necessary. Again, response should be acceptable.

(U) The main goals having been accomplished, some parametric analysis was performed on each system. Various ramp rates were investigated; the controller remaining unchanged. Faster ramp rates created larger transients for each system, with the series system being more sensitive. These effects can be seen in Fig. 12. The controller could probably be changed to produce better response at these higher ramp rates. Controller design will be investigated in more detail in the coming months.

(U) An investigation into the effect of turbopump time constants revealed that transient response deteriorates with an increase in the ratio of oxidizer-to-fuel pump time constants; that is, for best dynamic

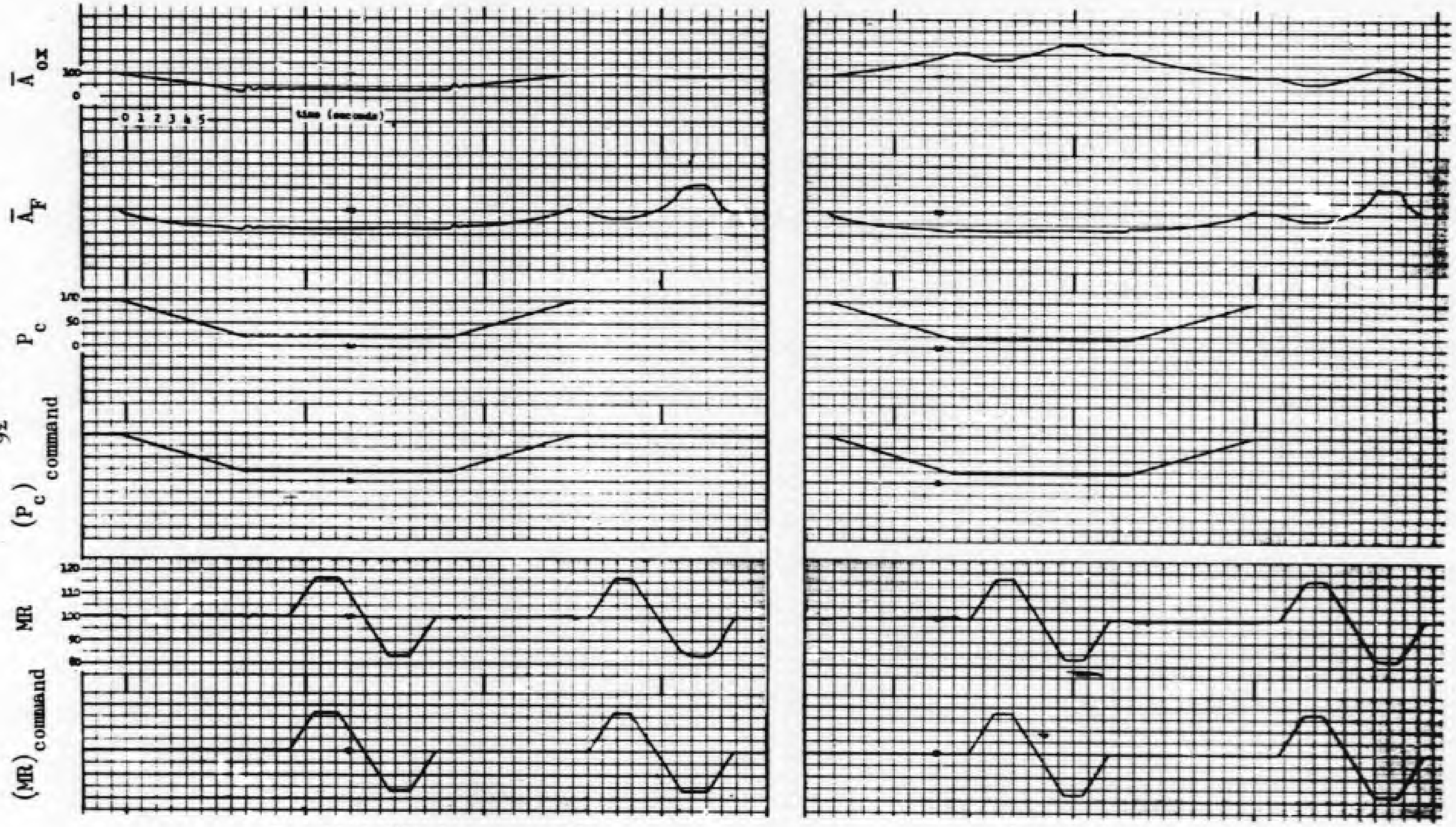

Figure 10. Response of Series and Parallel Systems to Standard Command Signals

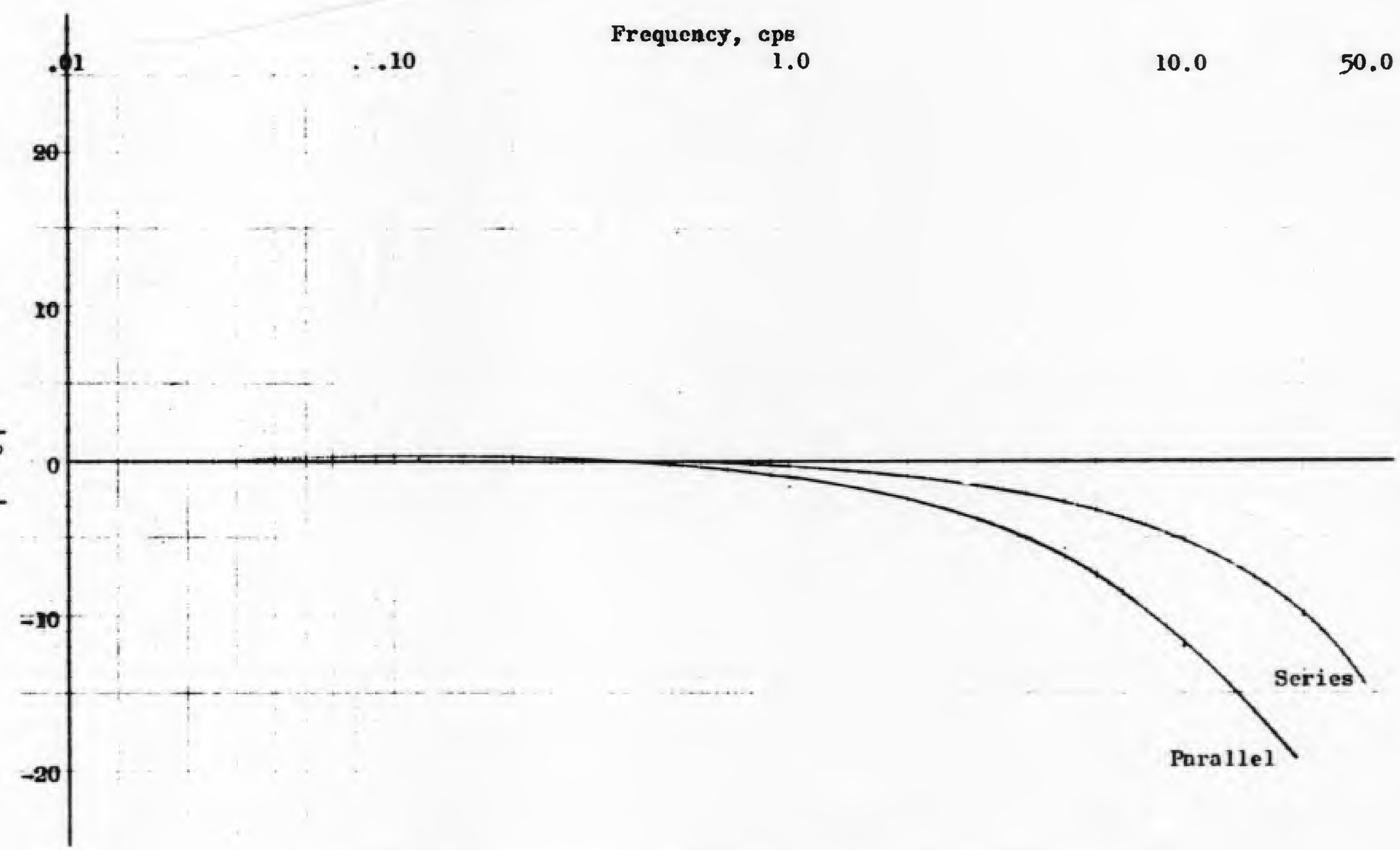

Figure 11. ADP Throttling Models, 100 Percent Thrust Level, Mixture Ratio Frequency Response

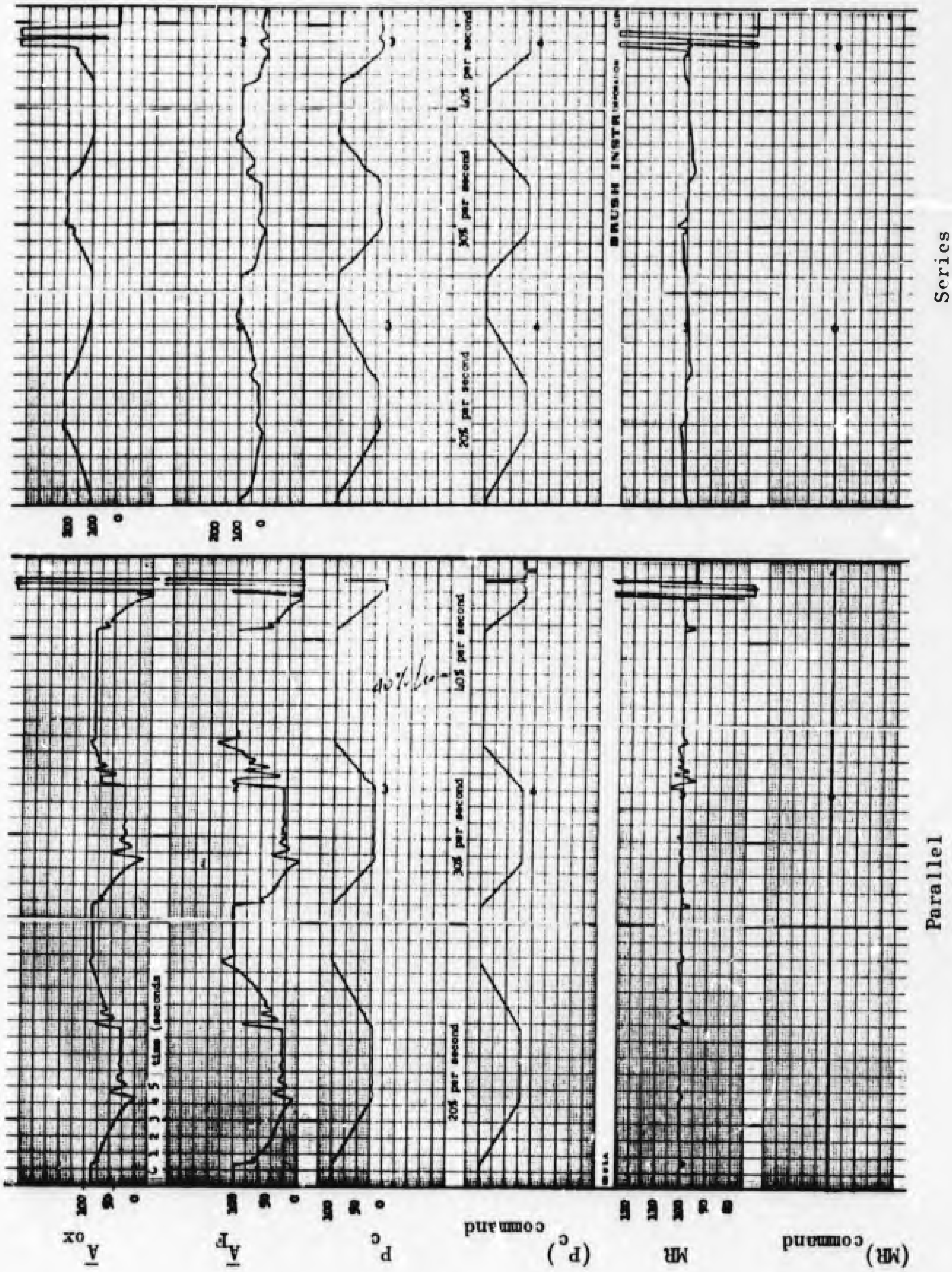

Figure 12. Higher Ramp Rate Performance of Series and Parallel Systems

performance,

$$\left(\frac{\pi}{30}\frac{JN}{\tau}\right)_F \geq \left(\frac{\pi}{30}\frac{JN}{\tau}\right)_{OX}$$

The primary effect of deviating from this condition is an increase in transient mixture ratio oscillation at low thrust levels. It was determined that the series system is much more sensitive to the time constant ratio. A parametric evaluation of the control valve pressure drops was made for both configurations. In the parallel system, the two turbine inlet valve pressure drops were varied from the design point in which one was choked and one unchoked. The conditions of equal pressure ratios across both turbines were evaluated where both are choked and both are unchoked. System response was improved with the use of equal pressure ratios.

(U) The series tapoff valve pressure drops was varied with the effect that a small pressure drop resulted in a wider range over which the valve must operate, especially in obtaining a mixture ratio of 5:1 at full thrust.

(U) Some additional studies included a minimum thrust analysis. Both systems were throttled to 6-percent thrust but stability was marginal. Also, thrust recovery to a step input from these low thrust levels showed essentially no difference at sea level or vacuum.

(U) Liquid control of both systems was briefly investigated with control valves in the pump discharge lines. While it was found that response was good, large control valve pressure drops were necessary and these pressure drops increase with throttling. The pumps, therefore, would be near a stall region, and some additional control devises might be necessary.

(U) In summary, it can be concluded that the series and parallel configurations are essentially equivalent from a controls standpoint with the selected criteria. The series system, is however, more sensitive to turbopump and design point variations. Also the required control valve pressure drops (if turbine inlet gas throttling is used) is much more easily obtained for the parallel system because much larger overall pressure ratios are available across each turbine.

(U) Conclusions.

1. There is no significant performance (specific impulse) advantage to either turbine arrangement over the other.
2. The parallel turbine arrangement results in an engine design which is lighter weight, provides better component accessibility and has fewer design problems.
3. Neither turbine arrangement appears to have a significant starting advantage.
4. The series system is more sensitive to turbopump and design point variations. Also, the required control pressure drops (if turbine inlet gas is used) is much more easily obtained for the parallel system.
5. The Demonstrator Module will use a parallel turbine drive arrangement.

(U) No further effort is planned in this tradeoff study.

Flight Module Design

(U) The requirements were established and effort initiated in May to accomplish the Flight Module Design tasks. Layouts are being prepared for modules of two thrust levels (250 and 350K) and three diameters (80, 100, and 120 inches). Parametric weight and performance data is being prepared for modules with thrust from 150 to 350K in 50K increments; chamber pressures from 750 to 2000 psia in 250 psia increments; and module diameters from 80 to 120 inches. Major emphasis is being placed on the 250 and 350K thrust levels during this study.

(U) Preliminary engine layouts and preliminary parametric weight and performance data will be completed by 1 July to permit initiation of the application studies during the next report period.

(C) Flight Module Layout (250K, 100 inch diameter). A typical preliminary flight module configuration layout for the 250K engine has been completed and is depicted in Fig. 13. The module has the following characteristics:

Thrust (vacuum), pounds	250K
Chamber Pressure, psia	1500
Engine Diameter*, inches	100
Mixture Ratio, o/f	6:1
Thrust Vector Control	mechanical gimbal
NPSH LO_2, feet	16
NPSH LH_2, feet	60
Nozzle Length, percent	25

*Dynamic and static

(C) The configuration is similar to the flight module engine system presented in the proposal (R-6360P-2). Some design modifications have been incorporated in the configuration to improve the performance and/or the ease of construction of the system. The combustion chamber walls have been altered from curved to straight parallel walls, making the cross section of the combustion chamber smaller and making it possible to move the exit throat outboard nearer the 100-inch diameter, thus changing the chamber centerline diameter from 91.5 to 93.0 inches.

(U) This change will result in increased performance associated with increased area ratio and will also result in a simplification of combustion chamber construction.

CONFIDENTIAL

PREVIOUS PAGE WAS BLANK THEREFORE WAS NOT FILMED

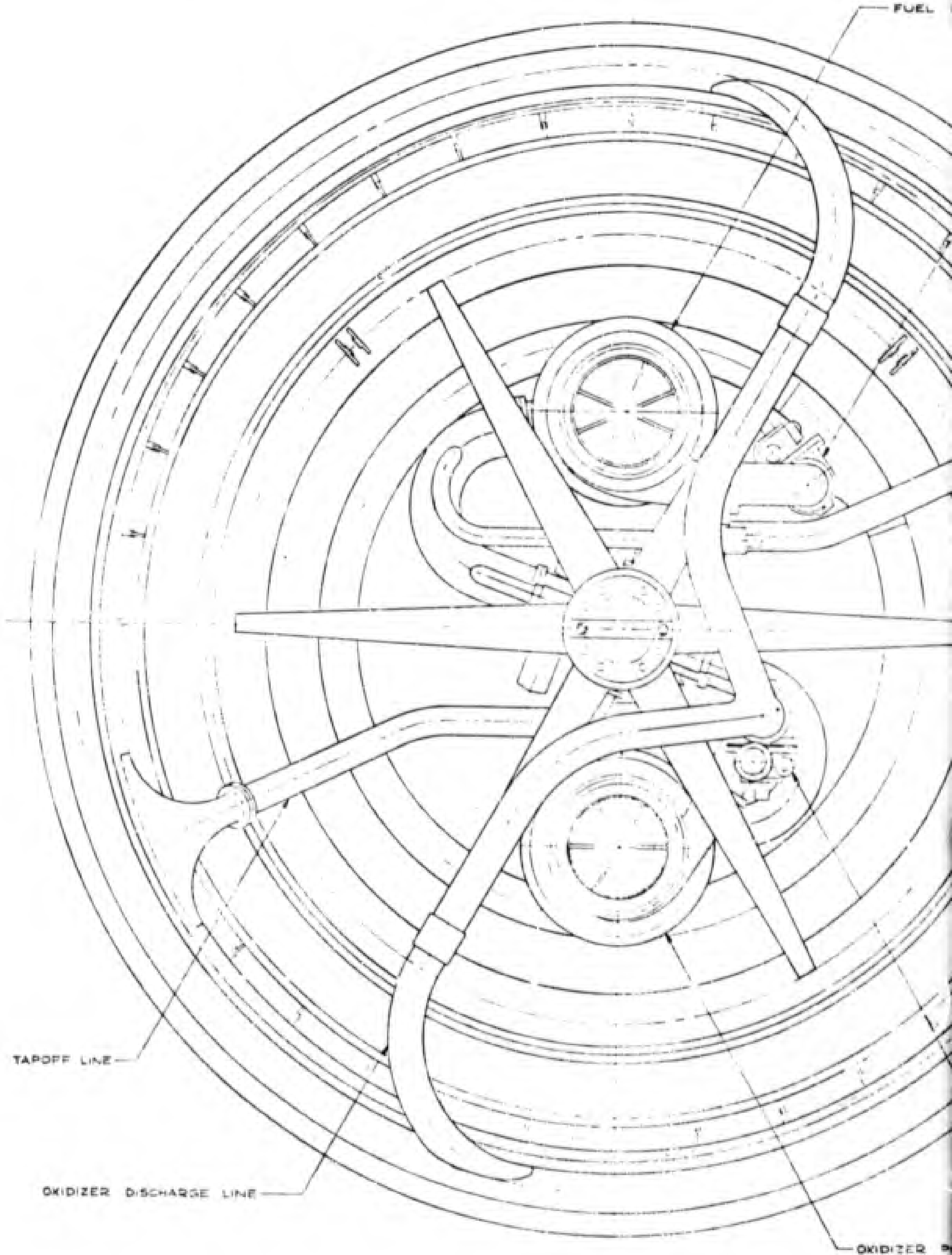

1

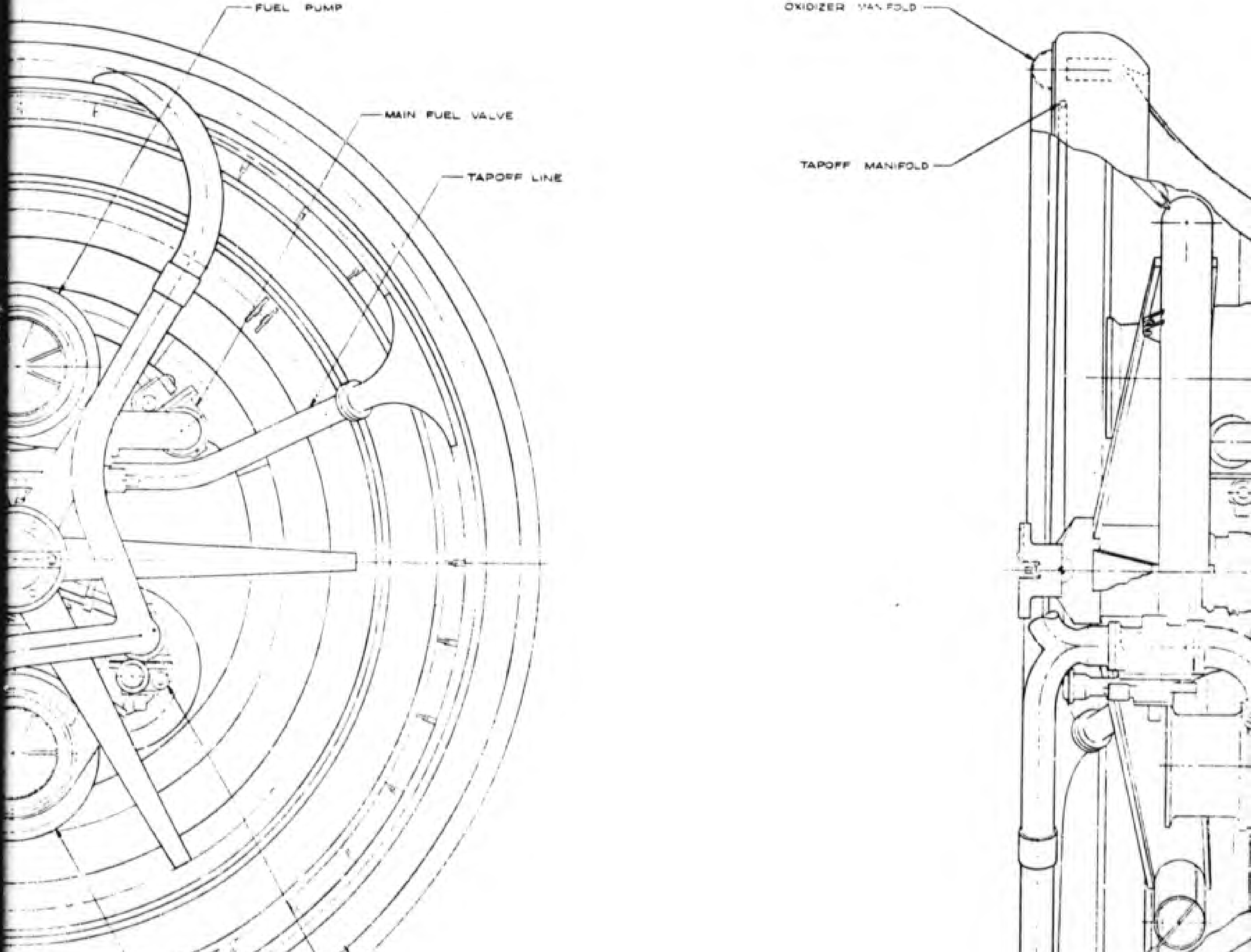
FUEL PUMP
MAIN FUEL VALVE
TAPOFF LINE
MAIN OXIDIZER VALVE
OXIDIZER PUMP
OXIDIZER MANIFOLD
TAPOFF MANIFOLD

2

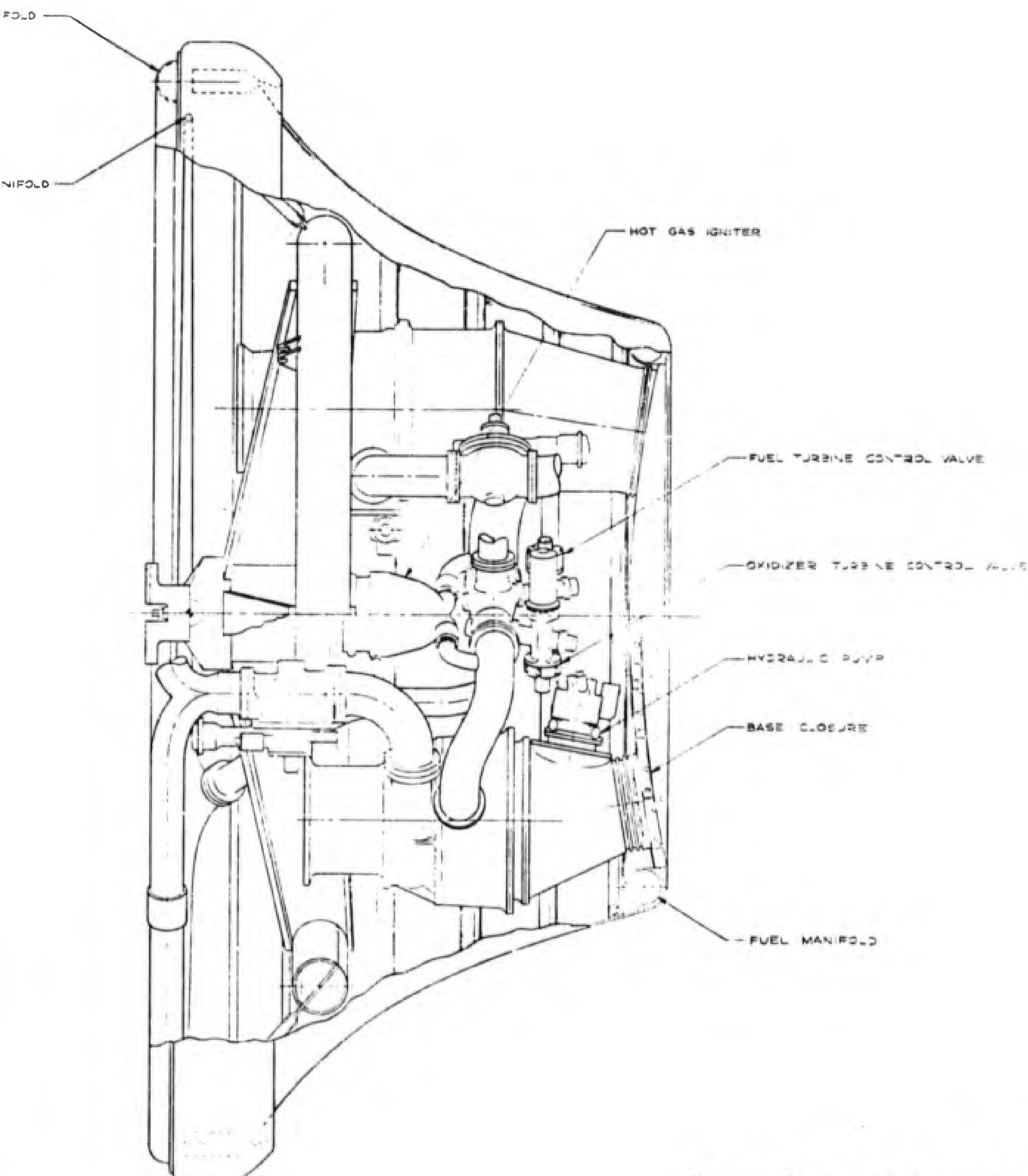

Figure 13. 250K Flight Module
(100 inch diameter)

3

CONFIDENTIAL

(U) The engine system plumbing has been integrated into a more compact package designed to provide better fluid flow control. A central plenum chamber has been established through which the turbine spin gas, the ignition gas, and the tapoff gas is distributed. This will result in improved tapoff gas control at the combustor chamber ports.

(U) The weight of the configuration is approximately 2527 pounds.

(U) A minimum flight module diameter envelope and a minimum length and diameter envelope was investigated at the request of the Air Force Project Office. Results are discussed below.

(U) Minimum Diameter Envelope. This study was conducted to determine the lower limit on diameter of a module that encompasses the components sized for the 250,000-pound-thrust engine system.

(U) Figure 14 presents an approach to this module design and shows that the turbopumps are the governing factors in sizing the overall envelope. The pumps are canted to obtain a small inner body diameter and to provide adequate clearance from structure and gimbal bearing.

(U) The thrust structure consists of 4 I-beams, cone and ring assembly. The I-beams are secured to the ring assembly 90 degrees apart at one end and to a center hub which is mounted to the gimbal bearing. Pumps and other components are mounted to the I-beam structure for their basic support. The thrust chamber is pinned to the thrust cone by multiple hinge assemblies to allow for thermal expansion or contraction between structure and combustion chamber. The nozzle contour is optimum for a 25-percent nozzle length.

(U) The base closure assembly provides controlled distribution of secondary base bleed of turbine exhaust gases. This closure assembly is removable and permits accessibility to components from the bottom.

CONFIDENTIAL

PREVIOUS PAGE WAS BLANK THEREFORE WAS NOT FILMED

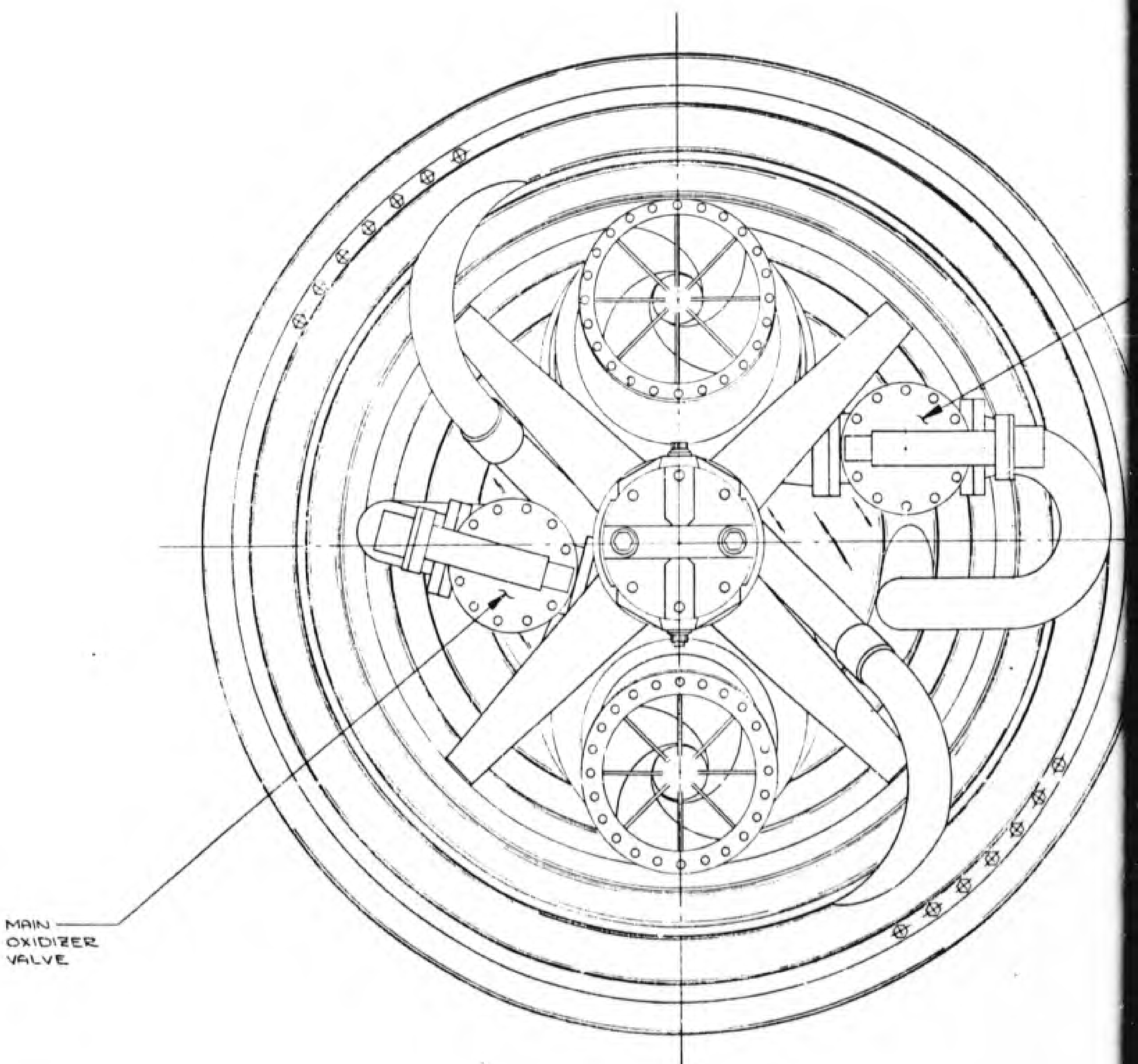

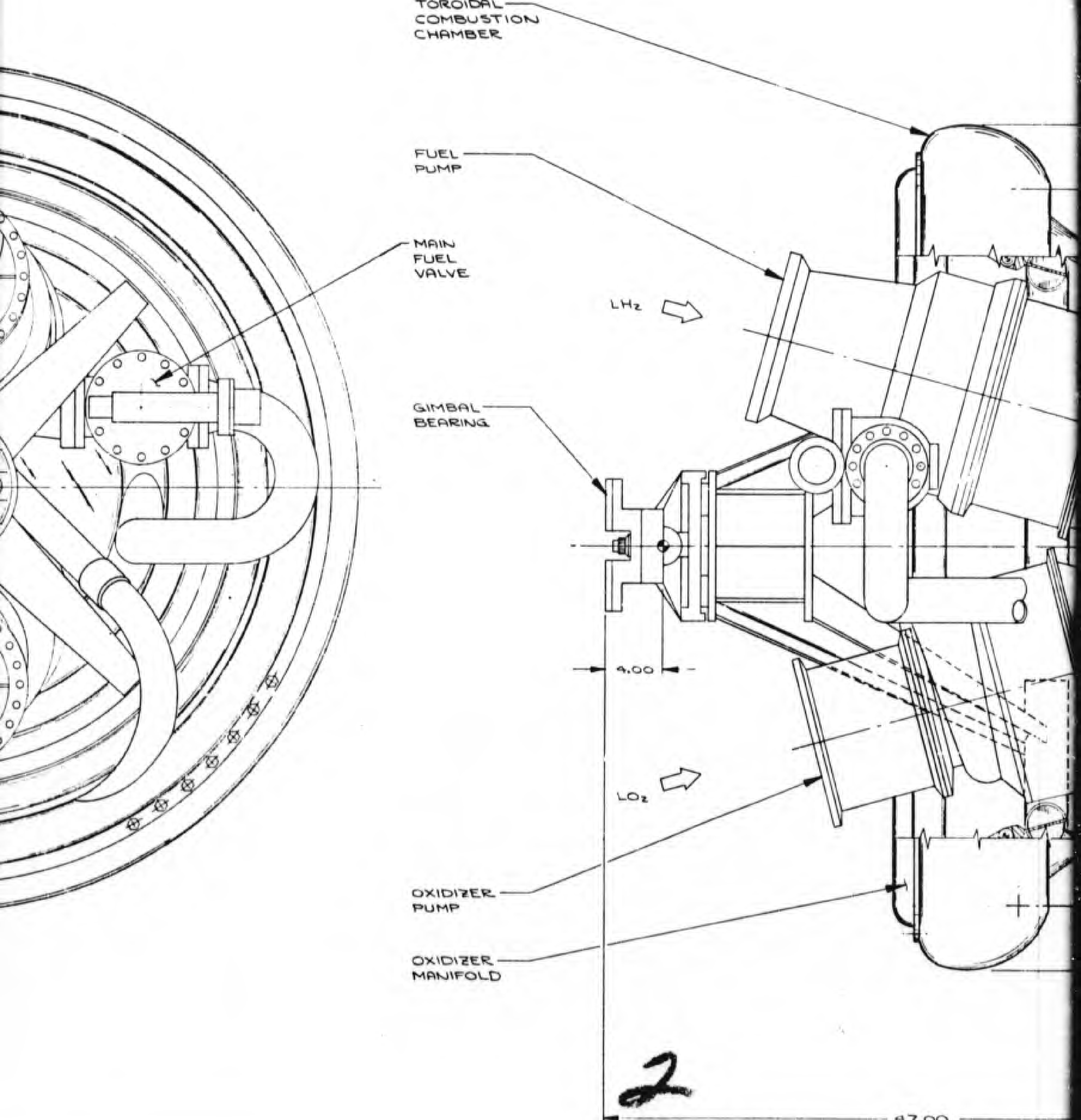

TOROIDAL COMBUSTION CHAMBER
FUEL PUMP
MAIN FUEL VALVE
LH_2
GIMBAL BEARING
4.00
LO_2
OXIDIZER PUMP
OXIDIZER MANIFOLD
2
47.00

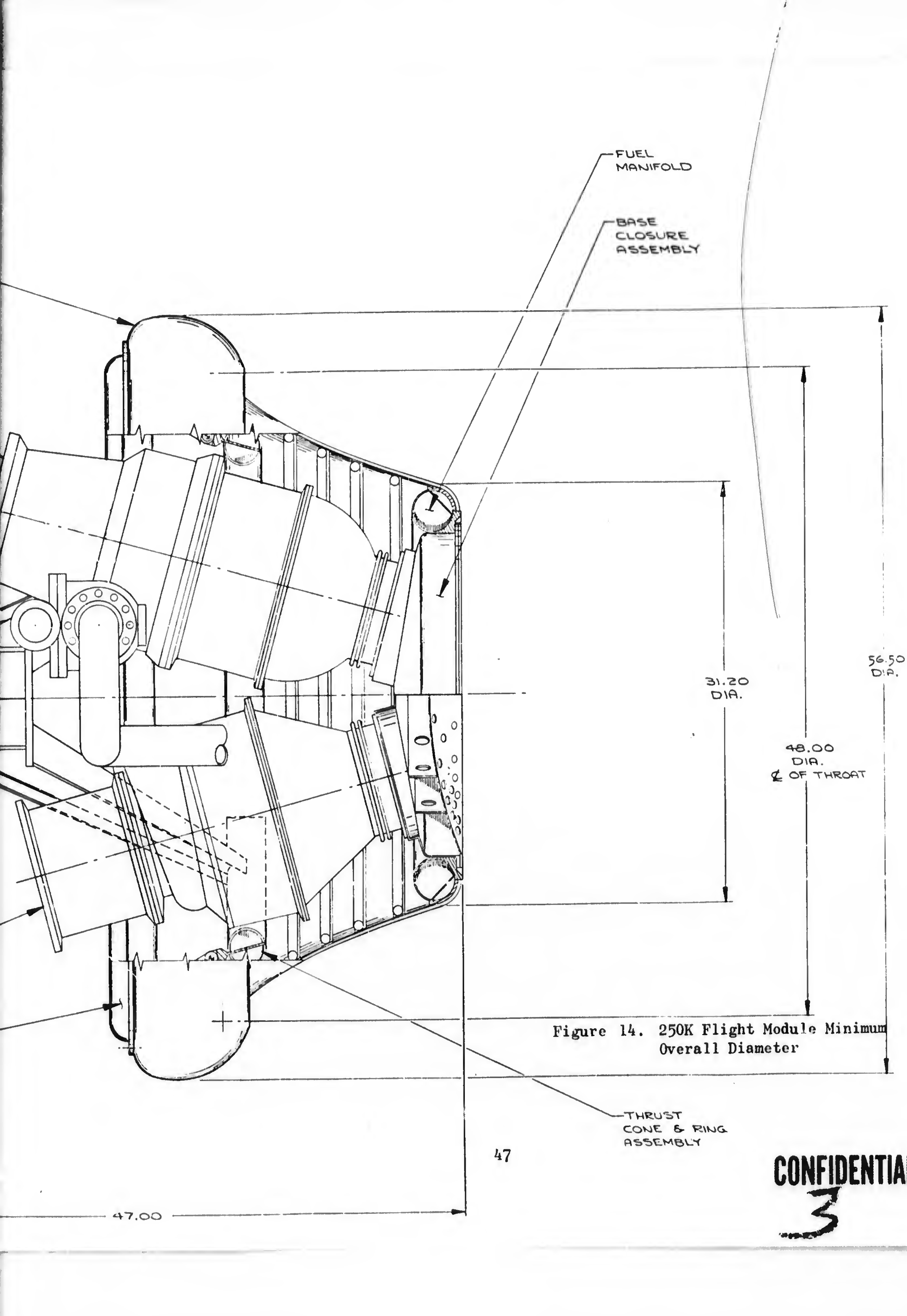

Figure 14. 250K Flight Module Minimum Overall Diameter

3

(U) The parametric weight of this module is 1960 pounds based on the 100-inch-diameter module. The minimum module diameter for this design approach is approximately 57 inches. The module length is 47 inches.

(U) Minimum Length and Diameter Envelope. Figure 15 presents a module designed for minimum diameter and length using the design philosophy and components previously sized for the 250,000-pound-thrust engine system. To establish this envelope, the gimbal point is located in the plane of the engine maximum diameter and the turbopumps are installed within the 25-percent-length nozzle. The innerbody diameter was determined by the turbopump arrangement.

(U) The two turbine housings are connected directly to the upper shell of the base closure assembly. The shell acts like a flex diaphragm and provides for linear thermal growth. The turbopumps are canted to clear the gimbal bearing structure and secured to the I-beam structure for their basic support. The primary structure consists of six equally spaced radial beams welded to an outer ring and central hub. The thrust chamber is pinned to the ring by multiple hinge assemblies to allow for differential thermal change.

(U) The base closure assembly provides controlled distribution of secondary base bleed of turbine exhaust gases. This closure assembly is removable and provides accessibility to components from the bottom.

(U) The parametric weight of this module is 1725 pounds based on the 100-inch-diameter module. The minimum module diameter for this design approach is approximately 60 inches. The module length is 32.6 inches.

Demonstrator Module

(U) Design. A preliminary schematic breakdown of the demonstrator module into subsystems has been completed. Figure 16 presents a composite of these schematics. The thrust structure, gimbal block and thrust chamber assembly (which includes the propellant injector, oxidizer and

CONFIDENTIAL

PREVIOUS PAGE WAS BLANK THEREFORE WAS NOT FILMED

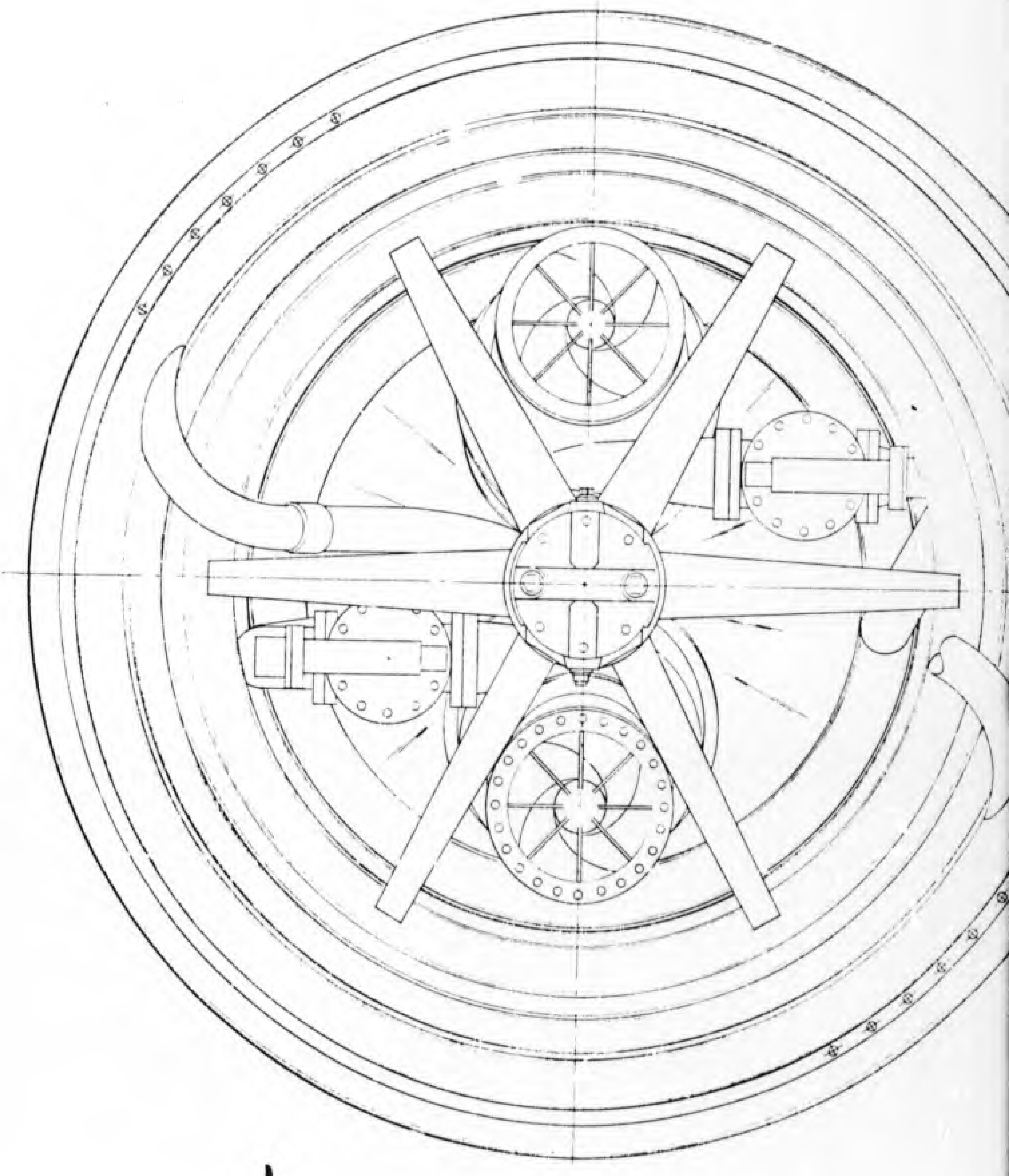

1

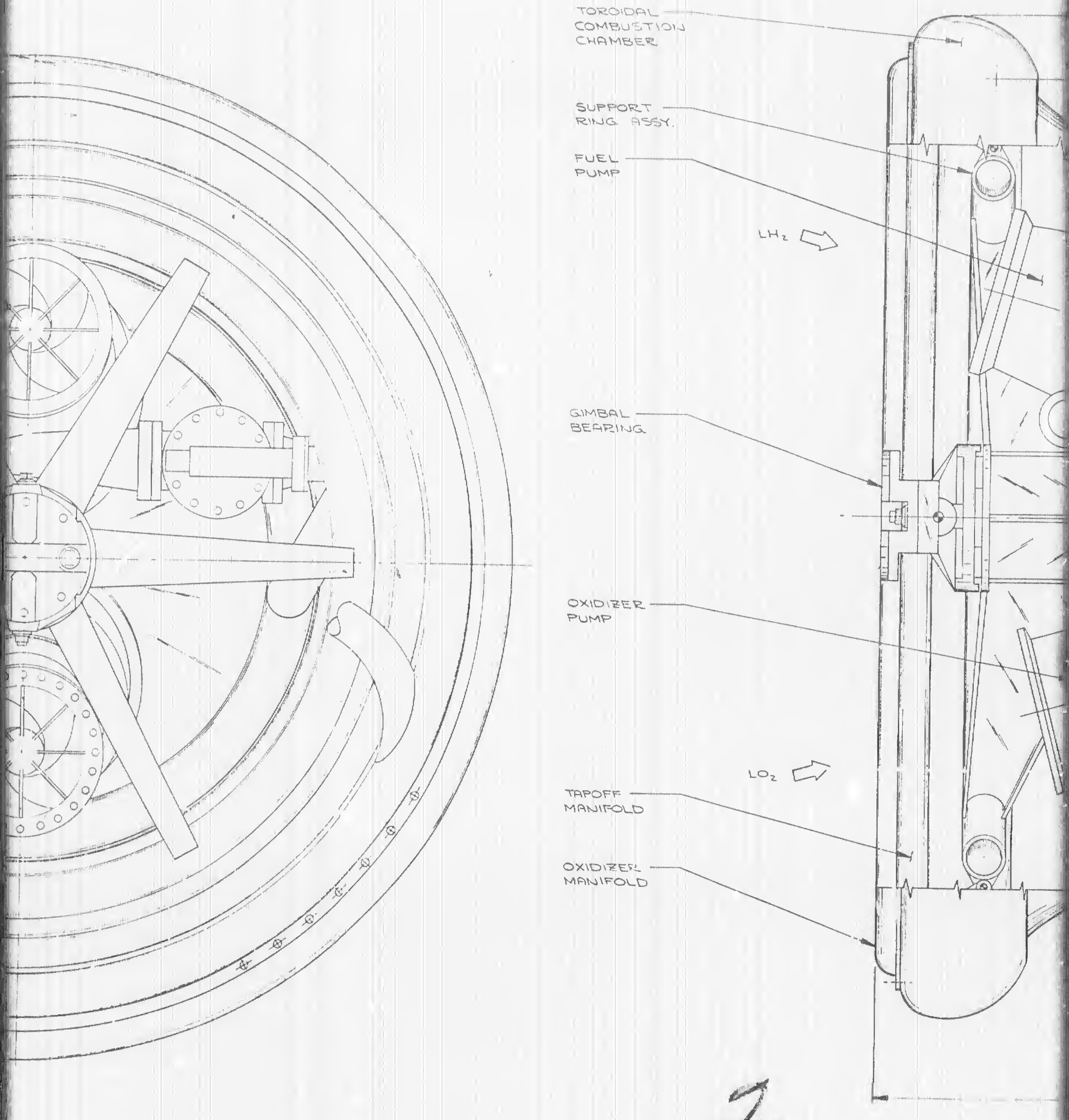
TOROIDAL COMBUSTION CHAMBER
SUPPORT RING ASSY.
FUEL PUMP
LH_2
GIMBAL BEARING
OXIDIZER PUMP
LO_2
TAPOFF MANIFOLD
OXIDIZER MANIFOLD

2

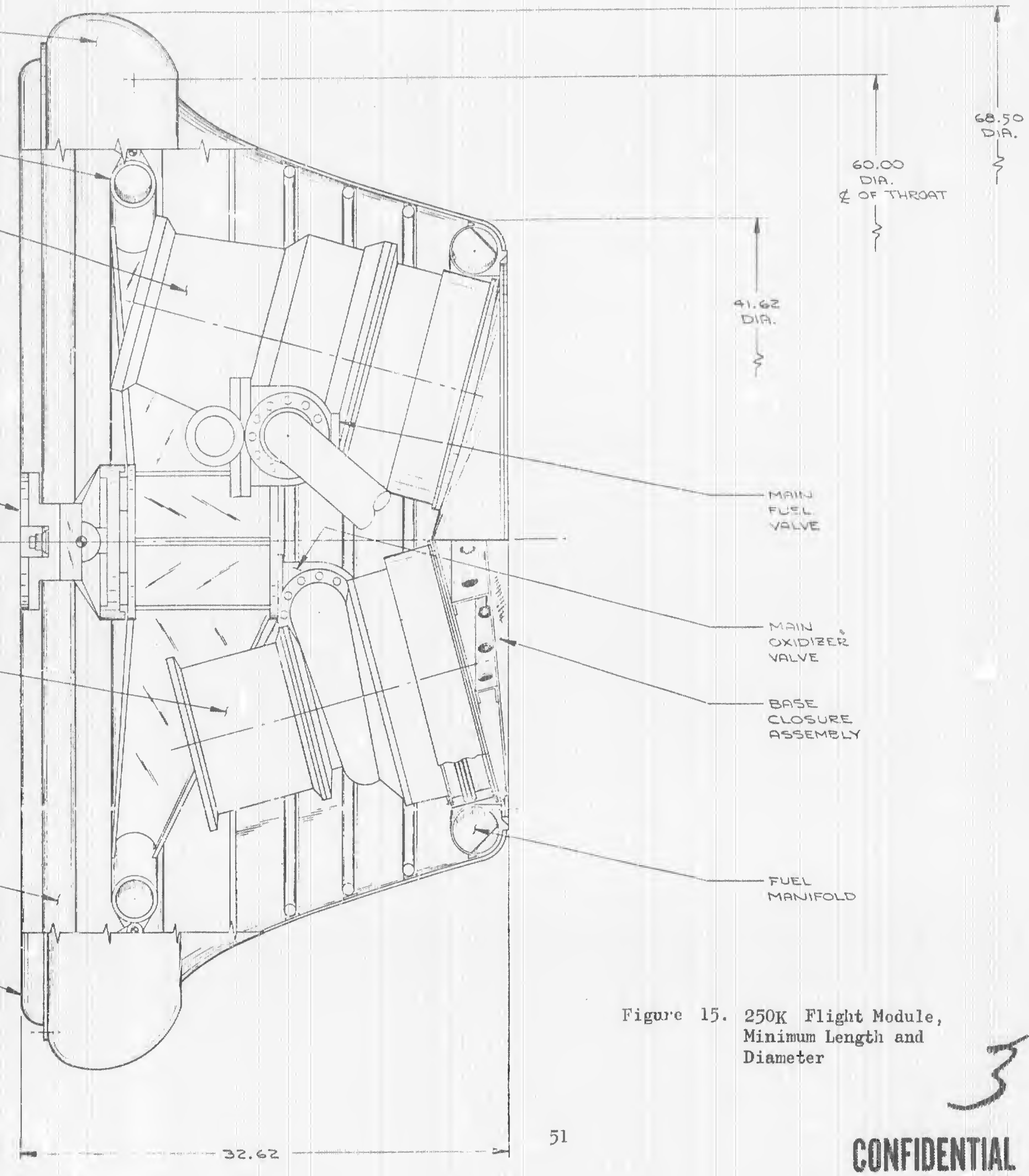

Figure 15. 250K Flight Module, Minimum Length and Diameter

3

CONFIDENTIAL

PREVIOUS PAGE WAS BLANK THEREFORE WAS NOT FILMED

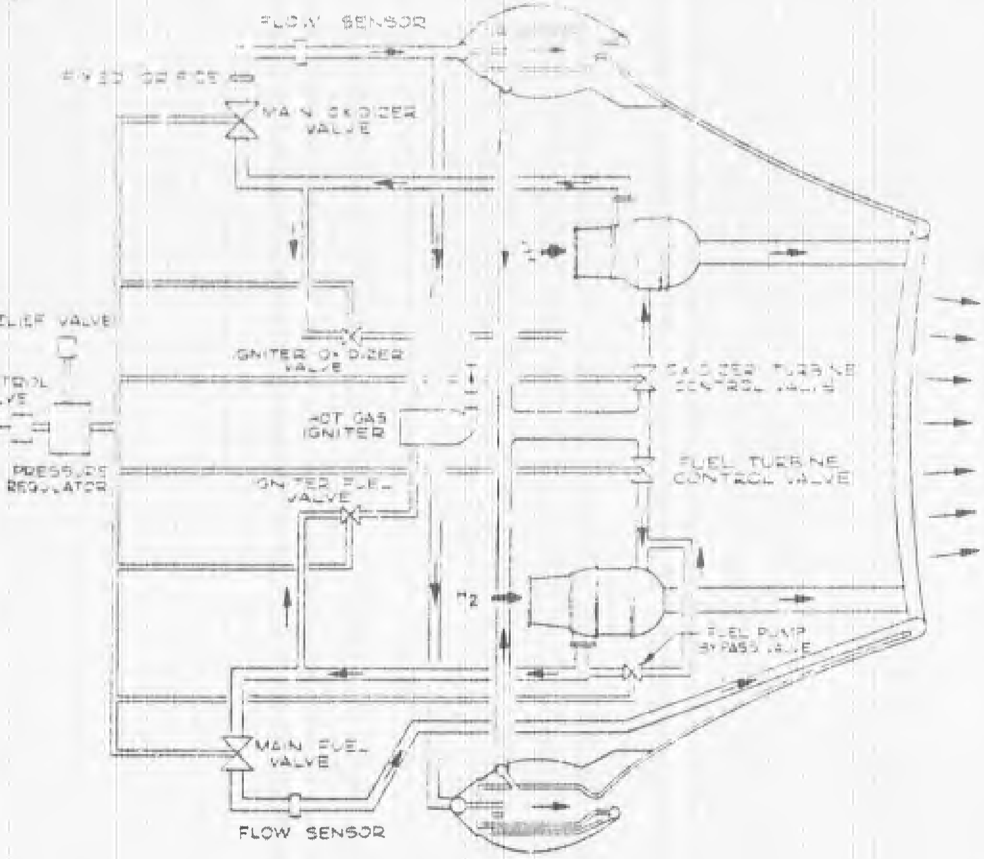

DEMONSTRATOR MODULE SYSTEM SCHEMATIC

SUBSYSTEM INTERFACE
LEGEND:
①-THRUST SUBSYSTEM
②-PROPELLANT FEED SUBSYSTEM
③-TURBINE DRIVE HOT GAS SUBSYSTEM
④-IGNITER HOT GAS SUBSYSTEM
⑤-PNEUMATIC CONTROL SUBSYSTEM

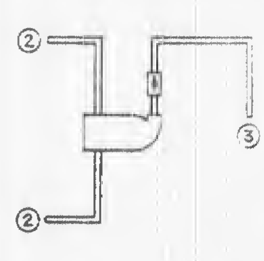

④-IGNITER HOT GAS SUBSYSTEM

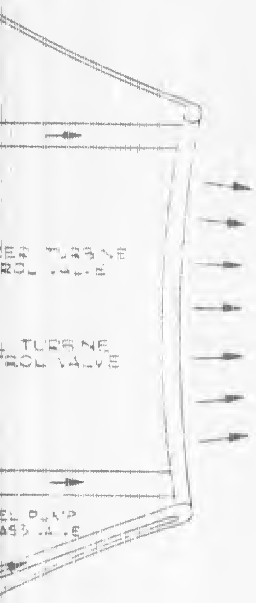

MATIC

TEM

M

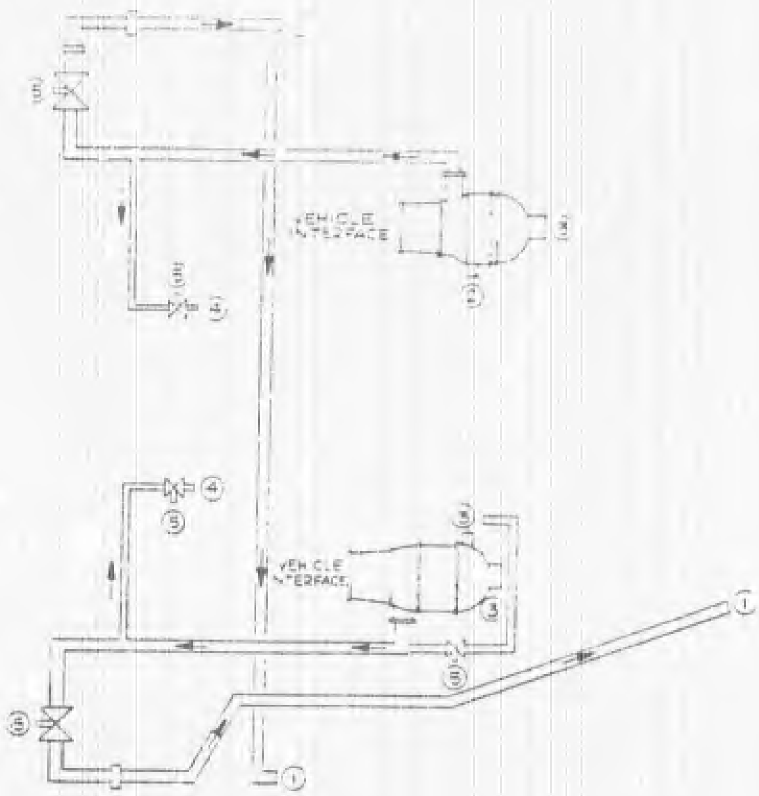

②—PROPELLANT FEED SUBSYSTEM

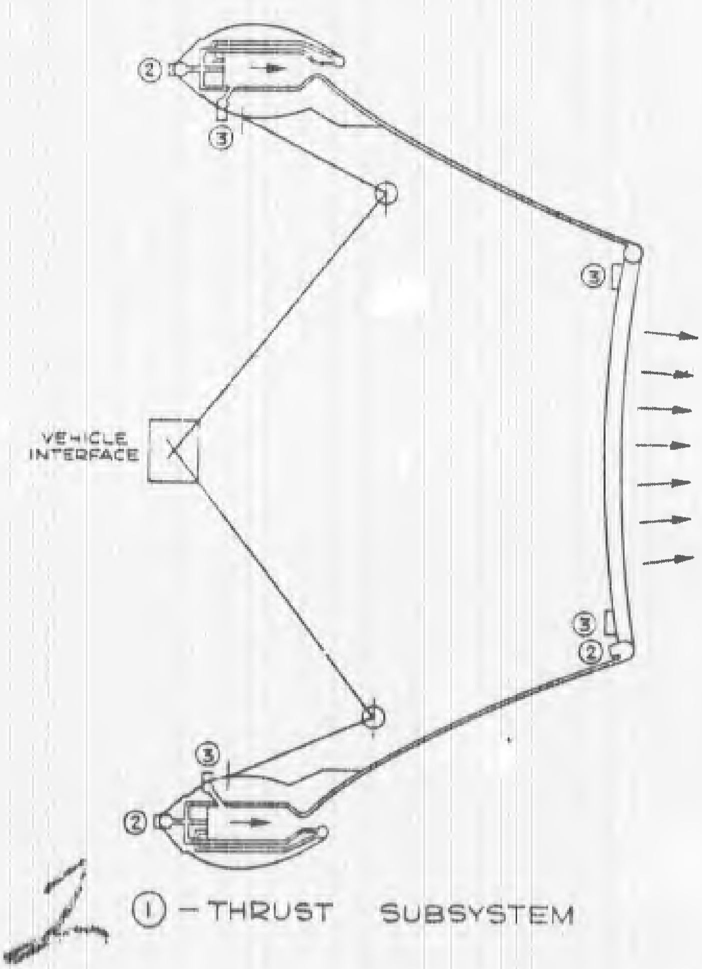

①—THRUST SUBSYSTEM

VEHI
INTER

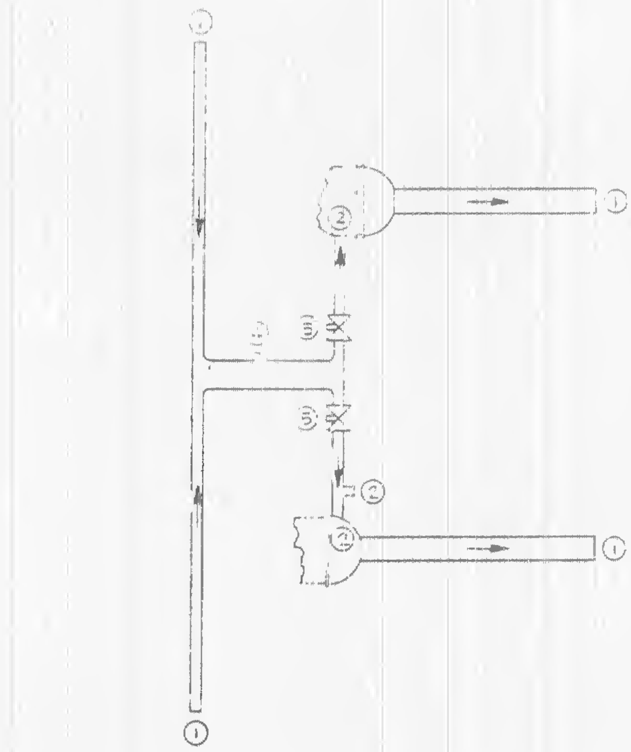

YSTEM

③–TURBINE DRIVE HOT GAS SUBSYSTEM

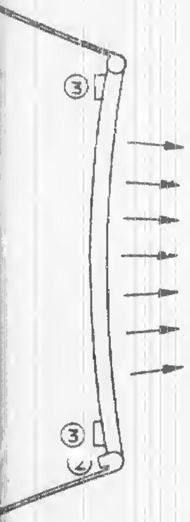

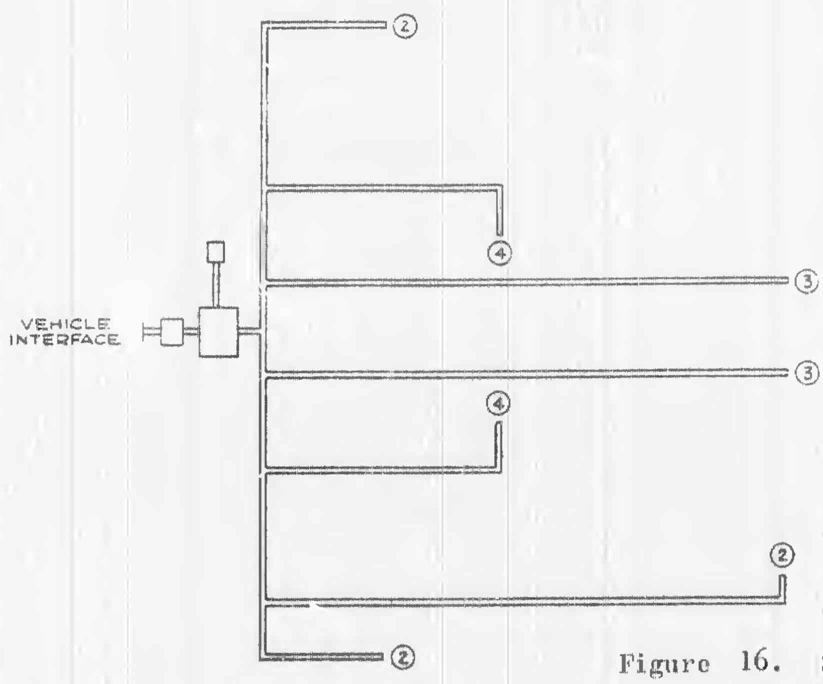

Figure 16. System and Subsystem Schematic

TEM

⑤–PNEUMATIC CONTROL SUBSYSTEM

3

(U) fuel manifolds, hot-gas tapoff manifold, innerbody, outerbody, and base closure) comprise the thrust subsystem. The turbine drive hot-gas subsystem includes the pump turbines, the hot-gas throttling valves, tapoff ducts,and turbine drive ducts. The igniter hot-gas subsystem includes propellant feed lines downstream of the control valves, injector, combustor, igniter hot-gas lines up to the turbine drive ducting and the hot-gas check valves. The propellant feed subsystem consists of the propellant pumps, main propellant valves, igniter propellant valves, fuel bypass valve, flow sensors, orifices, and propellant transport ducts and lines. The pneumatic control system is comprised fundamentally of pneumatic supply lines, regulators and control valves. It is expected that the individual propellant and hot-gas valve control and servovalves will be included in this subsystem at a later date instead of in the subsystem where the primary valve appears. The gimbal system, electrical, and instrumentation systems have not yet been defined.

(U) The igniter hot-gas subsystem provides the spin gas for the engine system turbines and the hot-gas ignition for the main combustion chamber. The subsystem (and the system directly related to its functions) is depicted in Fig. 16.

(U) The hot gas from the igniter is discharged into the tapoff lines which are primarily used to duct tapoff turbine-drive gas from the combustion chamber to the turbines. The tapoff lines along with the hot-gas valves in the lines are considered a part of the turbine drive hot-gas subsystem. Preliminary operating characteristics and conditions were established for the igniter hot-gas subsystem estimated at time of turbine spin start.

1.	Subsystem Minimum Oxidizer Inlet Temperature, R	175.6
2.	Subsystem Minimum Oxidizer Inlet Pressure, psia	39.8
3.	Subsystem Minimum Fuel Inlet Temperature, R	41.3
4.	Subsystem Minimum Fuel Inlet Pressure, psia	34.8
5.	Igniter Combustor Mixture Ratio, o/f	1.084 ±0.05
6.	Minimum Igniter Fuel Flowrate, lb/sec	0.508
7.	Minimum Igniter Oxidizer Flowrate, lb/sec	0.546

(U) The flowrates and subsequent line sizes are based upon preliminary calculations and are required for the iterative process of designing a low-pressure drop system.

(U) To size the propellant lines and the hot-gas lines for the igniter subsystem, several periods of engine system operation must be considered. The time periods of interest are:

1. Turbine spin start
2. Main combustion chamber ignition
3. 100-percent thrust

(U) At the time of turbine spin start, the central igniter must supply sufficient gas at sufficient pressure to initiate turbine spin, i.e., turbine break-away torque must be provided. Therefore, the igniter feed and discharge lines as well as valves and injector must be designed to produce a minimal pressure drop from propellant tank discharge to turbine gas inlet. The system as now designed allows hot gas from the igniter to flow into the main combustion chamber during the entire operation of the igniter. Thus, the tapoff port size effects the sizing of the igniter because there will be a flow into the main chamber during spin start.

(U) The tapoff ports are sized for 100-percent thrust at a gas velocity of Mach 0.25. At turbine spin start, the tapoff ports will flow sonic because the igniter gas pressure over the ambient pressure in the combustor will be greater than critical. A leakage rate can be calculated for the main chamber combustor at turbine spin start. At main chamber ignition, the same sonic condition will exist. Here again the flow into the main chamber can be calculated and compared with the required ignition flow.

(U) Taking the three time periods into consideration, a preliminary estimate has been made of the igniter line sizes. The primary purpose of the line sizing and flowrates is to estimate the pressure drops in the system at the time of turbine spin start. These pressure drops are a function of Reynolds numbers, friction factors, flowrates, system geometry, etc.

(U) The calculated pressure drop for the assumed system depicted in Fig. 17 will be compared with an acceptable pressure drop for the system. Adjustments can then be made in line sizes to optimize the system.

(U) The igniter subsystem pressure drops during the turbine spin start have been estimated and determined to be very low in value, and will dictate the igniter system configuration.

(U) A demonstrator module layout is in work to generate dimensional information for major component envelopes and interfaces. The information and data when determined will be added to the component design sheets. The configuration to date is similar to that in the proposal, R-6360P-2. The combustion chamber has been changed to reflect the straight wall design; the engine system plumbing has been integrated into a more compact package to provide better control; and the thrust mount attachment to the thrust chamber has been modified. Links are being provided to allow thermal expansion. A parting face at the end of each radial mount beam is being provided for easy removal of the thrust mount and attached components. The

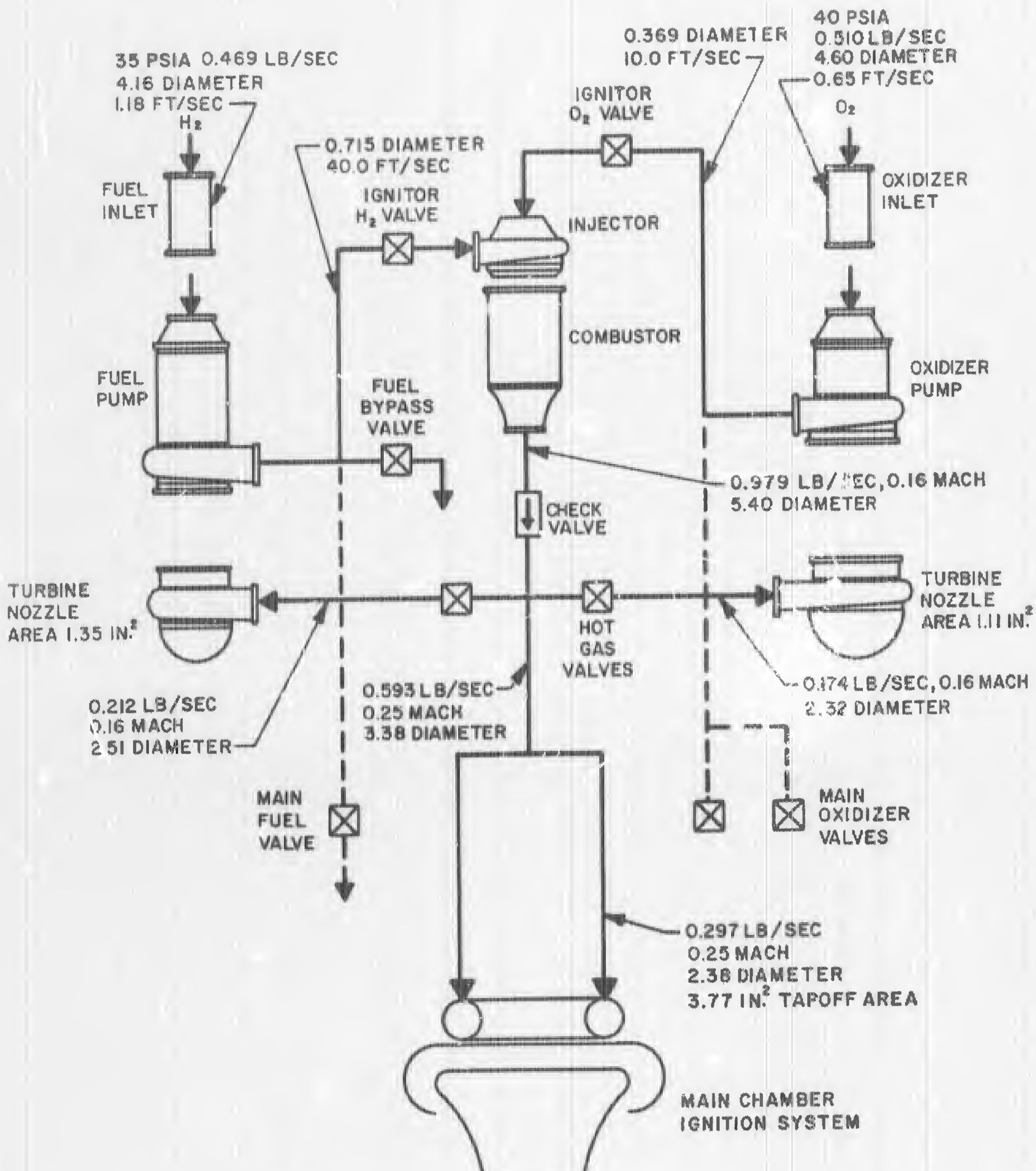

Figure 17. Igniter Hot-Gas Subsystem

(U) oxidizer duct is routed from the pump discharge interface through the radial beam structure to the forward side of the beams where it divides in two and proceeds to the oxidizer injector manifold. Each line supplies 180 degrees of the circular manifold. This routing allows more space below the beam structure for other critical components and provides a better line shape for thermal shrinkage on chilldown. The turbine control valves are now between the turbine spin gas source and the turbines, allowing one instead of two turbine spin hot-gas lines to be used between the central igniter combustor and the turbine drive ducts.

(U) During the next report period, system design and integration effort will be directed towards accomplishment of the following events: preliminary weight, envelope, and interfaces established; component design specification released; and the first Design Review completed.

(U) Steady-State Operating Characteristics. The derivation of steady-state operating characteristics of candidate parallel turbine control (thrust and mixture ratio control) configurations was initiated near the end of this report period. The following configurations are being considered in the investigation.

1. Two tapoff valves
2. Main oxidizer valve and fuel pump bypass
3. Main oxidizer valve and main fuel valve
4. Tapoff valve and main oxidizer valve
5. Tapoff valve and fuel pump bypass
6. Variable area cavitating venturis

(U) The objective of the study is to determine engine operating characteristics of each candidate configuration at full thrust over the entire mixture ratio range and if feasible extend the data to lower thrust levels. Preliminary results have been obtained for configurations 3 and 6. More complete data are available for configuration 1.

(U) Of the three configurations investigated to date, the two-tapoff valve configuration is the most attractive inasmuch as it minimizes pump head requirements. Satisfactory control is realized by providing for a total pressure drop from the thrust chamber to turbine inlet of 500 psi.

(C) A preliminary evaluation of configuration 3 indicates that in order to effect the desired mixture ratio excursion, the nominal valve pressure drops of 10 and 15 psi for the oxidizer and fuel valves respectively, have to be increased to 200 and 650 psi. The high pressure drop required by the fuel valve eliminated this configuration from further consideration. Similarly, the variable area cavitating venturis are also eliminated from consideration. If cavitation is maintained for the venturis at all times, a valve pressure drop of at least 15 percent of the upstream pressure is required, and in order to maintain this relationship the nominal pressure drop is far in excess of that required by configuration 3. At the extreme mixture ratios of 5 and 7, only 2-percent pressure drop remained for both the control elements where initially 9 and 20 percent was available at a mixture ratio of 6.0.

Next Quarter Effort

(U) Investigation of the steady-state operating characteristics of the six control configurations will be completed during the next report period.

(U) The investigation of maximum engine operating conditions based on component performance tolerances was initiated during the report period. These performance deviations will be statistically combined (to estimate expected 3σ engine operating conditions) in conjunction with the nominal characteristics during the next report period.

APPLICATIONS STUDY

(U) There has been no effort expended during this report period. The applications study will be initiated during the first week of August.

TURBOPUMPS

Design

(U) On initiation of the program, analytical work was undertaken to establish the overall turbopump performance specification. Series and parallel system turbine performance and turbopump inertia information was generated for use in determining engine operating characteristics using analog simulation. Complete turbine performance maps for both series and parallel operation were generated. Results of the series and parallel system evaluation show that the basic design of the pumps would not be affected by the system selected; the only differences are in the turbine area. The effect of the system on the fuel pump turbine would be relatively minor, and result from a higher discharge pressure and temperature with the series configuration. This would be reflected by slightly smaller blade height and discharge diameter which would be balanced by the increase in structural strength required.

(U) The LOX pump turbine operating in a series arrangement would have a much lower turbine inlet pressure than when operating in parallel. This would require a larger through flow area and consequently somewhat larger turbine blade heights and overall diameter. Structural requirements, however, are much less demanding because of the lower turbine inlet temperature and pressure and would be reflected by the use of less stringent material requirements and increased allowable stresses.

(U) Preliminary analysis work was initiated on the design of the pumps and turbines to assess in some detail preliminary design concepts and operating envelopes. Perturbations of LH_2 turbopump speed between 32,000 and 36,000 were studied and the effects of utilizing 1-1/2, 2, and staged radial impellers is under investigation. The result

(U) of this trade study will be the selection of LH_2 pump operating characteristics and design point. This, along with design sheets covering system requirements, will allow proceeding with design of both pumps

(U) It is expected that the turbopump performance specifications, which will firm the pump operating conditions, will be completed the first week in June which will then allow work to be started on the hydrodynamic analysis of the pumps and the thermodynamic analysis of the turbines.

Bearings and Seals

(U) Evaluation of the design of the bearings and seals was initiated and although it is not yet possible to establish the size, preliminary designs and materials have been established. Hardened stainless steel 440C has been selected as the material for the bearing races and balls, and the following materials are being considered for the cages:

1. Armalon
2. Polyimide, molybdenum impregnated 25 percent
3. Polyimide, graphite impregnated 25 percent
4. Polyimide, bronze impregnated 40 percent

(U) Shaft seal requirements of high rubbing velocity and long life favor a nonrubbing type of design. Of the two nonrubbing concepts considered (i.e., hydrodynamic type and hydrostatic type), the hydrodynamic type offers the least overall leakage and therefore has been tentatively selected for the preliminary turbopump designs.

Preinducer

(U) Stability of the hydraulically driven preinducer was investigated in more detail, and preliminary results show that over the range of

(U) operating conditions an almost constant preinducer to main inducer speed ratio can be maintained which will be stable.

(U) Preliminary analysis work in a test preinducer has been completed and detailed analysis and design is scheduled to be initiated shortly.

(U) The inducer runs at a blade speed (W_u) and adds rotation (ΔW_u) to the fluid. At the root-mean-square diameter, the velocity leaving the inducer is

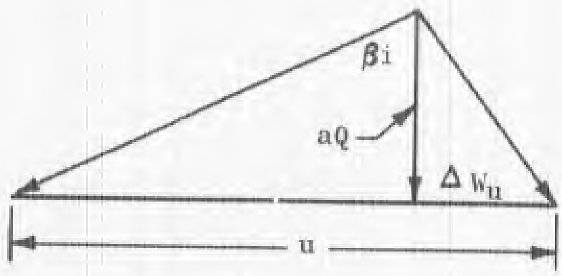

ΔW_u = u-aQtanβi

(U) The high-speed rotor following the inducer runs at a blade speed U and adds additional rotation so that the total rotation leaving the rotor is c_u. The velocity leaving the rotor is

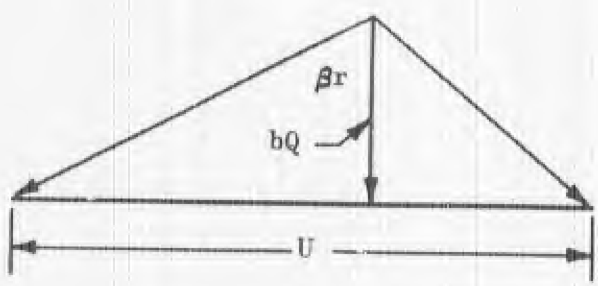

Cu = U-bQtanβr

(U) The rotor is followed by a turbine that drives the inducer. It runs at inducer speed u and removes the rotation added by the inducer; it must also supply the power absorbed in the bearings and the skin friction of the shroud, so the change in rotation in the turbine is K ΔW_u where K is greater than unity. The velocity entering and leaving the turbine is (assuming constant axial velocity)

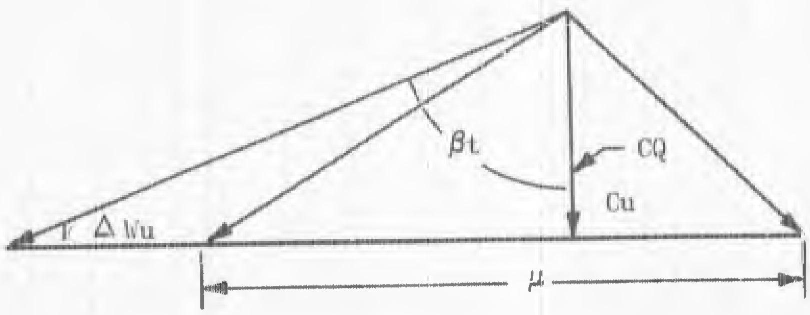

$$u + k\,\Delta W_u = C_u + CQ\tan\beta t$$

$$u + k\,(u - aQ\tan\beta_i) = U - bQ\tan\beta_r + cQ\tan\beta_t$$

$$\frac{u}{U} = \frac{Ni}{Nr} = \frac{1 + \frac{720}{\pi D}\,\frac{Q}{N_r}\left[c\tan\beta_t - b\tan\beta_r + ka\beta\tan_i\right]}{1 + k}$$

(U) Where Ni/Nr is the ratio of the speed of the inducer to the speed of the main pump (u and U are assumed to be at diameter D). If we desire that the speeds be "locked" at constant ratio, then a necessary and sufficient condition that this be true is for

$$\frac{Ni}{Nr} = \frac{1}{1+k}$$

Note that for no bearing losses, etc. k = 1, and the inducer runs at half the speed of the main pump.

(U) Some numerical calculations were made in which it was assumed that Ni/Nr at the design point was both lower and higher than the theoretical value for "locking". When Ni/Nr was low, then as Q was decreased at constant N_r, Ni increased. This would cause the flow coefficient to decrease more rapidly than normal and shorten the range over which good NPSH was obtained. When Ni/Nr was high, the reverse was true and the range was broadened.

(U) For the calculations it was assumed that k was 1.15 The calculations also showed that if the assumption were wrong (values of 1.0 and 1.3 were also tried), the inducer would run at some speed other than design value, but if the initial Ni/Nr ratio was made as close as possible to the "locked" value then the drift would be small.

(U) It was concluded that a unit designed at or near the locked value would be quite stable.

CONTROLS

(U) An analog throttling model for the parallel turbine engine configuration has been constructed. The model is capable of throttling in the range between mainstage to 20 percent of mainstage using a hot-gas control valve at each turbine inlet. Present effort is being applied to improve the cooling tubes description by adding the effects of heat transfer and flow dynamics.

(U) The simplified model (no cooling tube dynamics) has been used to study thrust chamber pressure and mixture ratio control during throttling. A throttling rate of 20 percent per second (four seconds required to throttle from mainstage to 20 percent of mainstage) was used. A mixture ratio of 6 was used during throttling with an excursion between 5 and 7 checked at the mainstage and 20 percent levels. The effect of variations in the hot-gas valve pressure drop to the fuel turbine and corresponding changes in fuel turbine nozzle area on throttling was examined. The fuel turbine hot-gas pressure drop was varied from the nominal value of 300 psi to 800 psi. The results showed good control of thrust chamber pressure for all cases. However, with the low fuel turbine hot-gas valve pressure drop for a mixture ratio near five at mainstage, control was marginal. By increasing the fuel turbine hot-gas valve pressure drop, adequate mixture ratio control was obtained for all required mixture ratio variations.

(U) A digital throttling model for the ADP engine which is being constructed to check the analog model is 75 percent complete. The model is being mechanized using a digital program, and an attempt is being made to more accurately mechanize nonlinear phenomena in the model such as gas flow-pressure relationships and pump coefficients using the expanded capabilities of the digital computer for function generation.

DEMONSTRATOR MODULE THRUST CHAMBER

(U) A study of the demonstrator module thrust chamber structure was initiated and is closely tied to the 20 K segment design. Two structural concepts were proposed for competetive design, namely a machined and welded Inco 718 structure and a titanium welded and bonded structure. The design will be selected in the next quarter and defined by specification.

THRUST CHAMBER PERFORMANCE EVALUATION, TASK II

APPROACH

(C) One of the major objectives of the current program is to demonstrate the performance capabilities of the aerospike thrust chamber. To accomplish this goal, a number of pieces of engine hardware are planned. This included two-dimensional 2.5K segments which will be used to select high-performance injectors capable of operating with high combustion efficiency at full thrust and throttled conditions. These segments will also be used to evaluate chamber heat transfer, tapoff locations, and stability characteristics. Solid-wall and tubular-wall thrust chambers with a nominal thrust rating of 250K will be used to evaluate nozzle aerodynamic efficiency at sea level and altitude, and full-size injector performance and stability.

(U) The noncooled 2.5K solid-wall chambers are versatile combustors designed for use in the program. A noncooled solid-wall engine is available for short-duration injector checkout tests. Spool segment change in this noncooled solid-wall chamber also converts it to a chamber for stability rating testing. A second spool segment change on this chamber converts it for use in tapoff evaluations.

(U) ew injector patterns or modified patterns are first checked out in this chamber for run durations of 300 to 400 milliseconds. Such checkouts provide data on structural adequacy of injectors both from an assembly standpoint as well as from a heat transfer standpoint. The solid-wall chamber is constructed with copper and has a 2-1/8 by 3-1/2 by 6-inches-long inner contour simulating the 250K chamber design. The chamber is closed with a nozzle end plate with three circular holes of total area equivalent to 2.5K toroidal segment. The nozzle plate is expendable and easily replaced.

(U) The water-cooled 2.5K solid-wall segment provides a versatile tool to obtain injector performance data over run durations long enough to stabilize propellant flowrates, as well as pressure, temperature, and thrust measurements. The chamber is made up of segments (chamber spacers and nozzle) to allow variable combustion length evaluations with selected injectors. The chamber also provides the capability of obtaining detailed local heat flux measurements through calorimetric measurements on the cooling passages. A section of the chamber assembly is shown in Fig. 18.

(U) The 250K solid-wall chamber is a workhorse chamber designed primarily to provide a test vehicle for injector checkout prior to tube-wall chamber runs. The injector checkout includes determinations of durability (structural and heat transfer), ignition characteristics, and stability evaluation. Secondary data which may be obtained with the chamber include inner body wall pressure data for aerodynamic evaluation, selected chamber temperature data for heat transfer analysis, structural data on pressure, and temperature load effects. Consideration is also being given to the use of this chamber for obtaining overall thrust chamber performance data.

(U) The 250K tube-wall chamber is a tubular chamber with heavy weight backup structure designed to provide nozzle and combustion operating data on extended duration runs over a 5:1 throttling range, a broad mixture ratio range, and various nozzle gas flows. In addition to sea level performance data, the chamber provides the capability to obtain altitude compensation data with base bleed gases provided by an auxiliary gas generator.

2.5K SEGMENT INJECTOR PERFORMANCE INVESTIGATIONS

(C) The primary effort in this phase of the program is associated with the determination of injector performance data. The basic approach is to implement previously obtained toroidal injector design and performance criteria into injector designs for use over an operating range of 300 to 1500 psia. Analytical considerations for maximum performance over this range have been well formulated. The results

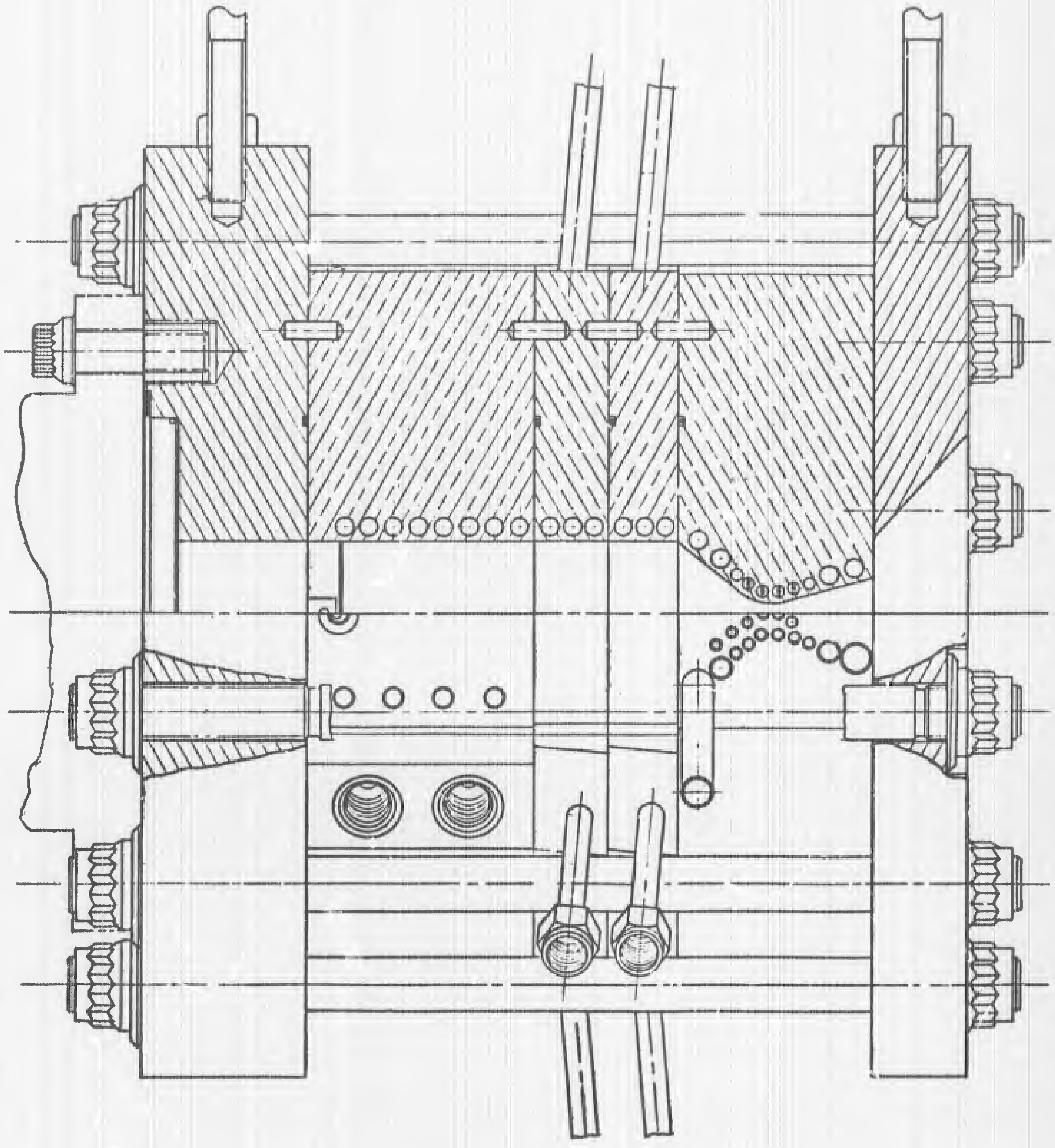

Figure 18. 2.5K Solid-Wall Thrust Chamber

indicate that atomization and mixture ratio control are the strong factors in design. This control is effected through primary atomization of the LO_2 at early locations in the chamber and velocity control of the hydrogen. The analytical studies show that above 1200 psia, the thermochemical properties of LO_2 droplets are such that for 200-micron droplets the equilibrium temperature in ADP-type chambers is always above the critical temperature; consequently, combustion control is through turbulent diffusion. For this reason, almost any type of injection configuration which produces moderately sized LO_2 drops through LO_2 impingement and H_2 jet velocity atomization and reasonable H_2 mixing will provide high combustion performance at design pressures (1500 psia). Therefore, attention can be directed to injector durability and thrust chamber interaction effects at high pressures. Below 1200 psia, high performance combustion required manipulation of atomization and H_2 mixing because the LO_2 drops burn to depletion in the liquid state. Based upon these considerations, the approach to the injector evaluations is to provide durability at 1500 psia while concentrating on performance optimization at the reduced chamber pressures. Coupled with this approach is a matching of the injector to the chamber primarily from a heat transfer standpoint

<u>2.5K Water-Cooled Segments</u>

(U) The chamber assembly consists of four copper sections, forming the body of the chamber. Chamber operating parameters are:

Thrust, pounds = 2,500

Chamber pressure, psia = 1500 to 300

Mixture ratio = 5.0 to 7.0

(U) The copper water-cooled sections of the chamber are internally machined to define the chamber cross-section when stacked together. The No. 1 copper block, the forward body assembly, and the two following spacers define the combustion zone of the chamber. The above-mentioned blocks contain coolant passages which cover all four walls of the combustion zone in circuits normal to the chamber (Fig. 18). The remaining copper section forms the throat and nozzle. The nozzle employs 15-degree divergent half angles with an area ratio of 3.60. The low area ratio value was chosen for full nozzle flow (underexpanded) over all chamber pressure values.

(U) The higher heat flux regions of the throat section utilize coolant passages with bent 321 CRES ribbon flow swirlers to improve heat transfer coefficient coolant side values. The balance of the throat section is cooled passages without swirlers. The part has been designed to incorporate H_2 gas film cooling on all surfaces should this modification be desirable for certain test conditions.

(U) A heat transfer analysis of the 2.5K water-cooled chamber was conducted, with particular emphasis being placed on the drilled holes in the throat region. The analysis was based on a copper chamber with a minimum "reach" (distance from coolant wall to gas wall) of 0.070 inch and a maximum reach of approximately 0.10 inch. Both water and hydrogen cooling were considered. Using water cooling at 1500-psi pressure and 65 F temperature, the coolant wall temperature under nucleate boiling conditions would be about 600 F. Under these conditions, the required water velocity would be about 200 ft/sec, including a 50-percent factor of safety over the burnout velocity. The corresponding gas wall temperatures are 1350 and 1560 F for the minimum and maximum reach respectively.

<u>Injectors (2.5K) and Preliminary Results</u>

(C) Four injectors have been made available for the 2.5K evaluation efforts from an in-house IR&D effort and the ADP program. A total of four patterns have been started through evaluation during the past quarter (Fig. 19, 20, 21, and 22. These patterns are all basically triplet patterns with LO_2 jets as fans impinging on center. Testing

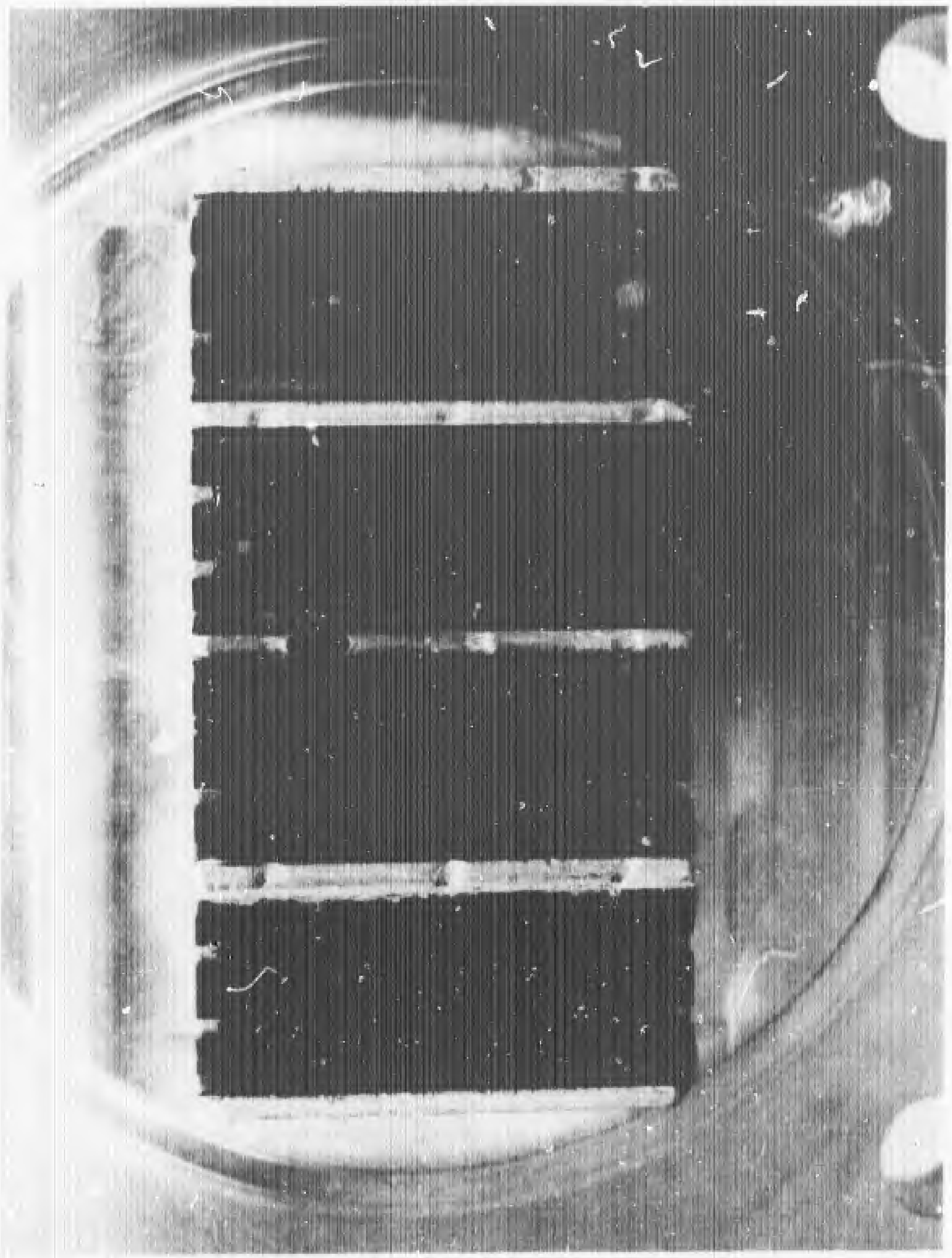

LXV45-5/10/66-S1B

Figure 19. LOX Fan Injector Pattern

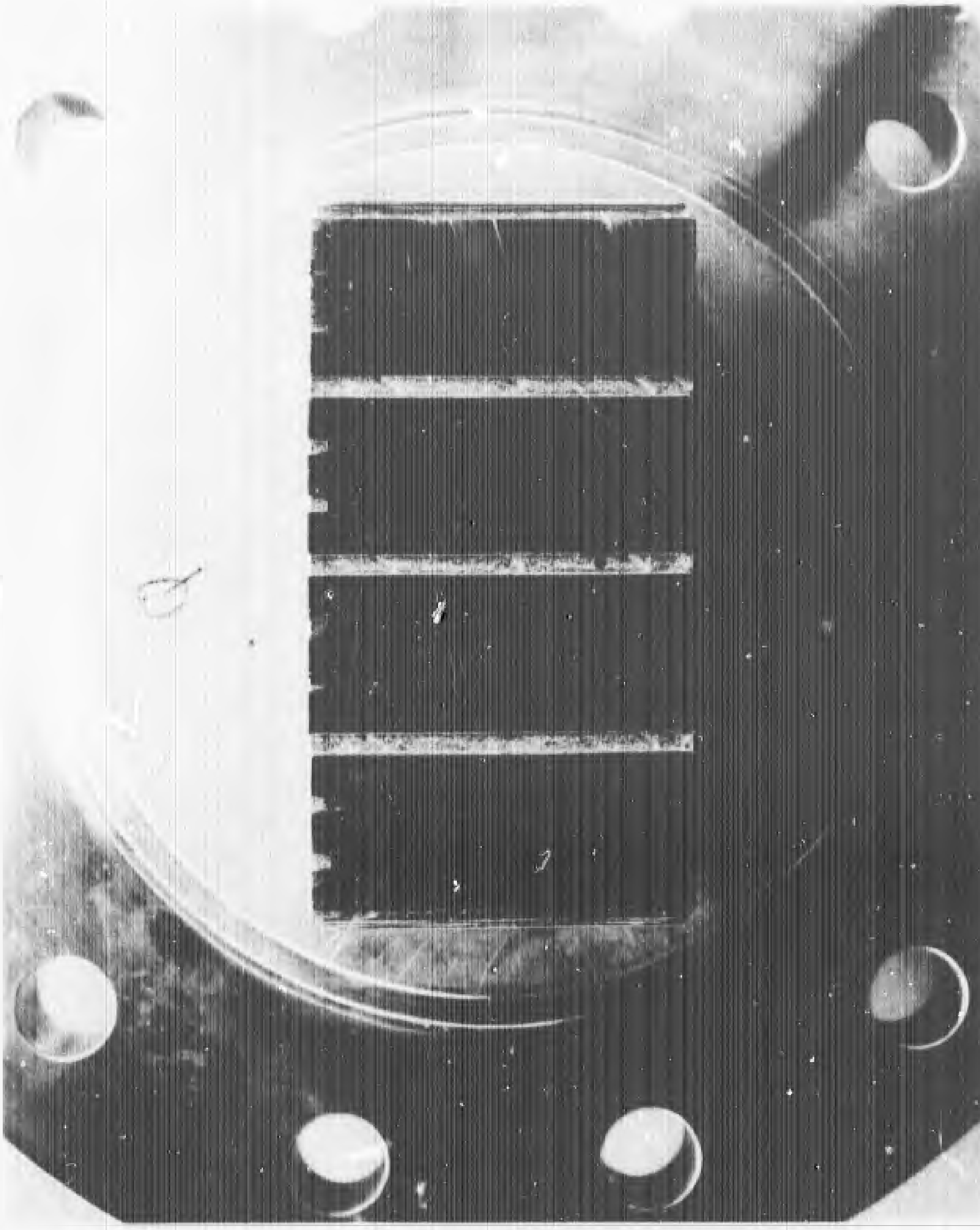

5AA36-5/24/66-S1A

Figure 20. Reversed Pattern, 80-Degree Fuel on LOX Fan

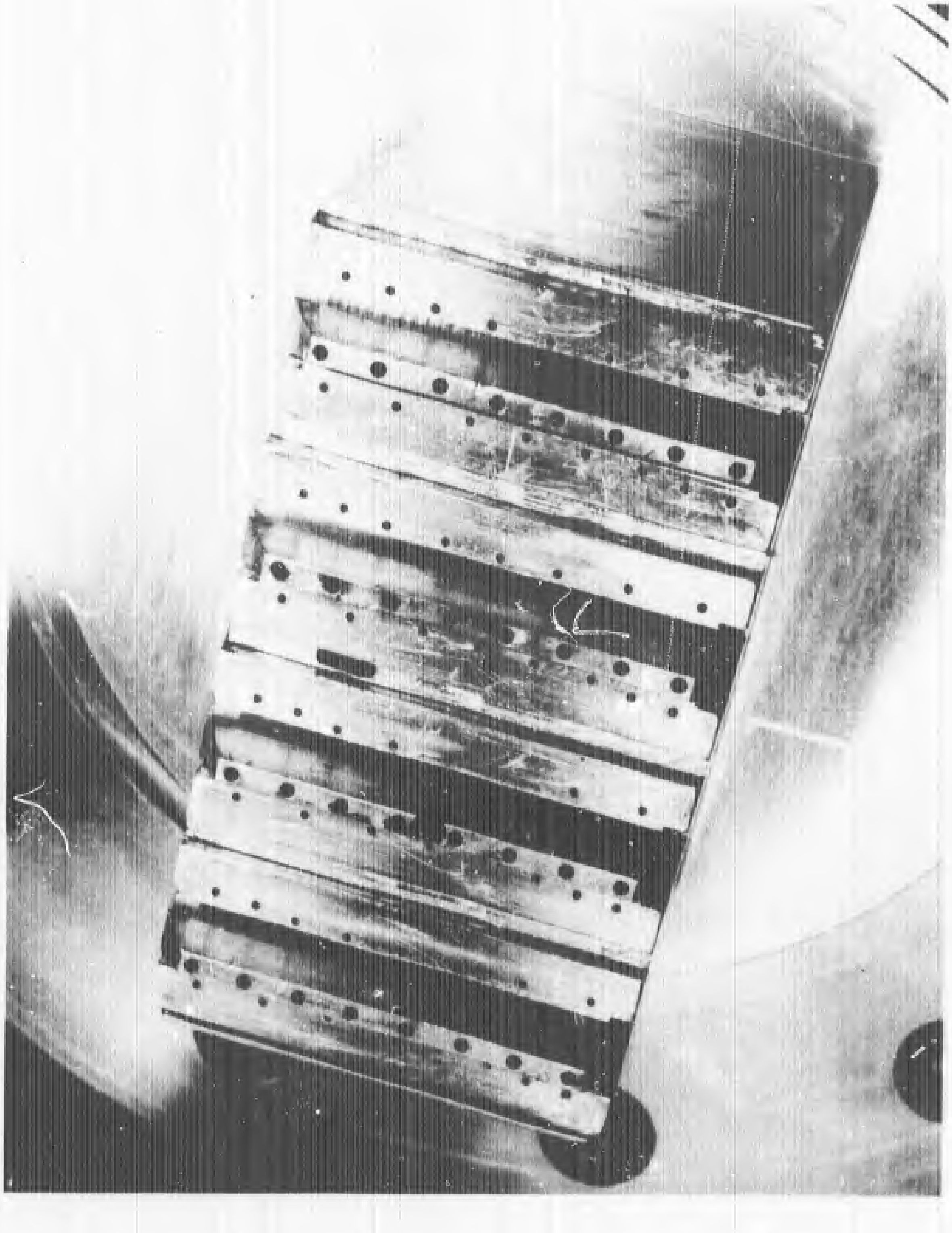

5AA34-4/20/66-S1A

Figure 21. 60-Degree LOX Impinging Triplet with Fuel Post

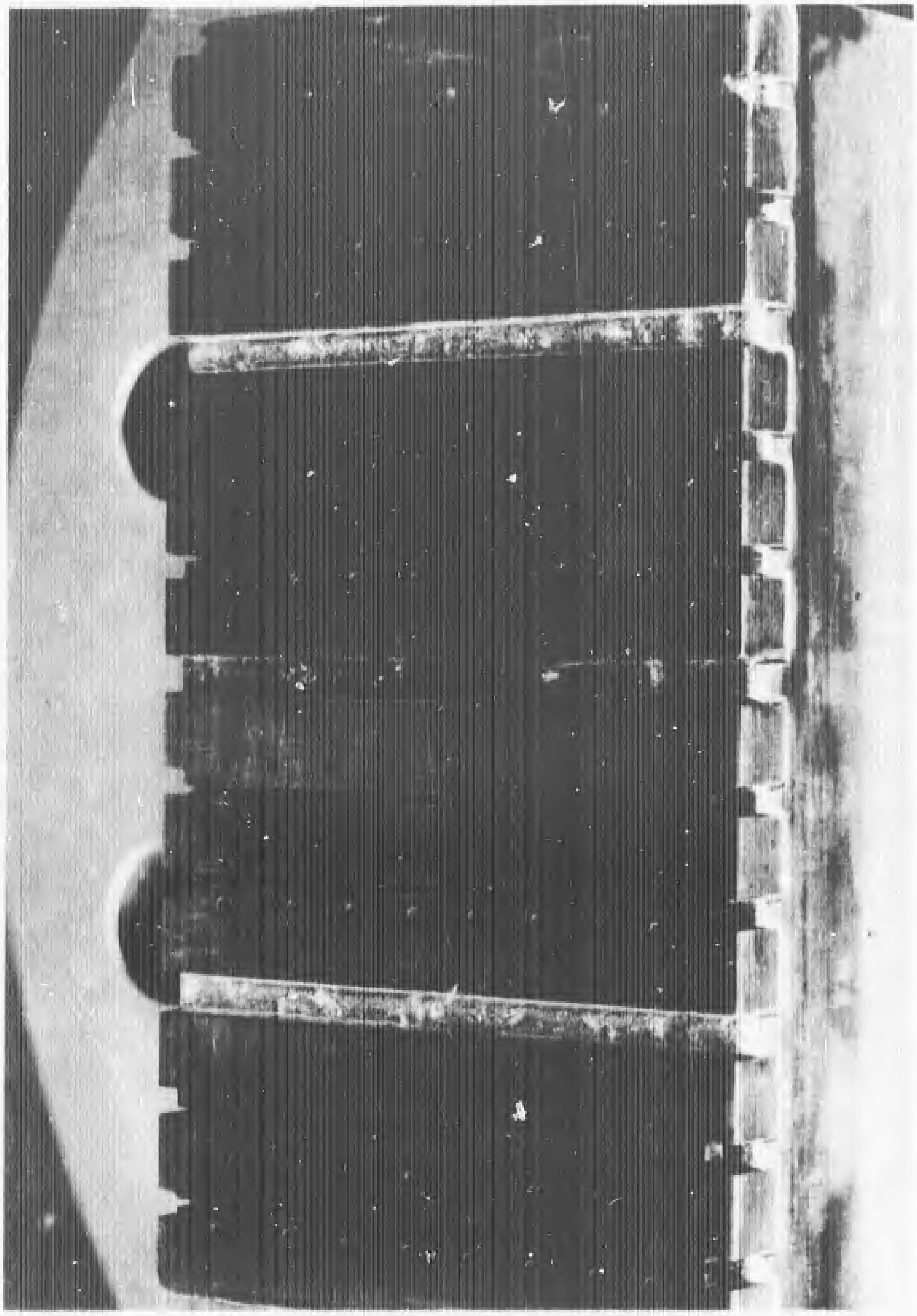

1XV43-5/19/66-SID

Figure 22. Reversed Pattern, 60-Degree Fuel on LOX Fan

to date has consisted of two checkout tests for durability, and preliminary stability evaluation. The checkout durability tests (Table 4) were conducted at 1500 psia in uncooled hardware for run durations of 300 to 600 milliseconds, a period long enough to determine face-cooling characteristics. The durability results show the 60 degree triplet and reverse flow patterns to be acceptable. A preliminary stability evaluation of the 60-degree reverse-flow pattern with a 5.5 grain bomb (200-psia overpressure) showed damping in 1 cycle (2 milliseconds) at 1500 psia.

(C) Next Quarter Effort. During the coming quarter, the injector performance evaluations will be fully implemented. Performance data over the 5:1 throttle range will be acquired as well as heat transfer data for selected injectors. In addition, stability bombing tests will be conducted at selected operating points to verify the stability characteristics over the entire throttle range. Tapoff studies will be initiated to obtain data on tapoff gas composition and temperature control.

250K THRUST CHAMBER NOZZLE INVESTIGATIONS

250K Solid-Wall Thrust Chamber

(C) A 250K solid-wall chamber will be utilized to provide advanced information regarding operational characteristics of a full 360-degree aerospike thrust chamber assembly. Specific items to be evaluated during hot-fire testing are: (1) hypergolic and hot-gas ignition within a compartmental combustion zone, and (2) injector assembly performance, stability, and structural integrity at rated and throttled conditions. In addition, the inherent ruggedness of this type of hardware will make it a valuable tool during test facility shakedown periods.

TABLE 4

2.5K ADP INJECTOR SEGMENT TESTING DURING MAY 1966

Test No.	Injector Description	Test Objective	Test Comments
031	80-degree fuel, reversed pattern	Injector durability evaluation	Chamber pressure was 1560 psia, no injector face erosion
032	60-degree fuel, reversed pattern	Injector durability evaluation	Chamber pressure was 1540 psia, slight injector face erosion in spots, bomb induced instability damped in one cycle

(U) In order for this hardware to provide maximum utility during the early phases of the aerospike chamber development program, the following basic design requirements were established:

1. Inner and outer body chamber contour identical to that of the planned Demonstrator Module Chamber
2. Ease of manufacture and repair
3. Maximum accessibility
4. Hot-fire duration of approximately 0.7 second at full thrust
5. Interchangeability with subsequent chamber hardware
6. Minimum fabrication time and cost

(U) The solid wall chamber is composed of two major units: one consists of the outer section of the combustion chamber and expansion shroud, the other consists of the inner section of the combustion chamber and expansion nozzle. Each unit will be fabricated from 304L CRES steel forgings machined to the desired contour. Three types of material were originally considered for construction of the solid-wall chamber inner and outer bodies (347 CRES steel, 1018 carbon steel, and OFHC copper). For maximum hot-firing duration, OFHC copper was the best selection; however, unavailability of necessary forging sizes precluded its use. Based on experience acquired from the F-1 solid-wall thrust chamber, 1018 steel was eliminated because of severe cracking after repeated operation. The 304L CRES steel was finally chosen over the 347 CRES steel because of lower cost and improved fabricational capabilities. Between machining operations, the combustor bodies will be annealed to minimize residual stresses and ensure dimensional integrity.

(U) Radial and axial positioning of the inner body with the outer body is maintained by attachment to the injector, and is facilitated by shear lips on the inner and outer body interface at the attach bolt circles. The shear lips also provide resistance to thermal and pressure loads encountered during hot firing. The solid combustor bodies provide the required structural restraint for control of the annular throat gap. Thrust loads will be transmitted through the inner chamber body, utilizing an eight-point thrust mounting structure.

(U) To provide sufficient thrust duration, water film cooling is utilized in the throat section. The film coolant is injected through orifices located approximately 1.5 inches upstream of the throat. A 0.750-inch-thick copper inlay is utilized in the throat region. The high thermal conductivity of the copper will provide a margin of safety during operation and provide potential for brief operation without coolant. As a result of Rocketdyne laboratory testing, the method of applying the copper will be by weld buildup utilizing a short-arc machine technique. This method provides a copper deposit with good ductility and thermal conductivity needed to meet heat transfer requirements in the throat region.

(U) The injector to be used with the solid-wall chamber assembly is identical to that planned for subsequent tube-wall assemblies. However, because there is no circulation of fuel in the injector crossover passages during solid-wall chamber testing, two pressurizing ports will be directed into the manifold in this area to maintain an inert gas pressure greater than the chamber pressure across the seals between the injector and chamber bodies.

(U) A transient heat transfer analysis was conducted to determine the maximum gas-side wall temperature in the combustion zone and the throat region of the solid-wall chamber during 1500-psia chamber pressure testing. The analysis at the throat region assumed that the total water coolant is injected through 0.043-inch-diameter orifices with a 0.36-inch centerline spacing and assumed no film-coolant spreading; i.e., 0.043-inch-wide strips. The maximum gas-side wall temperatures in the combustion zone and the throat region are shown in Fig. 23 as a function of test duration. The design water film-coolant flowrate will be sufficient to maintain a liquid

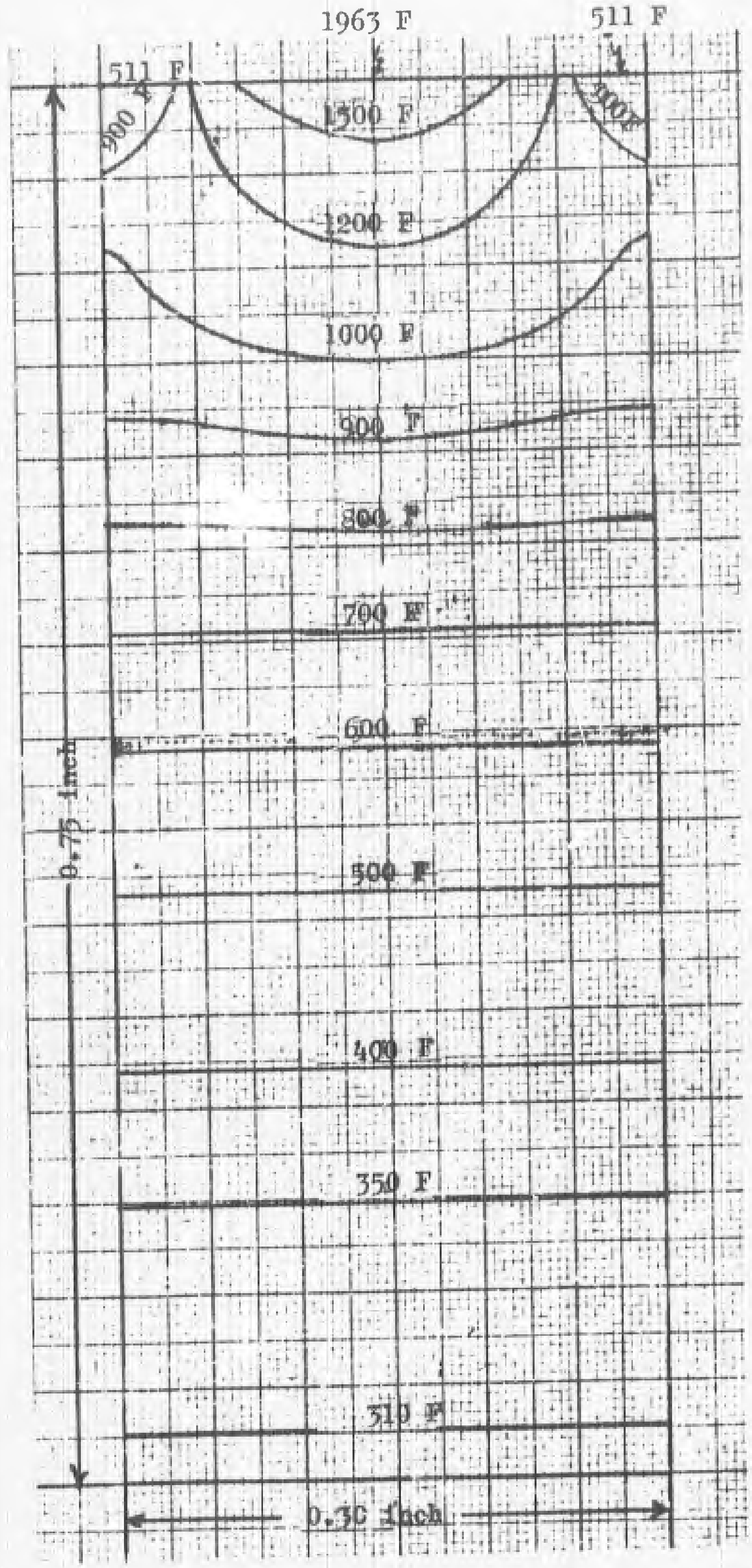

Figure 23. Wall Temperature Distribution in Throat of ADP Water Film-Cooled, Solid-Wall Chamber After 0.72 Second

film over the entire length of surface to be cooled and sustain nucleate boiling from the wall surface in contact with the film coolant while providing a substantial margin on the wall burnout heat flux. Adequate test duration of approximately 0.7 second without chamber erosion in the combustion zone or the throat region appears completely feasible with the present solid-wall design.

(U) The potential of improving preliminary injector performance data during testing with the solid-wall chamber by utilizing a high-speed actuated water valve in series with a multi-holed venturi orifice plate is being evaluated. This concept will allow precise shutoff of the film-coolant flow before termination of the hot-fire test to obtain performance data which will not be complicated by a film-coolant correction factor.

(U) Load cells will be utilized in the thrust system to measure lateral thrust, roll thrust, and main thrust displacement. It is anticipated that analysis of load cell data will provide information such as throat concentricity and data relative to any movement of the inner and outer chamber bodies.

(U) Analytical and design efforts pertaining to the solid-wall chamber have been completed. The detailed drawings are undergoing final review in preparation of release for manufacturing.

250K TUBE-WALL THRUST CHAMBER

Structure

(C) A complete design review of the structural arrangement for the 250,000-pound-thrust tube-wall thrustors was conducted during this report period. A number of concepts for the experimental thrust chamber were reviewed in terms of ability to meet overall program objectives, fabrication cost and schedule, braze inspection and realloying potential, and dimensional control. All factors appeared to be equally weighted except schedule and cost which dictated a final solution of a structure based on solid forgings (Fig. 24). This choice was then thoroughly analyzed from both a stress and thermal standpoint.

(C) The area of stress analysis can be summarized through examination of Fig. 25, 26, and 27, which show the particular forces of concern on the structure. The forces result in moment, tension, and shear loads on the bolts connecting the inner and outer bodies and the injector. Primary pressure force restraint is in inner and outer body hoop stress retention. Thermal loading accounts for only a small percentage of the available distortion forces.

(C) The temperature distribution of the tube backup structures is shown in Fig. 28 after a 5-second chilldown, using 60 R hydrogen, and after a 5-second firing, the 350 R coolant bulk temperature corresponding to the outer body and the 200 R to the inner body throat region. An initial temperature of 100 F was assumed for the backup structure, which would be somewhat conservative if the engine were fired in winter. A complete stress and thermal tolerance analysis of the throat gap shows that the throat gap will be 1.09 to 1.14 times the assembly dimension at 1500 psia.

Nozzle Contour

(C) Aerodynamic Analysis. Rocketdyne's method for the design of aerodynamic spike nozzles employs a double expansion shroud design coupled with the ideal spike design procedure. The method consists of starting with an ideal spike exit flow field and computing the nozzle required to give this flow field. A double expansion shroud is then designed to match this flow field at some point downstream of the throat. Depending on the point in the flow field where this match is made, mean throat flow angles (β^*) from approximately 5 to 90 degrees can be obtained. The advantage of this type of design

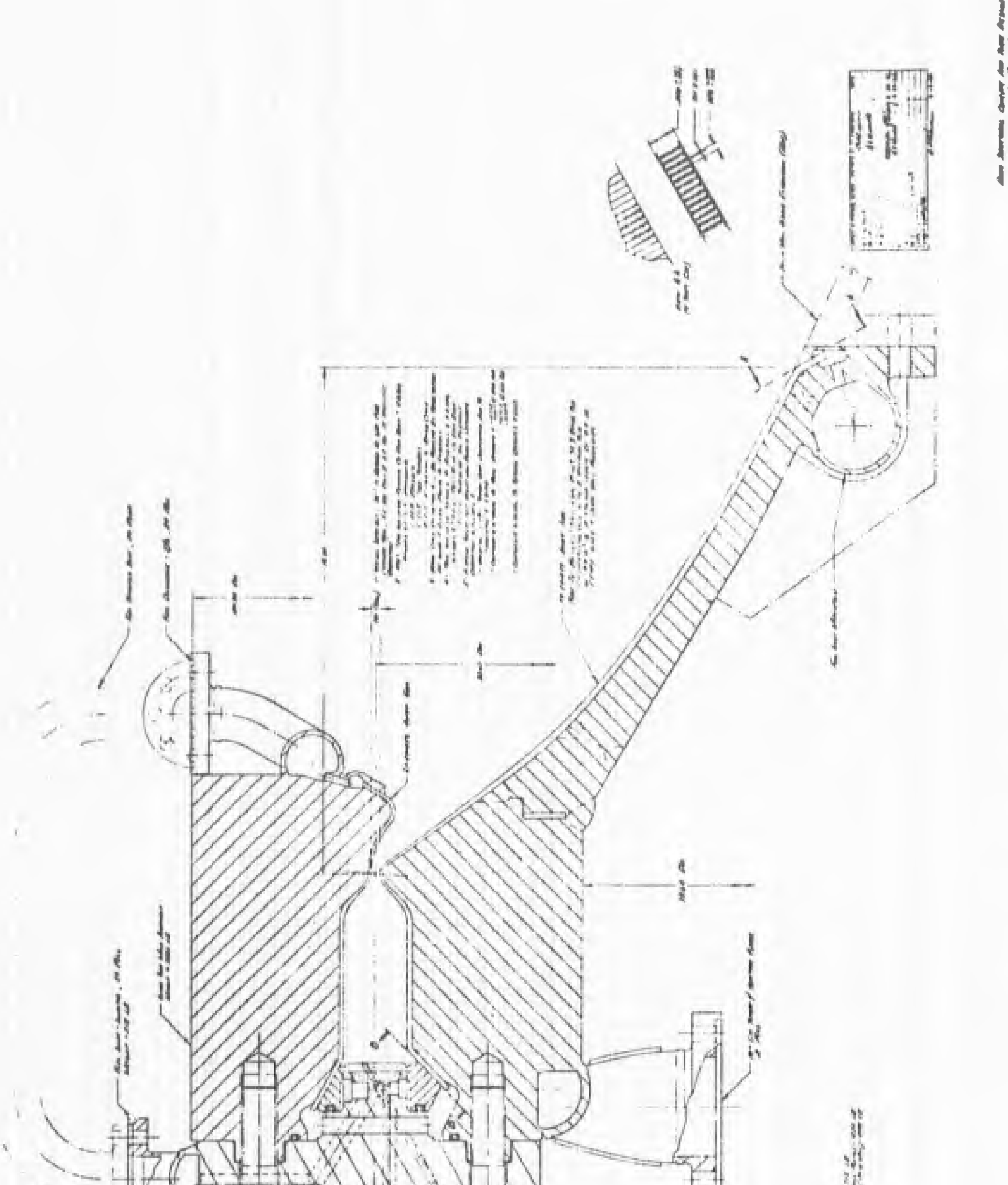

Figure 24. 250K Tube-Wall Thrust Chamber

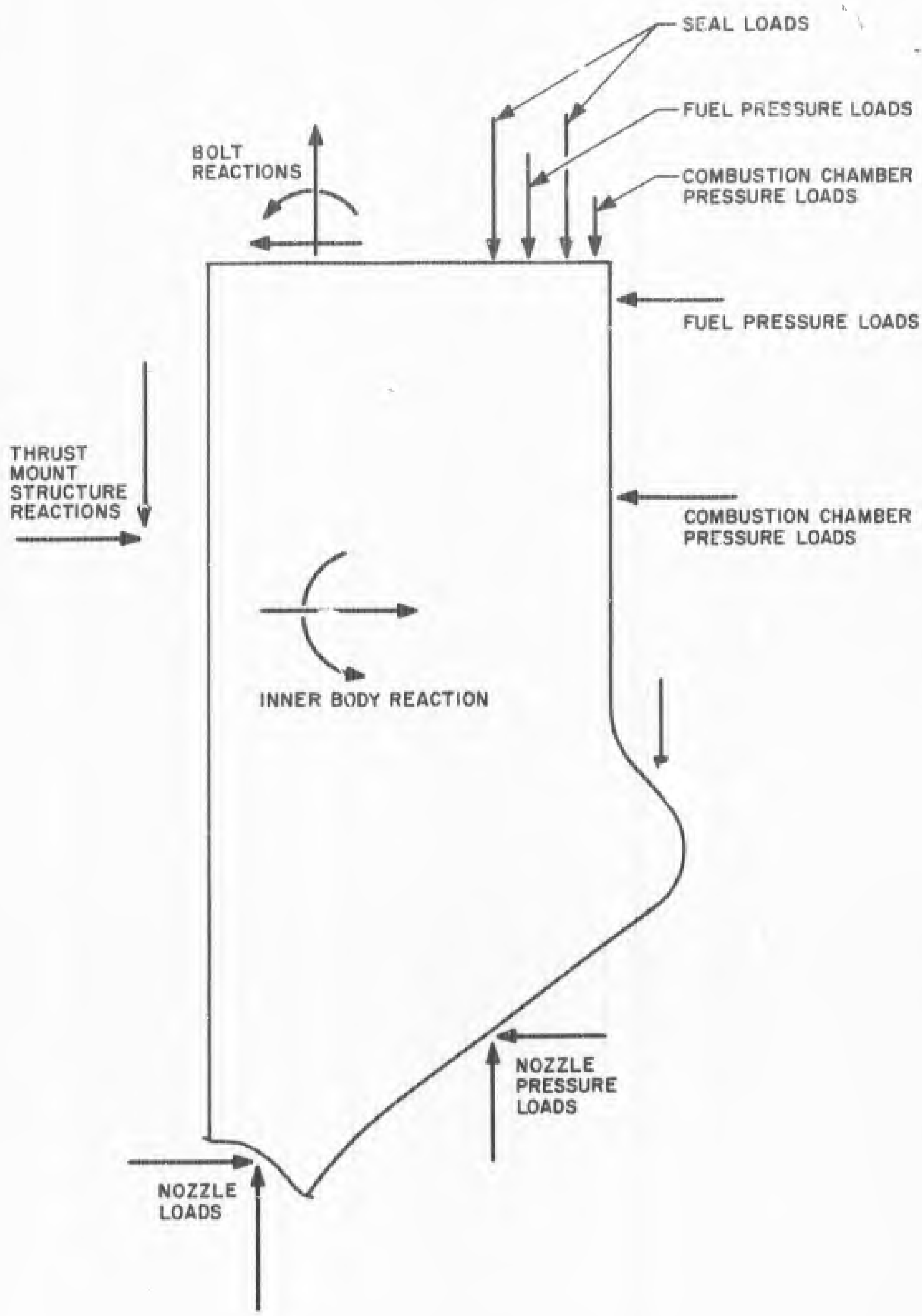

Figure 25. Forces Acting on Inner Body

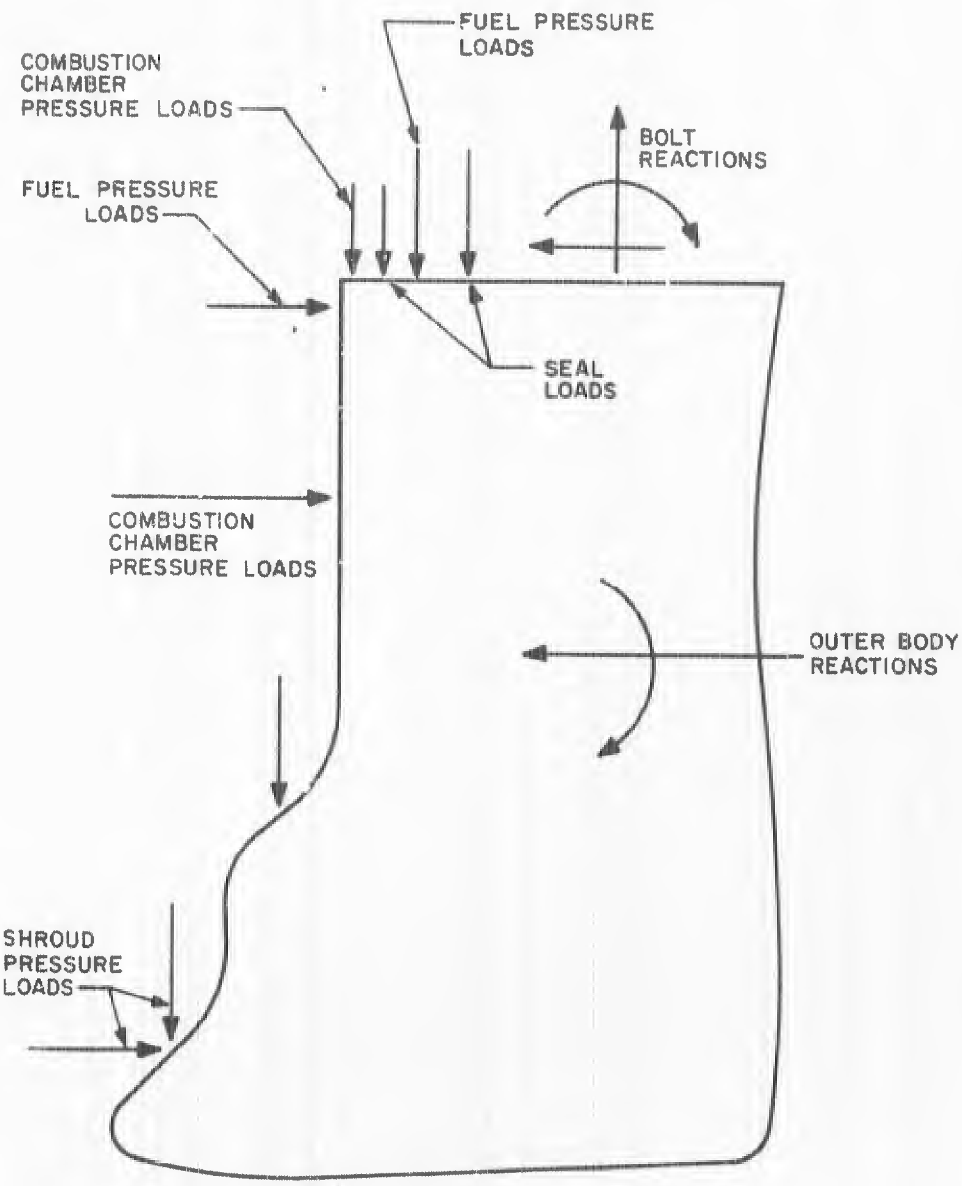

Figure 26. Forces Acting on Outer Body

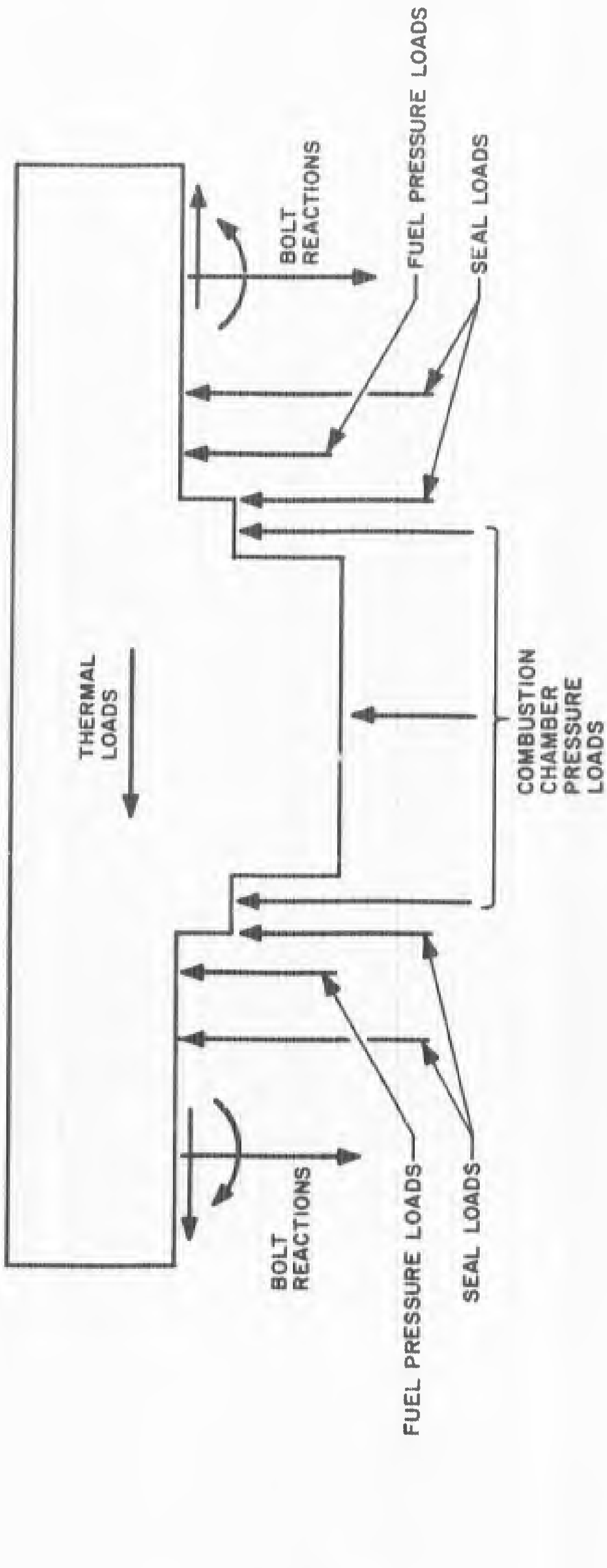

Figure 27. Forces Acting on Injector

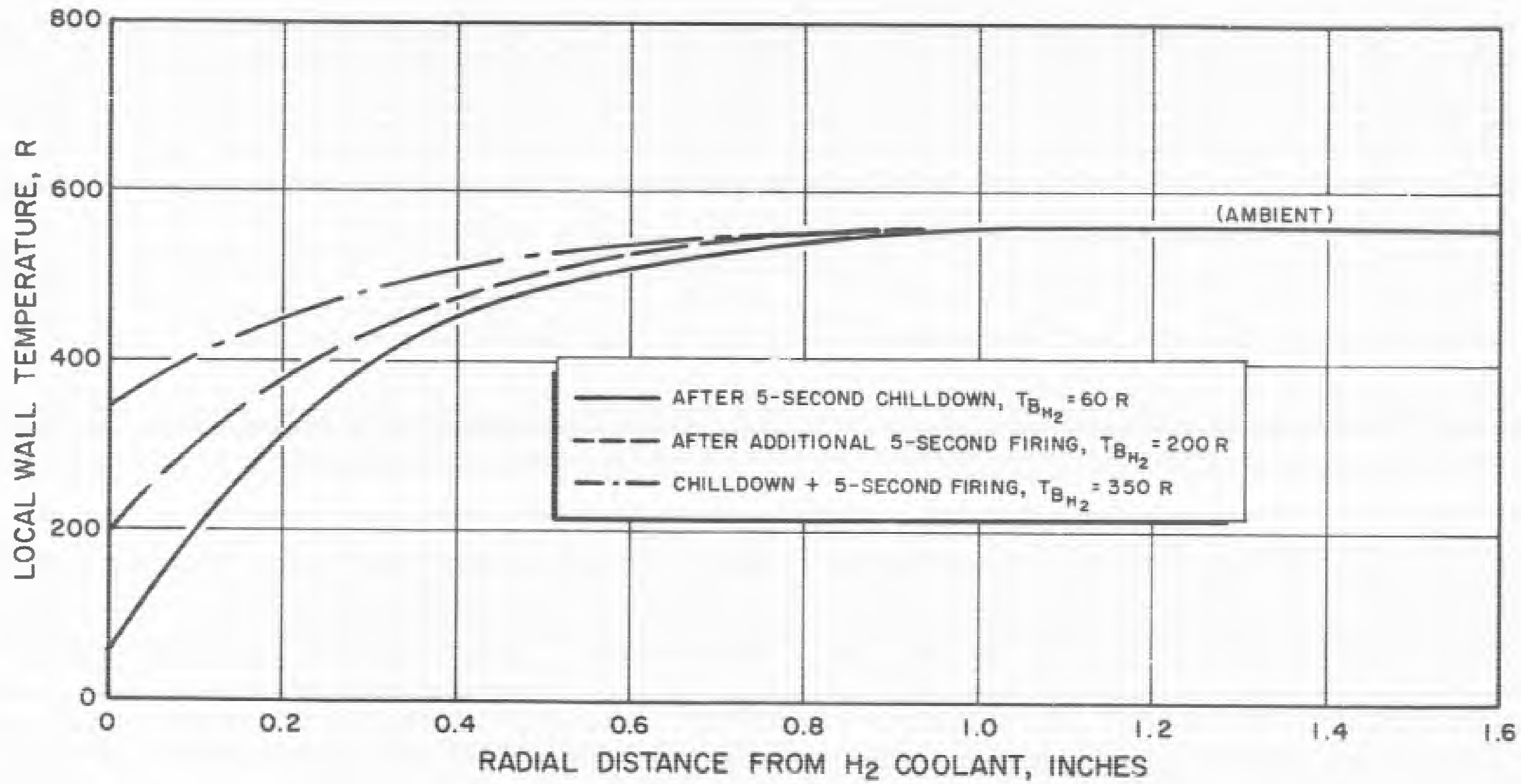

Figure 28. Transient Wall Temperature Profile (250K Solid Structural Backing for Tube Bundle, 304 L Stainless Steel)

is that a nozzle with nearly axial throat flow and a throat design suitable for maximum regenerative cooling can be obtained.

(C) Contours designed for mean throat flow angles of 4.5, 14.5 and 23 degrees are shown in Fig. 29. As the throat approaches an axial flow condition, the length at the shroud and overall length of the nozzle are increased. However, as the flow field downstream of the shroud approximates the flow field of an ideal spike, the nozzle performance is the same for all shroud lengths, provided that the spike length (positive X/RL, as shown in Fig. 29) is the same. The criterion to maintain a near-axial mean throat angle resulted in the selection of the β = 4.5-degree design.

(C) Shroud Length Reduction Study. As an alternate approach to obtaining reduced shroud lengths and maintaining the nearly axial mean throat flow angle, the shroud on the β = 4.5-degree nozzle was truncated to various lengths, as shown in Fig. 30. The method of characteristics nozzle analysis programs was used to generate the primary flow field and compute nozzle performance for each reduced shroud length case examined. Base pressure calculations were made to determine the change in base pressure for 1.7-percent secondary flow for a range of shroud lengths. The results of the reduced shroud length performance calculations for vacuum performance are shown in Fig. 31.

(C) The nozzle performance (exclusive of base pressure contributions) results (Fig. 31) clearly indicate that the full-length shroud nozzle was not an optimum configuration for vacuum operation; otherwise, any change such as reduced shroud length should produce a loss in thrust coefficient. The nozzle thrust coefficient shows a maximum for shroud axial length, X/R_t = 0.3. The base pressure was found to remain nearly constant from full length to X/R_t = 0.3, then drop for further reductions in shroud length. These performance results indicate that a reduced shroud length of X/R = 0.3 should be selected (Fig. 31) to obtain the optimum vacuum performance.

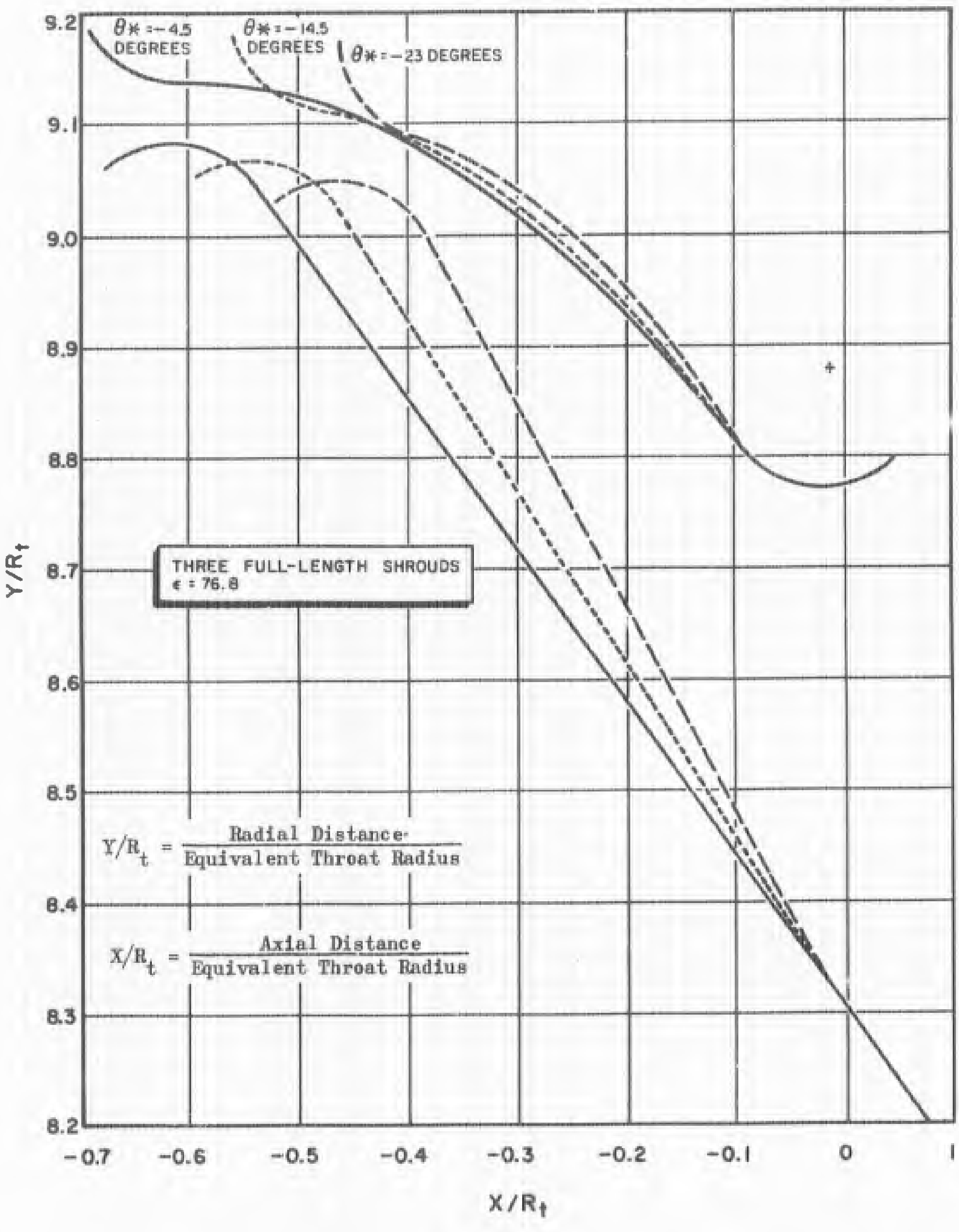

Figure 29. ADP Nozzle Contour

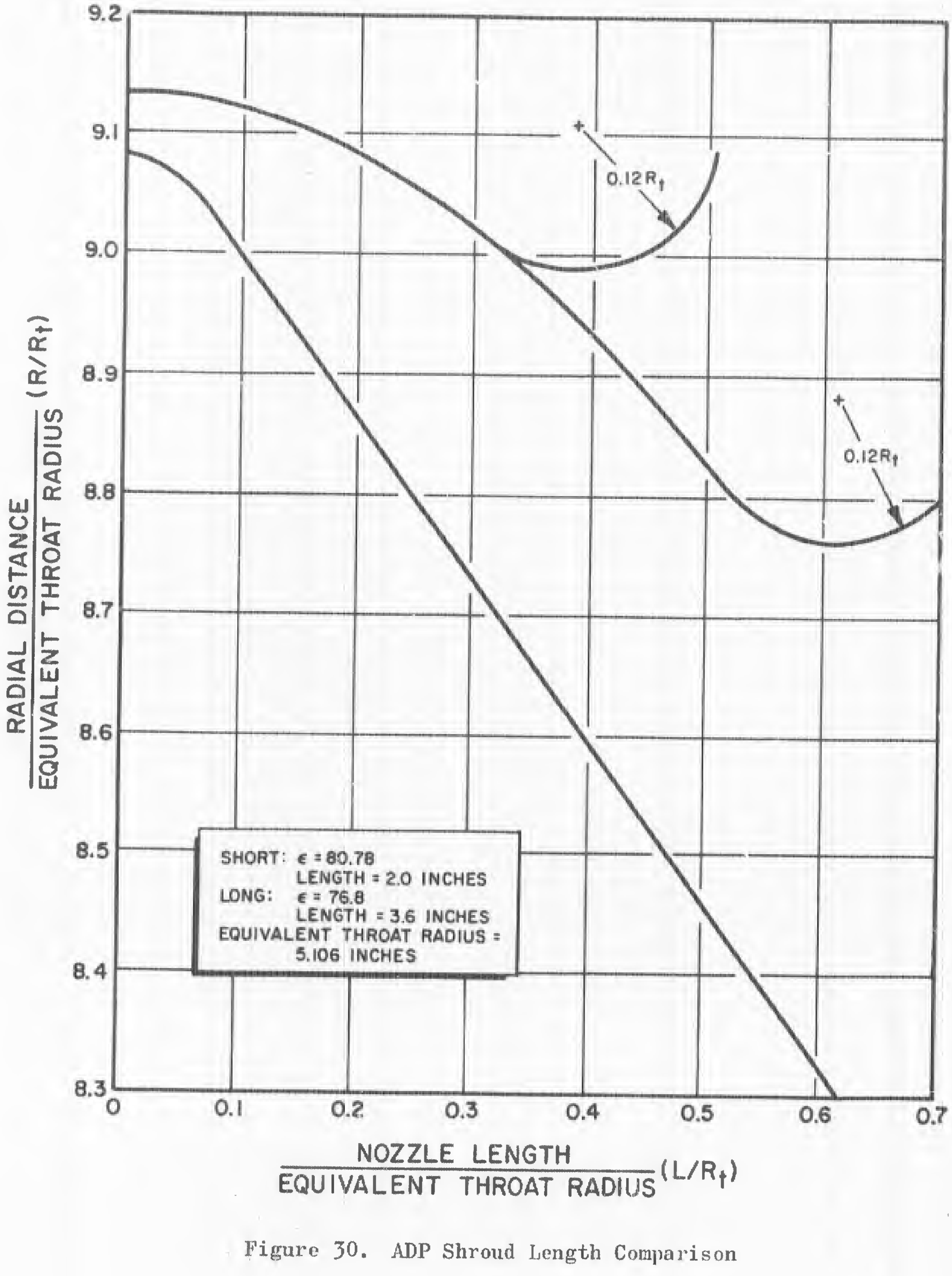

Figure 30. ADP Shroud Length Comparison

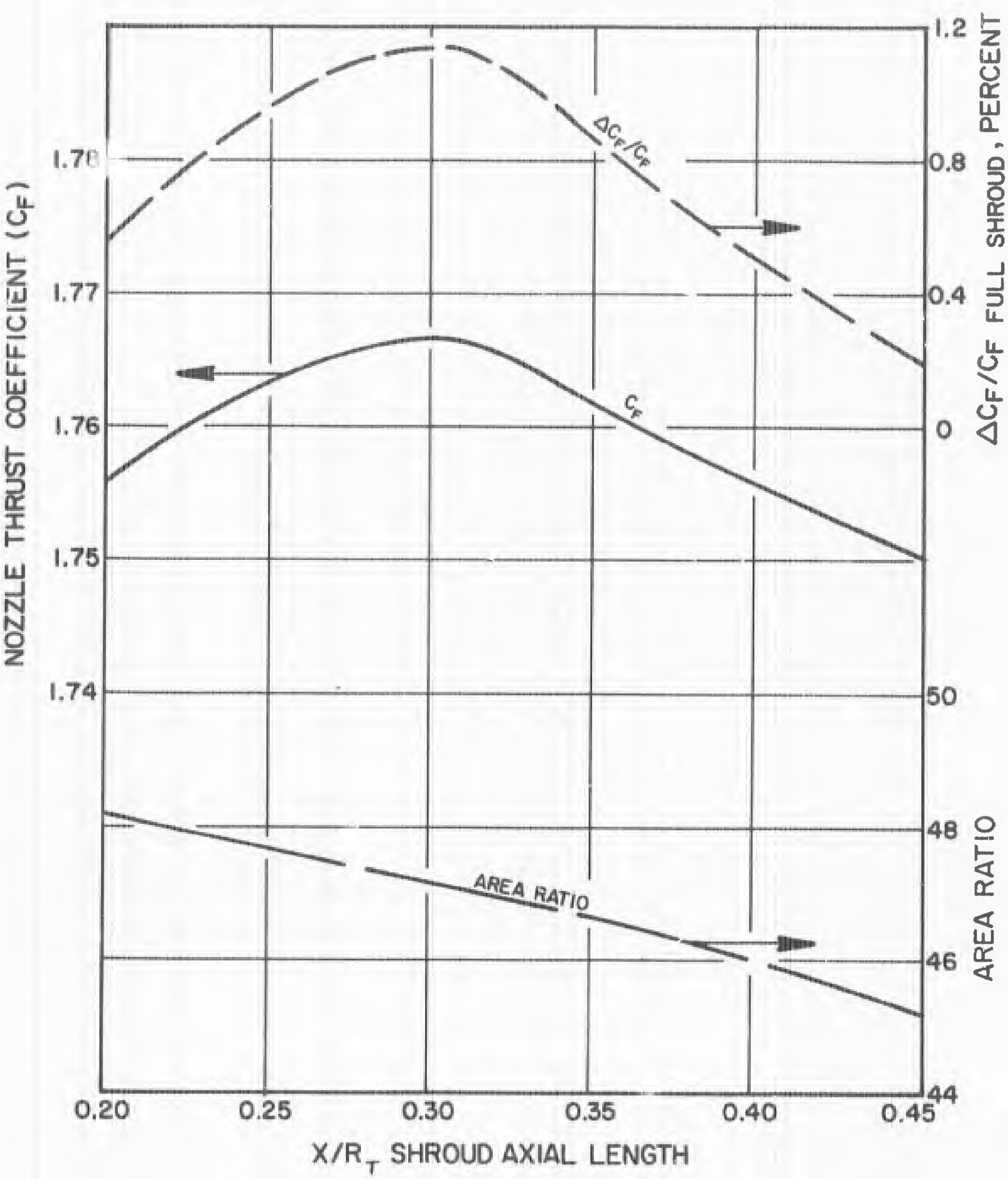

Figure 31. Performance vs Shroud Length

(C) <u>Low-Pressure Ratio Performance Analysis</u>. In addition to the vacuum analysis, a low-pressure ratio analysis (of the mean flow angle design of 4.5 degrees) of the effects of shroud length was also investigated. The shroud lengths (Fig. 30) corresponding to the vacuum optimum and full length were analyzed.

(C) Outer shroud and spike nozzle wall pressures are shown in Fig. 32 for the full-length shroud design, for chamber pressures of 300, 600, and 1500 psia operating at test stand altitude and vacuum conditions. The increases in the low-pressure wall pressure are caused by a recompression effect. Typical flow patterns for an aerospike nozzle operating at low-pressure ratios are shown in Fig. 33. For the ideal case, as shown in Fig. 33 (View B), expansion waves from the shroud are reflected from the contour as expansion waves and are then reflected from the free-jet boundary as compression waves. At high-pressure ratios, the compression waves from the free-jet boundary do not intersect the contour; however, at low chamber-to-ambient pressure ratios (Fig. 33), the compression waves from the free-jet may intersect the contour, resulting in recompression. The chamber-to-ambient pressure ratio below which there will be recompression on the contour is a function of the area ratio, the ratio of specific heats, percent length, the nozzle contour, and the geometry of the cowl. However, if the flow field downstream of the shroud does not approximate that of an ideal spike, the recompression waves coalesce into a shock wave (Fig. 33, View A). The strength of this shock wave depends on the nozzle flow field departure from that of the ideal spike.

(C) A comparison between the wall pressure profiles resulting from the short and full-length shrouds is shown in Fig. 34. The pressure rise associated with the long shroud is less severe than that of the short shroud. Although it is not apparent from the data given in Fig. 34, the wall pressure profiles associated with the long shroud are the result of isentropic recompression, while the short-shroud wall pressure profiles are the result of the impingement of strong oblique shocks on the nozzle wall.

CONFIDENTIAL

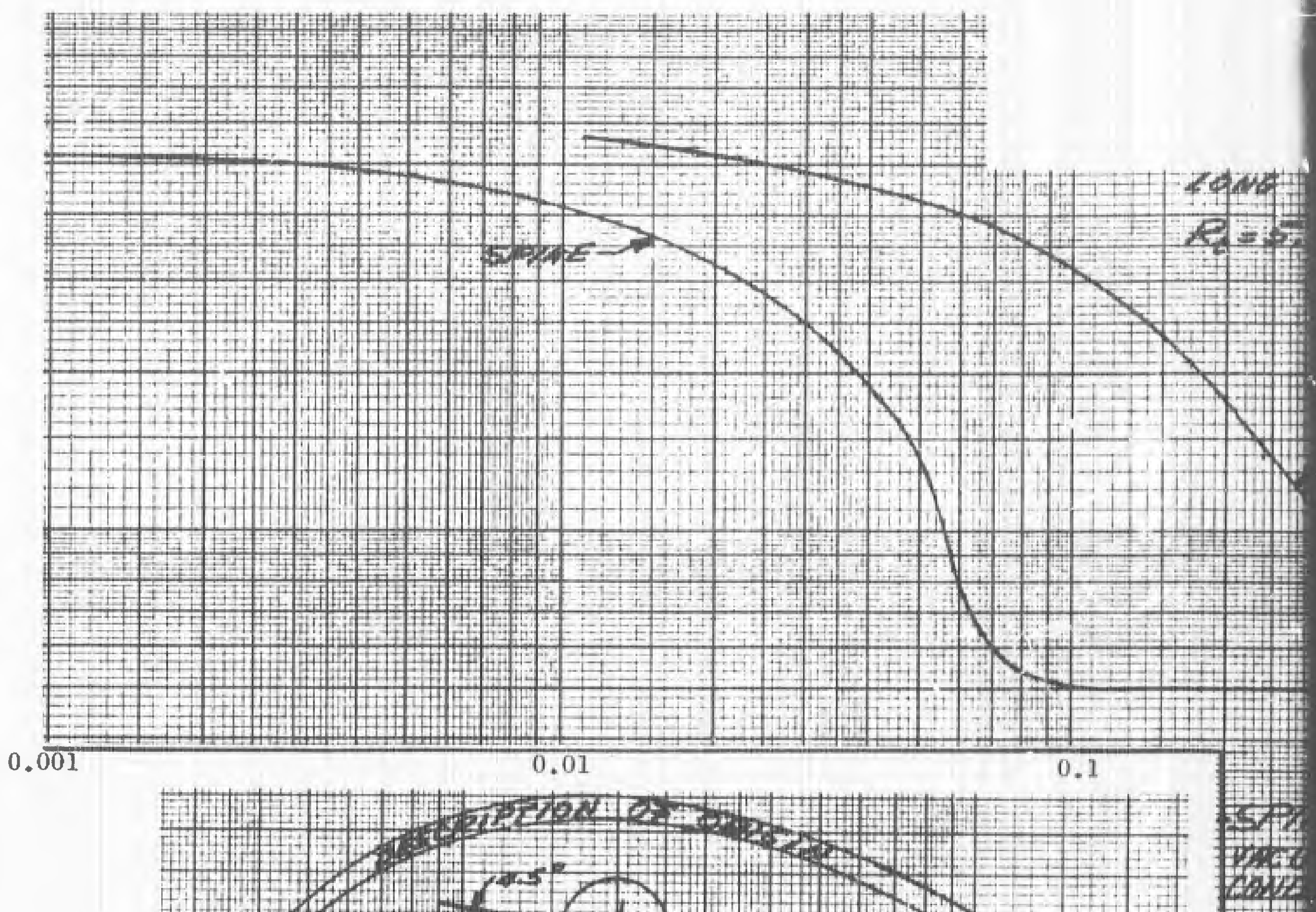

1

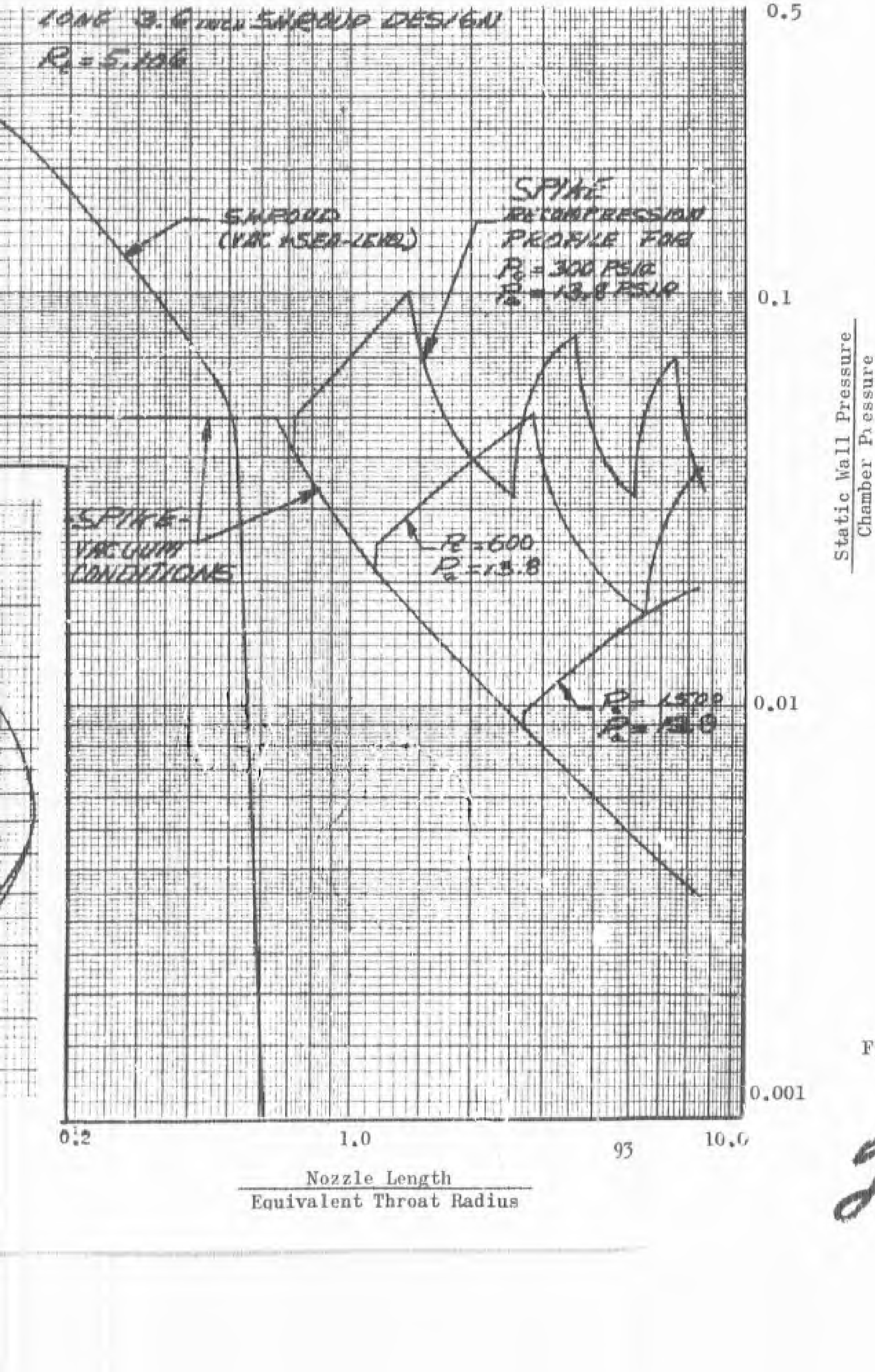

Figure 32. Shroud and Spike Pressure Profiles

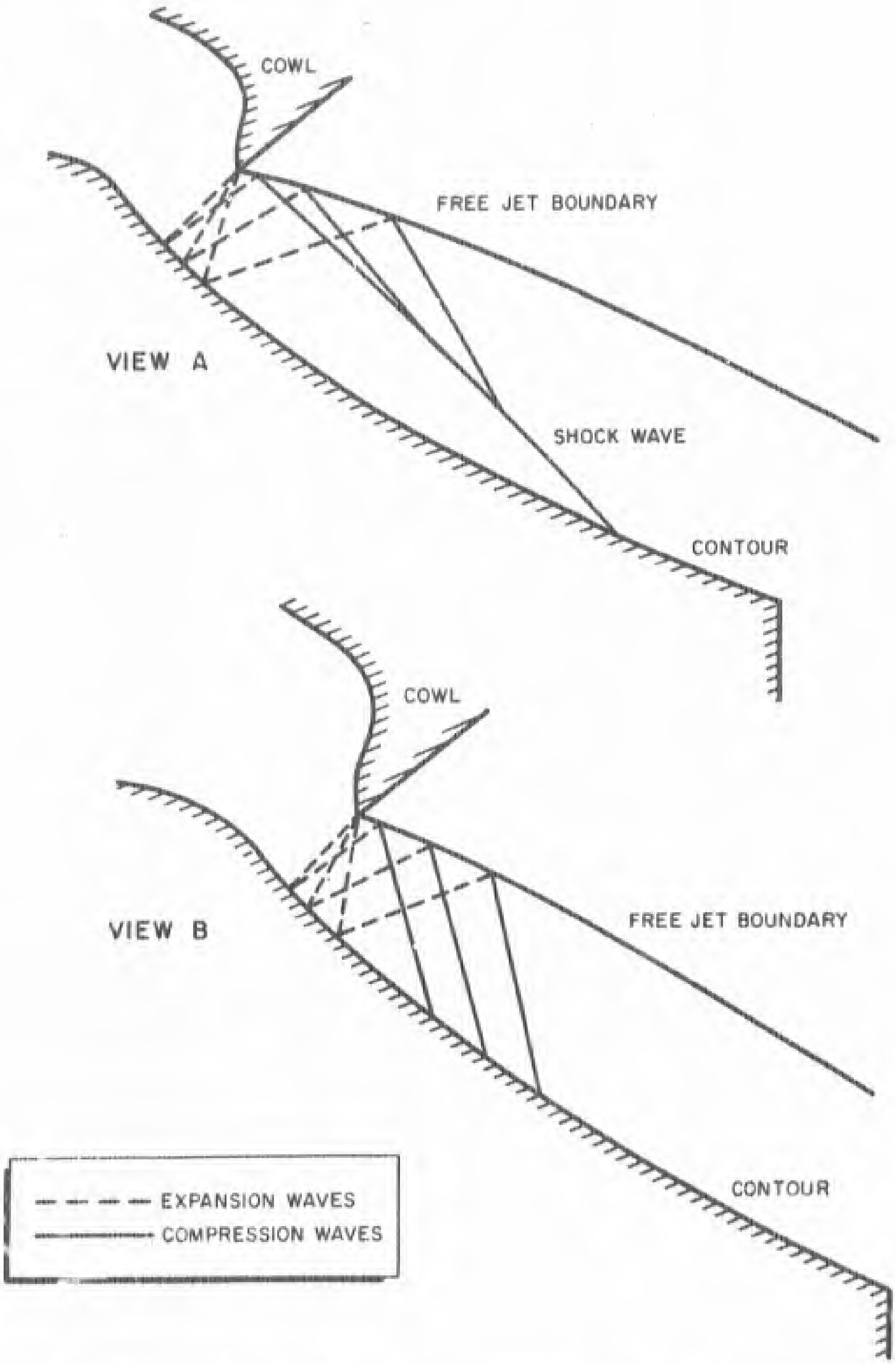

Figure 33. Expansion and Compression Waves in Aerodynamic Spike Nozzle Flow Field Analysis

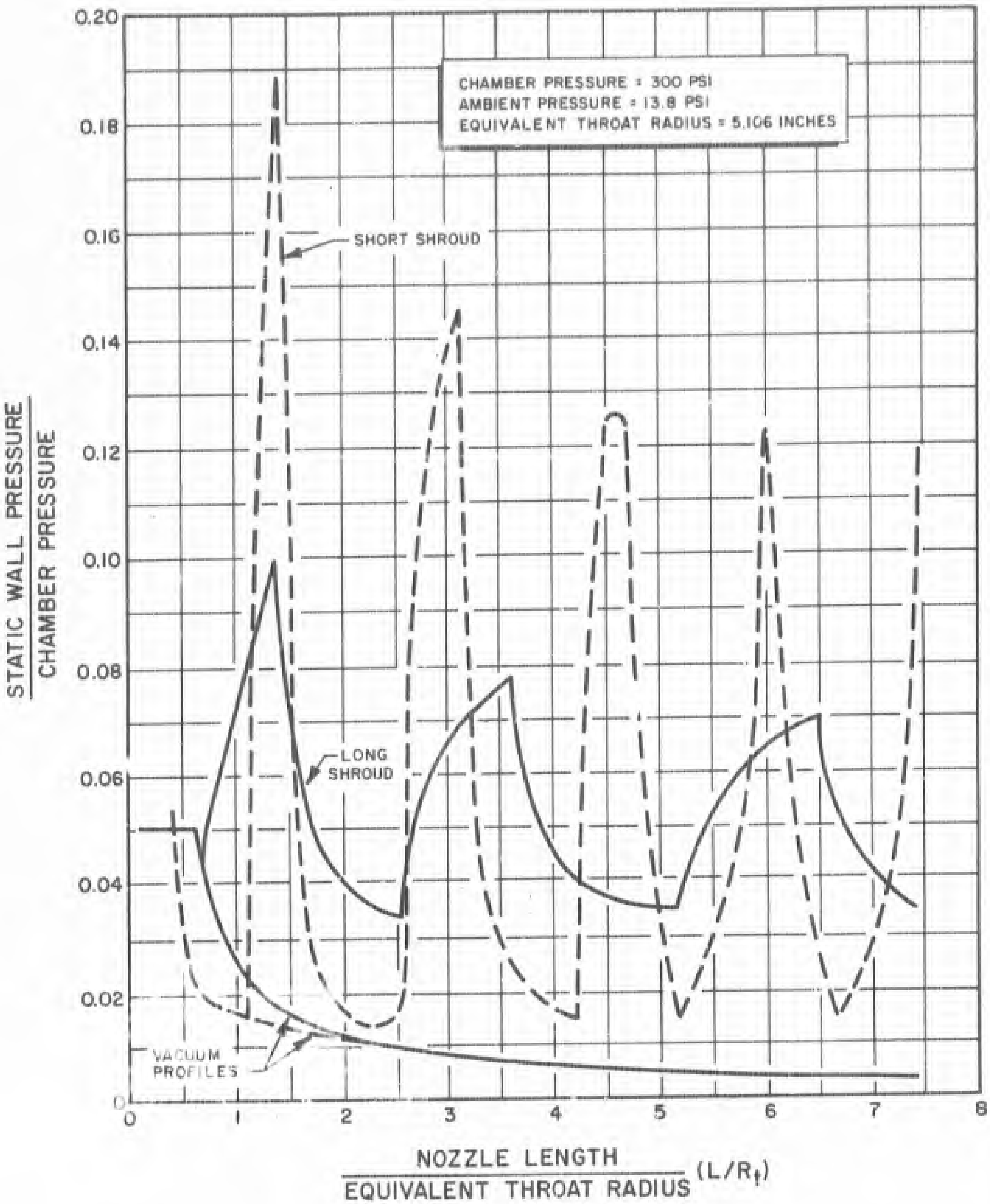

Figure 34. ADP Sea Level Centerbody Spike Wall Pressure Profiles

(C) In a supersonic flow field bounded by a solid surface, the interaction of a shock wave with a boundary layer causes the attending pressure rise to propagate in the subsonic portion of the local boundary layer. For a shock of sufficient strength (i.e., pressure ratio), the adverse pressure rise may cause the boundary layer to separate from the wall upstream of the shock impingement location, and reattach on the wall downstream of the shock. One criterion dictating the shock strength necessary to cause separation of a turbulent boundary layer has been derived by A. Mager.* The peak pressure along the wall, for both attached and separated boundary layer conditions, is equal to the pressure rise across the shock. The Mager criterion has indicated that, while local separation could result from the reduced shroud case, the full-length shroud should not separate.

(C) Although the short-shroud design shows a performance advantage over the long-shroud design at vacuum operation, the long-shroud nozzle has been selected based on good performance at all altitudes and heat transfer considerations.

<u>250K Tube Design Considerations</u>

(U) During the past quarter, the regeneratively cooled tube bundle was designed and parametric analysis conducted to determine the cooling requirements in the throat region, this being the region of highest flux. In addition, specifications were written to check each tube dimensionally and for flow characteristics.

(C) The cooling circuit, consisting of a single up-pass on the inner body and a single downpass on the outer body, was chosen to optimize the heat transfer requirements for the engine. This cooling circuit results in a maximum curvature enhancement effect to the coolant heat transfer coefficient. Typical predicted heat transfer operating conditions are shown for the inner body of the experimental chamber in Fig. 35. The analytical and some experimental heat flux data are

*Technical Consultant (Ref. 3)

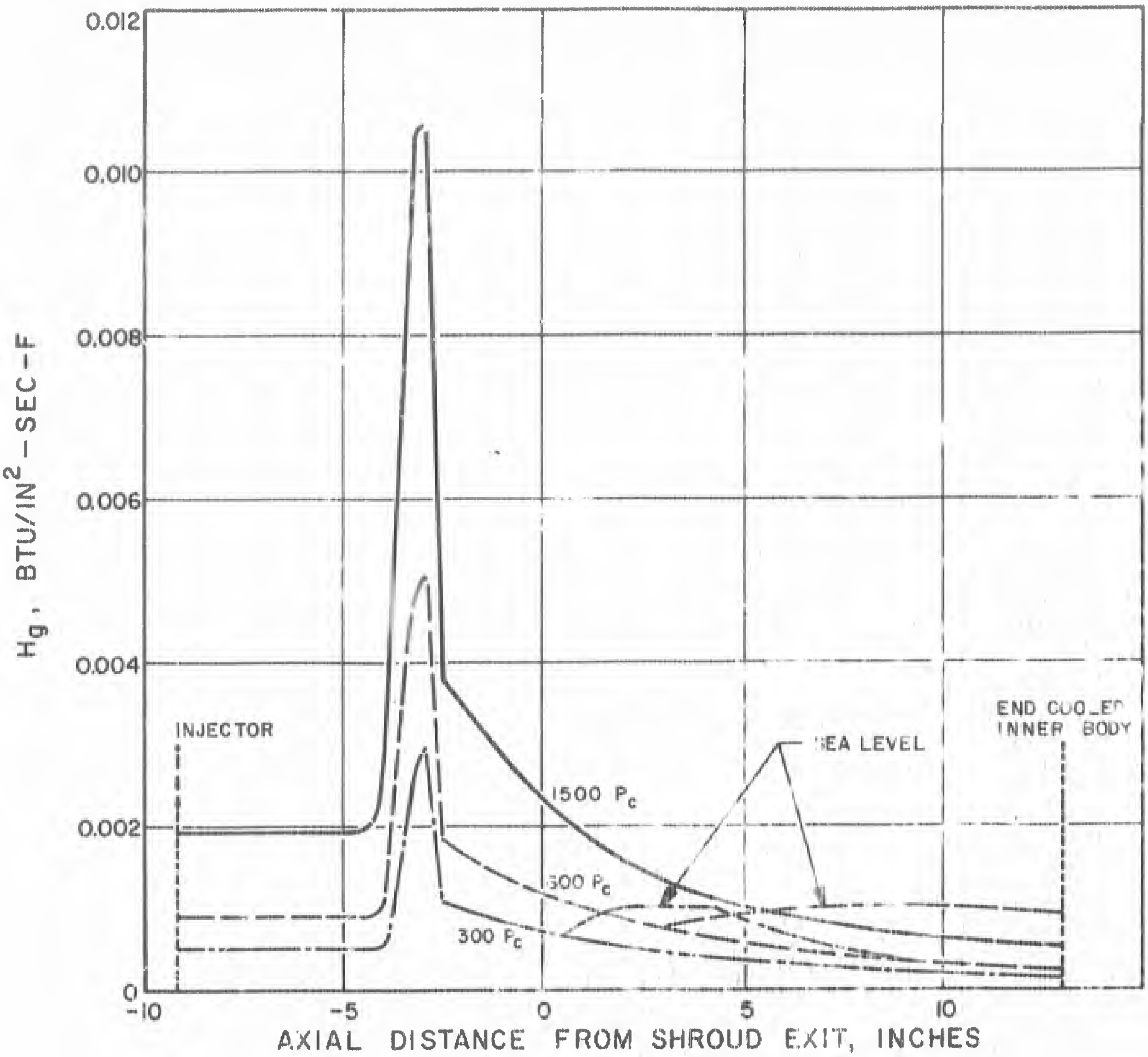

Figure 35. Theoretical Nozzle Gas-Side Heat Transfer Profiles at Vacuum and Sea Level Conditions (250K Experimental Chamber, MR = 6.0)

shown in Fig. 36. These heat fluxes were used to determine the tube-wall temperature, shown in Fig. 37, at a chamber pressure of 1500 psia and a mixture ratio of 6.0. Also shown are the curvature enhancements used for the analysis, based on previously obtained, Rocketdyne experimental, electrically heated, curved-tube data for hydrogen and coolant mass velocities resulting from the chosen tube taper.

(C) Throttled operation should not pose a heat transfer problem at vacuum conditions. However, at sea level, high local wall pressure increases exist locally on the nozzle wall because of aerodynamic shock patterns. Resulting wall temperatures at sea-level operation will be determined in the next quarter using the anticipated gas-side heat transfer coefficient distribution for the inner body.

(U) To define accurately the operating characteristics of the ADP thrust chamber, knowledge of the GH_2 cooling capability in a small-diameter, tapered, and curved tube must be determined experimentally. Accordingly, an experimental effort was undertaken to determine the heat transfer capabilities of gaseous hydrogen in an actual ADP thrust chamber tube sizing having a configuration of current interest. A tapered and curved, 347 stainless-steel tube was fully instrumented for recording local temperatures and local power generation within the tube wall.

(U) A total of 14 heat transfer runs were conducted. The first 11 runs were conducted without a restrictor downstream of the test section, so that the GH_2 flow was sonic at the minimum area portion of the tube and supersonic in the subsequent diverging section. The first four of these supersonic runs were conducted with hydrogen inlet temperatures of approximately 160 R. The remaining 7 runs were conducted at inlet temperatures of 230 to 450 R. The inlet pressures were in the range of 1000 to 1900 psia.

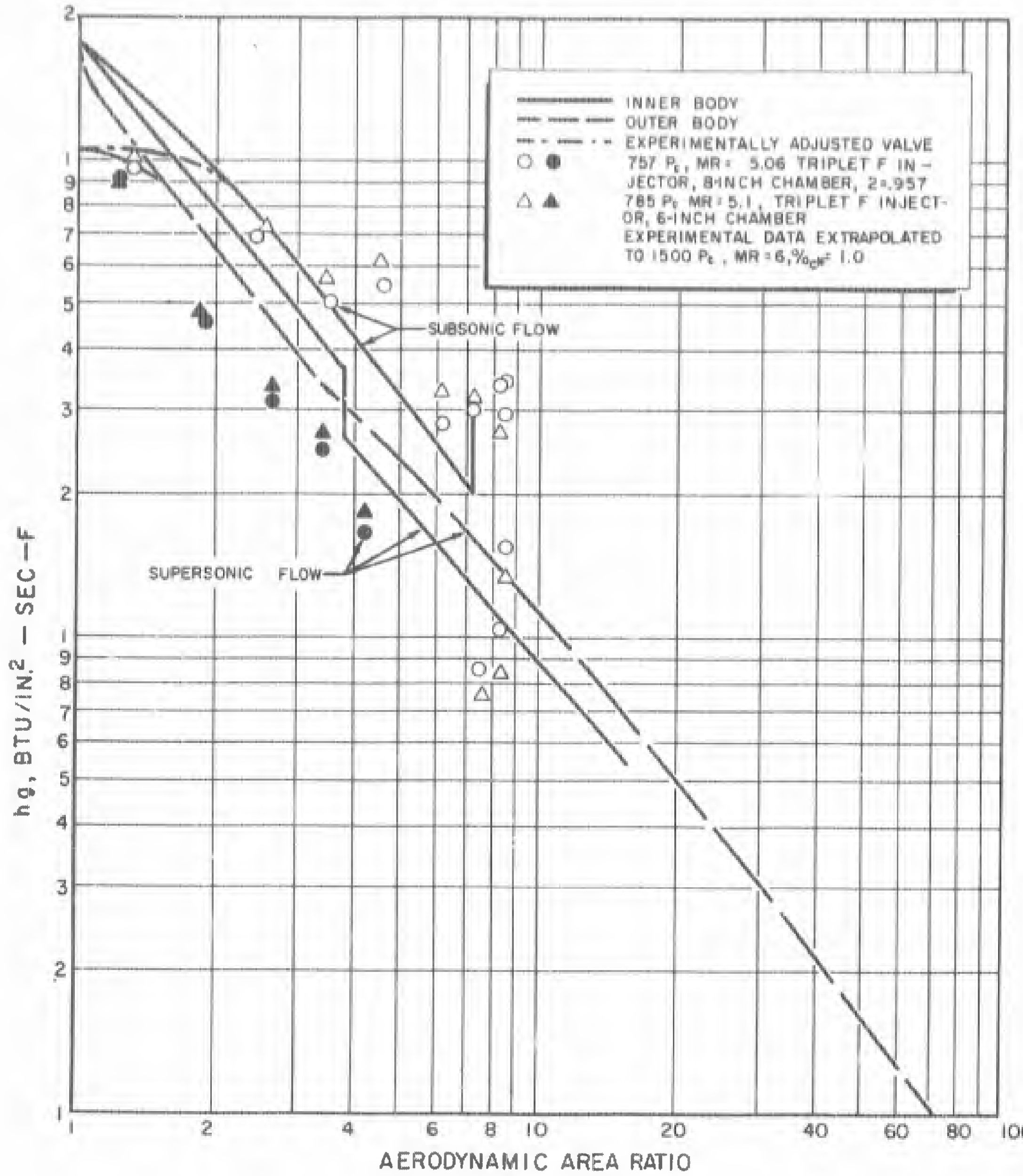

Figure 36. Theoretical and Experimental Heat Transfer Coefficients, 250K Experimental Thrust Chamber Breadboard Engine, O_2/H_2, MR = 6.0, P_c = 1500 psia, Vacuum Operation

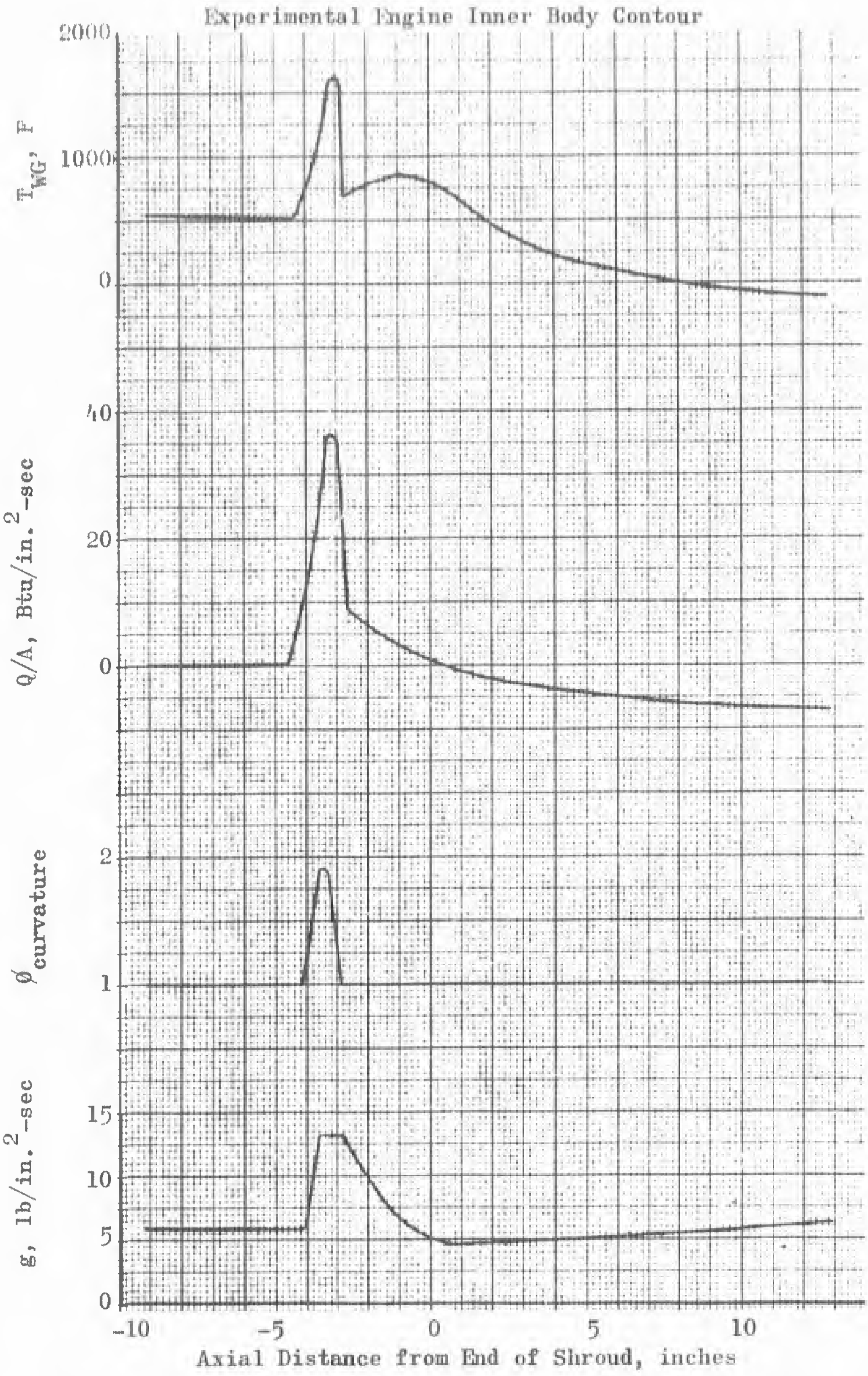

Figure 37. Gas-Side Wall Temperature, Heat Flux, Curvature Enhancement, and Coolant Mass Velocity Profiles, (O_2/H_2, P_c = 1500 psia, MR = 6.0, W_c = 150 lb/sec)

(U) At the conclusion of this series of runs, a downstream flow restrictor was installed in the system to ensure subsonic flow conditions throughout the test section. This also provided an exit pressure comparable to thrust chamber injection pressures.

(U) Three heat transfer runs were conducted with the downstream restrictor. During an attempted fourth test, an inadvertent power surge overloaded the electrically heated test section, causing a test section rupture with a subsequent termination of experimental activities.

(C) The 347 stainless-steel test section is schematically shown in Fig. 38. Before forming, the tube had an outside diameter of 0.156 inch and a wall thickness of 0.008 inch. After forming, the tube had the outside dimensions given in Fig. 38.

(U) The temperature of the outside surface of the heated test section was measured at 16 axial stations, each station having two chromel-alumel thermocouples attached on diametrically opposite surfaces of the tube, as shown in Fig. 38. Because d-c current introduced through the copper bus bars provided the electrical heating power, the 32 thermocouples were electrically insulated from the wall to prevent a possible emf pickup. The fully instrumented test section is illustrated in Fig. 39.

(U) Twelve Inconel taps were used, being closely spaced to accurately monitor the power consumed in each increment because of the varying cross-sectional area.

(U) The ranges of experimental variables covered by this investigation are listed below:

Inlet Bulk Temperature, R	152 to 451
Exit Bulk Temperature, R	283 to 731
Inlet Pressure, psia	1043 to 1868
Inlet Mach Number	0.059 to 0.159
Exit Mach Number	0.117 to 2.66

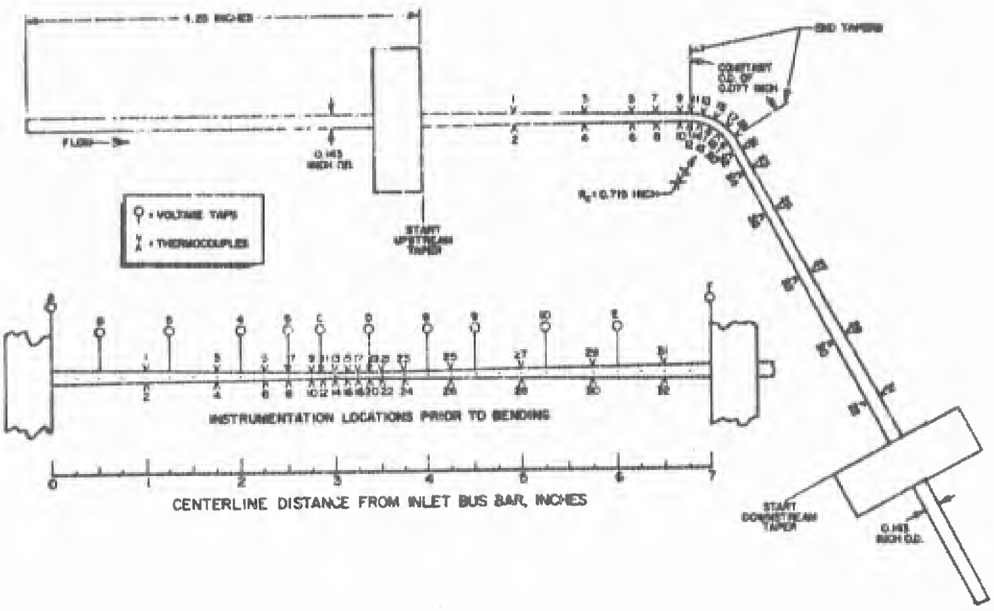

Figure 38. Simplified Curved Gaseous Hydrogen Heat Transfer Test Section (66-1)

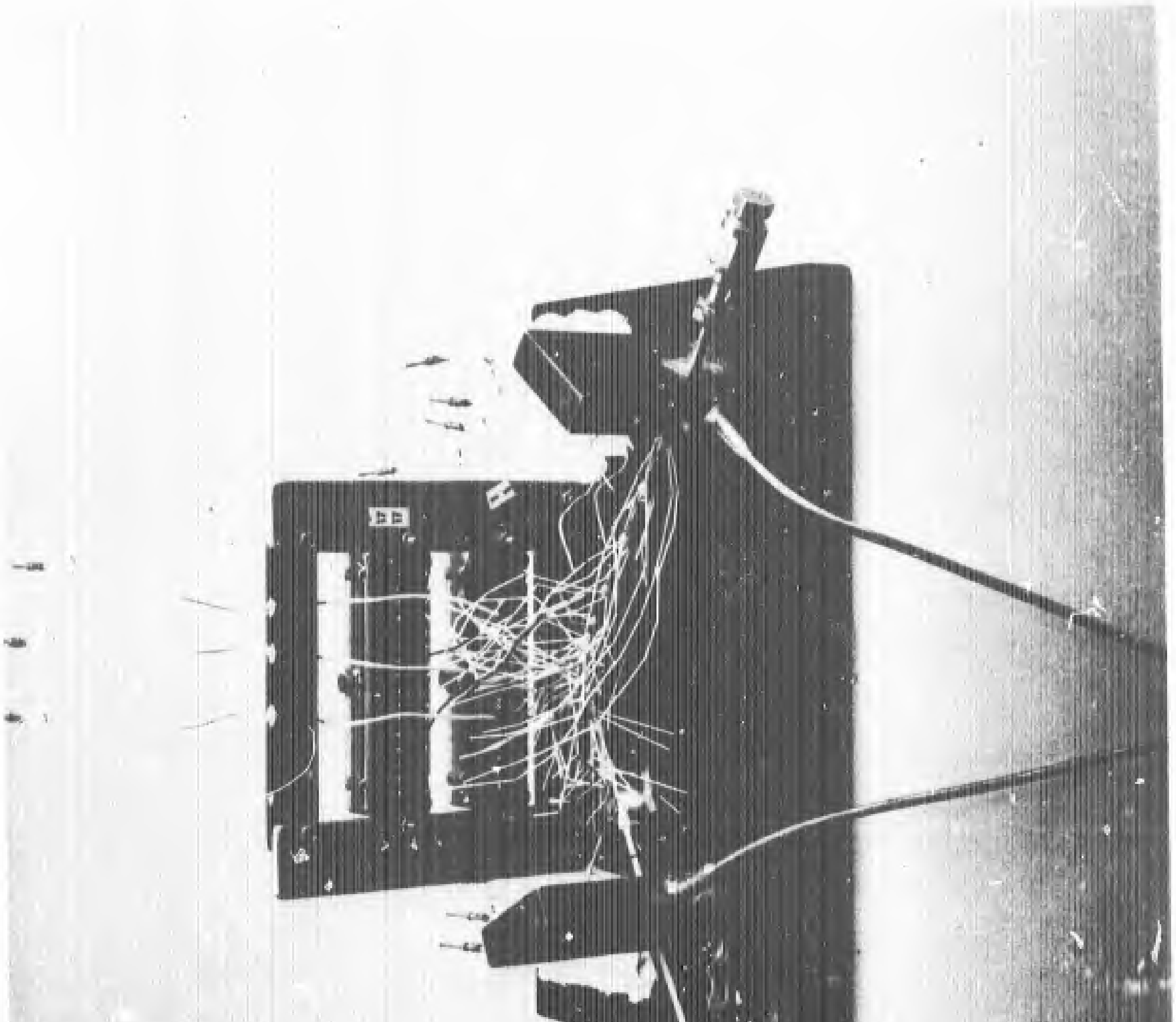

5AF23-4/11/66-S?

Figure 39. Instrumented Tapered and Curved Stainless Steel Simulated ADP Tube Used for Tube Curvature Heat Transfer Studies

Throat Region Heat Flux, Btu/in.^{2}-sec	
Inside Surface of Curvature	12.09 to 30.08
Outside Surface of Curvature	11.05 to 26.7

(U) For design purposes, it is pertinent to compare the heat transfer data with the prediction of the straight-tube correlation of McCarthy and Wolf currently in use at Rocketdyne.

$$Nu = 0.025\ Re^{0.8}\ Pr^{0.4}\ (T_w/T_b)^{-0.55} \tag{1}$$

(U) For each measuring station, Eq. 1 was solved for a straight-tube value of h using the ID, Re and (T_w/T_b) at the station considered. The actual heat transfer data were then compared to the computed straight-tube values in the form of curved-to-straight ratios of heat transfer coefficients.

(U) All supersonic flow runs displayed similar temperature and heat transfer profiles. Therefore, three such runs are adequate for comparison with those obtained at completely subsonic conditions. Heat transfer results for the supersonic flow runs are presented in Fig. 40 where the ratio of heat transfer coefficients is:

$$\frac{h_o}{h_s} = \frac{\left[(Nu/Pr^{0.4})\ (T_w/T_b)^{0.55}\right]}{0.025\ Re^{.8}} \tag{2}$$

(U) Equation 2 relates a measured outside-curvature heat transfer coefficient, h_o, to a computed value for a straight tube having the ID, Re and T_w/T_b of the measuring station considered. The (h_o/h_s) ratio is shown to be between 1.4 and 1.6 for the inlet straight portion of the heated test section. Apparently, the heat transfer enhancement in this section is caused by entrance effect and/or an unknown taper effect. At the onset of curvature (axial length of 3 inches), the ratio increases rapidly to a value slightly above

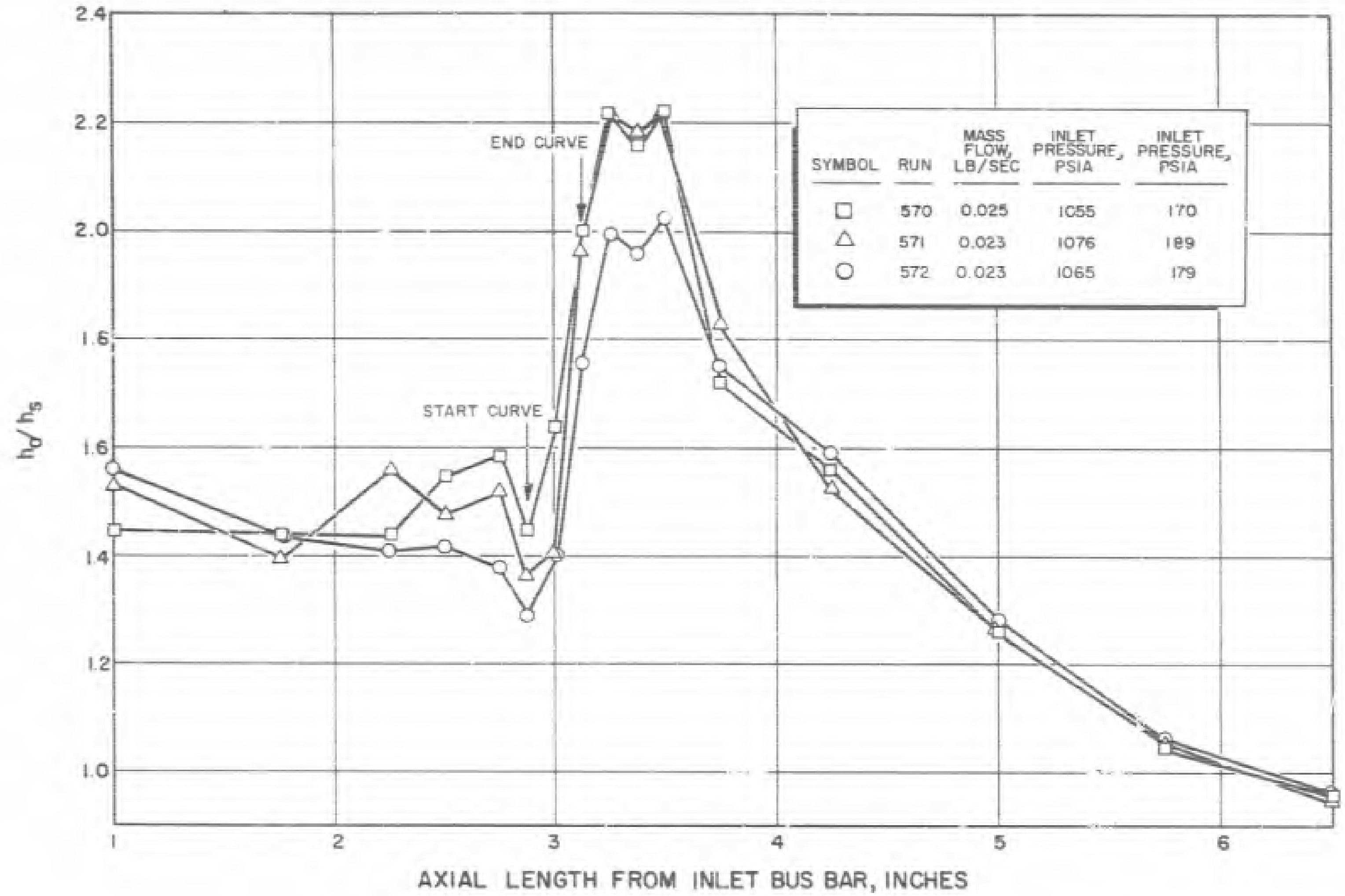

Figure 40. Heat Transfer Results for Supersonic Exit Conditions; Ratio of Outside-Curvature Heat Transfer Coefficient to Straight-Tube Prediction

2.2 for two of the runs and over 2.0 for the other run. At the end of curvature, which is also the beginning of the diverging section, the ratio h_o/h_s drops off rapidly to a value below 1.0 at the exit. In the diverging section, the flow is apparently supersonic and undergoing shocks and/or separation towards the exit. This could explain a value lower than one at the exit.

(U) A similar presentation of the same heat transfer ratio for the subsonic flow conditions is given in Fig. 41. Again, a relatively high ratio is observed for the inlet straight portion of the heated test section. However, in this case the ratio tends to decrease with distance as entrance effects normally do in straight-tube flow.

(U) Previous experiments with liquid hydrogen and gaseous hydrogen show the entrance effect to be a function of x/D only. A ratio of x/D for a tapering area is not readily defined. However, for a critical x/D value of 30 the axial length for entrance effects would have to be between 1.9 and 4 inches based on the extremes of the diameters (maximum and minimum). For the ADP test section, the flow passage is tapered for the first 2.75 inches and then encounters the curved portion. Therefore, it appears that even if the inlet portion were of straight tubing (not tapered), entrance effects would still be prominent when the bulk fluid entered the curved portion of the tube. The curved portion is approximately 6 diameters in length and through this length the heat transfer ratio, h_o/h_s, increases from a value of approximately 1.4 to a value slightly over 2.2. The maximum enhancement is achieved directly after the end of curvature at an axial length of 3.5 inches and reaches a value on the order of 2.2.

(U) As shown, the enhancement does not fall off as rapidly as in the supersonic flow experiments, and near the end of the test section has a value of approximately 1.3 for all subsonic runs conducted. In fact, the peak heat transfer enhancement in the subsonic case persists more than 3/4 inch downstream of the end of curvature. In the supersonic case, no enhancement was noted beyond 1/4 inch of the end of curvature.

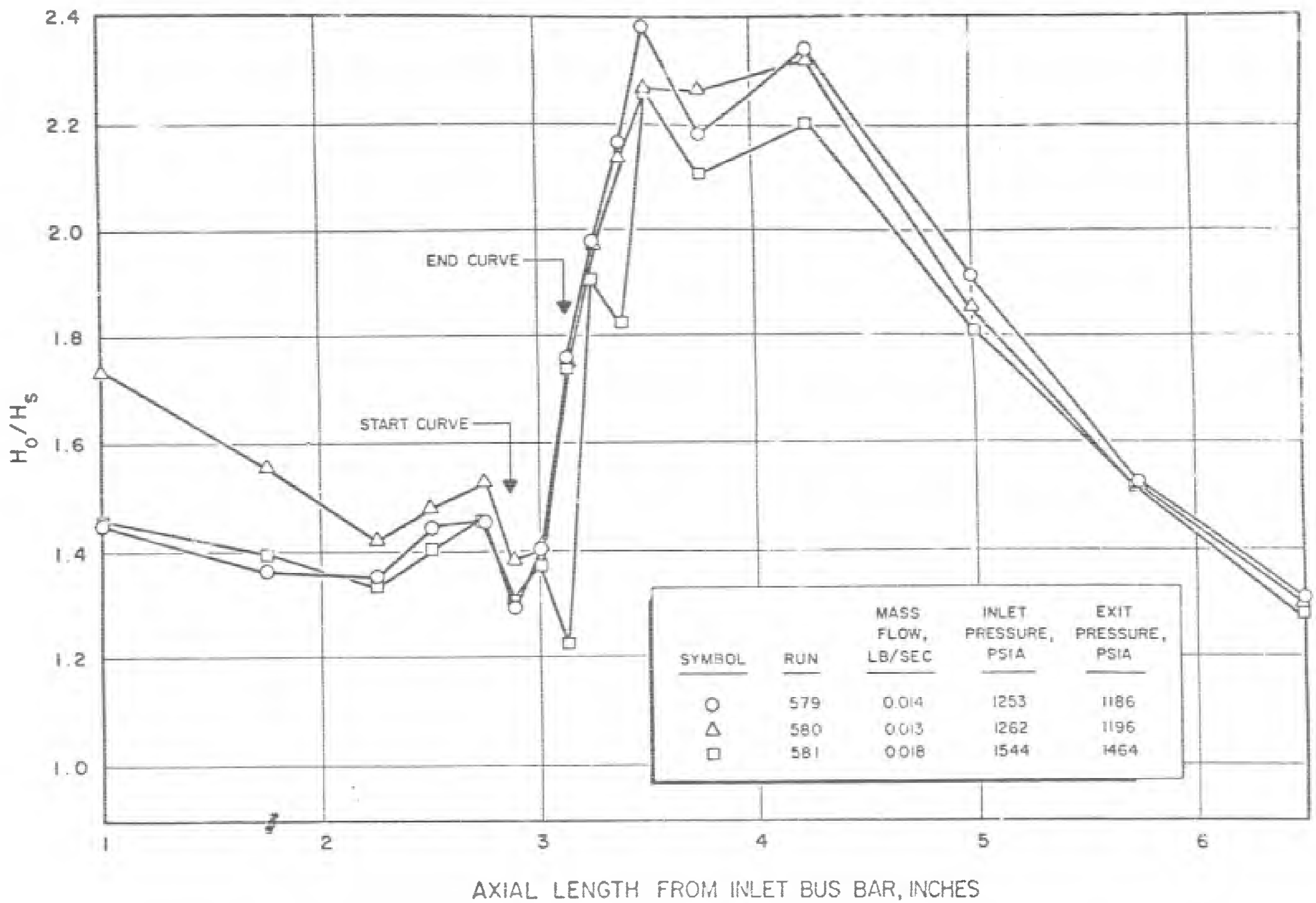

Figure 41. Heat Transfer Results for Subsonic Flow Conditions Throughout the Test Section: Ratio of Outside-Curvature Heat Transfer Coefficient to Straight-Tube Prediction

(U) Another unknown, with the h_o/h_s ratios, is the wall roughness effect (if any). Only a small absolute roughness (ϵ) will result in a significant relative roughness (ϵ/D), because D is only 0.062 inch at the minimum point. To the degree that a wall roughness effect did exist in these experiments, it is lumped in the reported h_o/h_s values.

(U) Experimental data obtained from tubes of larger diameter but approximately the same radius of curvature-to-tube radius were used for the ADP tube design. Comparison of the most recent experimental results with those used for the ADP tube design is presented in Fig. 42. The most recent experimental data reflect a 20- to 40-percent safety margin in the current design technique.

(U) Tolerance Effects. A sensitivity analysis of the theoretical maximum side wall temperature in the inner body throat region, in terms of the coolant mass velocity and the tube tolerance specifications, was conducted. The tube thickness is seen to have an appreciable effect (Fig. 43) of approximately 80°F increase per 0.001 increase in wall thickness. Coolant mass velocity has a somewhat lesser effect, with a 10-percent change producing a 50°F change in wall temperature. The roughness band represents about 25°F, while the effect of the tolerance in tube height is only about 10°F.

(U) As a result of this sensitivity analysis, tubes with a wall thickness over 0.008 inch will be sorted out. This, along with the use of air-flow calibration to sort tubes by their resistance (principally minimum flow area), will permit stacking a chamber with minimum tube-to-tube flow variation.

(U) Air Flow Checks. A reasonable rapid means of nondestructive testing to determine the tube inside dimensions and surface characteristics is to flow fluid through the tubes. Water was initially considered but was found to be too insensitive to changes in minimum tube cross-section area. For example, a change of 10 percent in the minimum

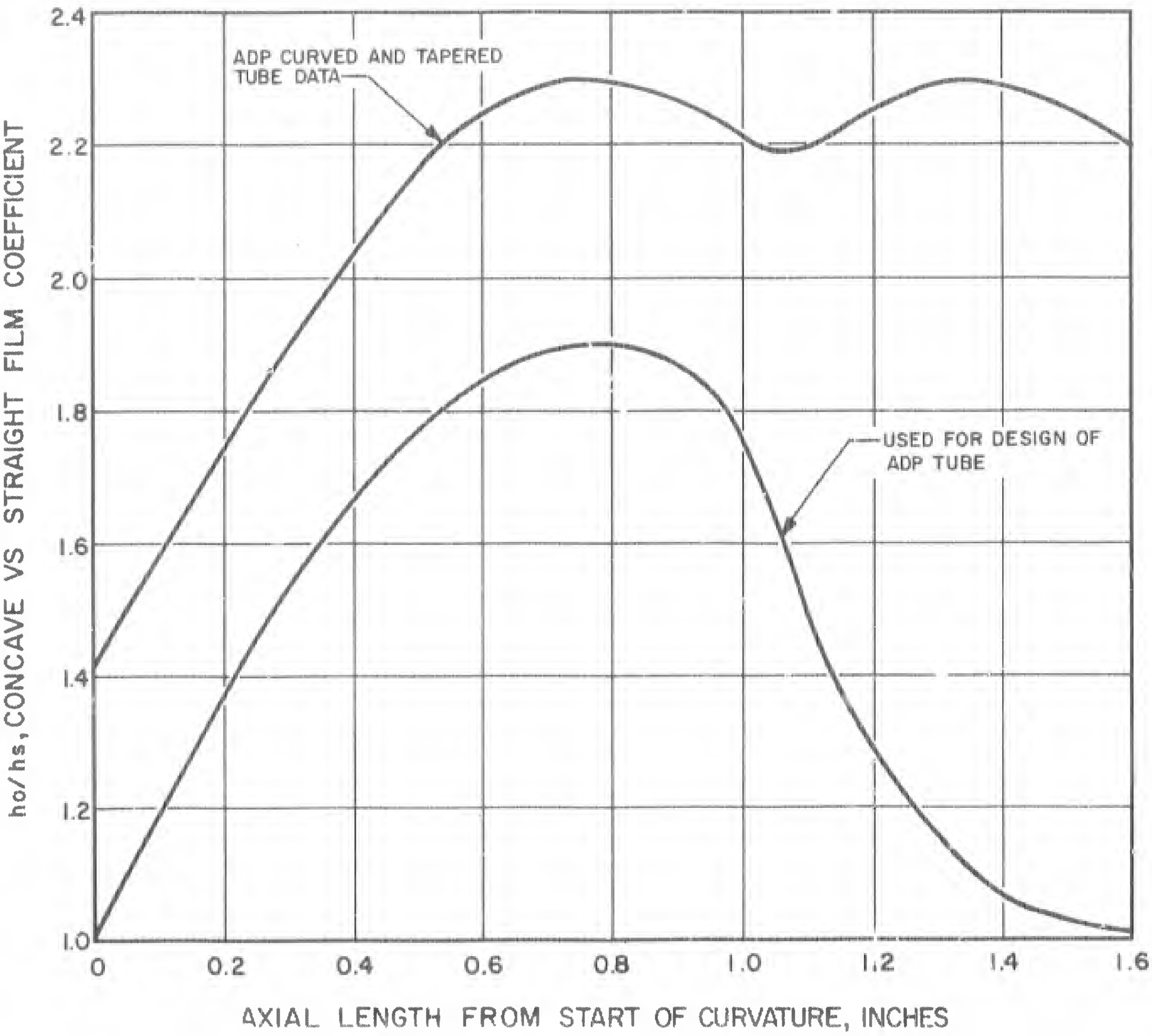

Figure 42. Comparison of Film Coefficient Enhancement Factor used for ADP Design with ADP Tube Experimental Results

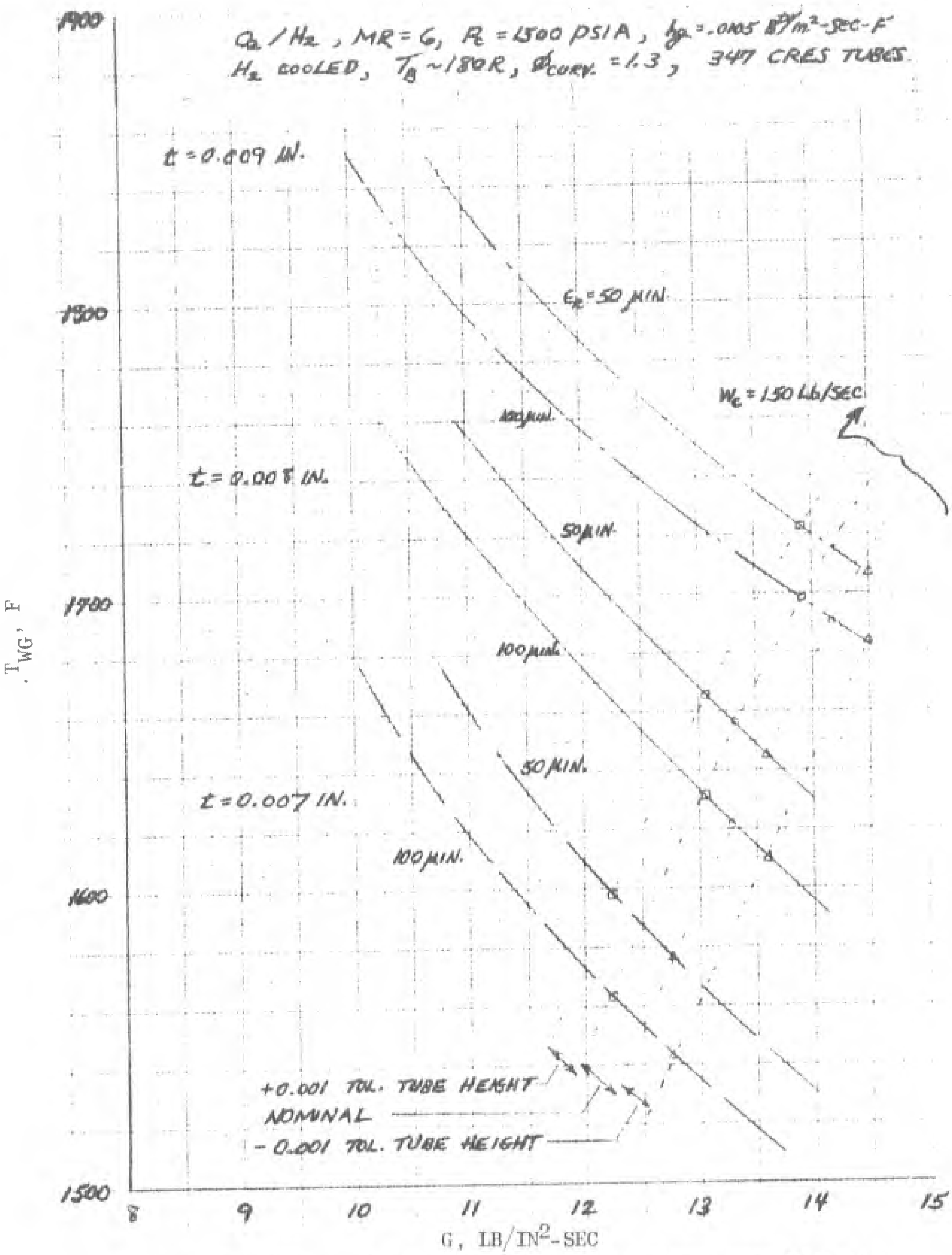

Figure 43. Effect of Tube Tolerances and Coolant Mass Velocity on Gas Wall Temperature

cross-section area resulted in a change of only 2.5 percent in the pressure drop through the inner body tube.

(U) Air flowrates are also relatively insensitive to tube area and surface condition unless a sonic condition (Mach No. = 1.0) exists. With some flow, the air flow is directly proportional to the minimum cross-sectional area of the tube. It was thus decided to air flow the tubes with 45 psia at the tube inlet, the air to flow in the same direction as the hydrogen coolant. This results in a sonic condition at the downstream end of the minimum area section (throat) of the tube. Changes in air flowrates using 60 F inlet air temperature were predicted for both the inner and outer body tubes using the specified dimensional tolerances. The results of this analysis are shown in Table 5. The tubes after being air tested will be classified into groups according to the actual measured air flowrate (corrected to standard flow conditions).

TABLE 5

AIR FLOWRATE VARIATIONS

Tolerances	Uppass	Shroud Downpass, scfm
Minimum Tolerance Area, percent	-14	-8
Nominal, percent	0	0
Maximum Tolerance Area, percent	+11	+10

Injector

(C) The injector is a one-piece, stainless-steel, annular assembly having a mean diameter of 93.010 inches and a width of 2.000 inches. The injector hole pattern (to be defined from segment tests) will be drilled in oxidizer and fuel strips. The injector will be uniformly divided into 40 compartments formed by baffles which simulate the internal support structure of a lightweight chamber.

(C) Connection of the annular injector to the inner and outer combustion chamber sections will be provided by bolts on the inner and outer combustion chamber sections. Shear surfaces at each periphery restrain thermal and pressure loads. The injector body is designed so that any bending will not adversely effect throat and seal dimensions. The structural design of the major areas in the injector body is 90 percent completed. The body cross section, the shear lips, the bolt and bearing plate, and local section moduli have been determined.

(C) Injector Body Design. Hydrogen is distributed to the injector from 20 risers to an externally mounted manifold. The flow is distributed uniformly to the fuel downcomers. Two-thirds of these passages feed the fuel annulus; the remaining passages cool the baffles and then discharge into the fuel annulus. Hydrogen is fed to the injector strips from the fuel annulus through slots designed to provide uniform flow along the length of each strip.

(C) Liquid oxygen is distributed to the injector feed passages from a tapered annular manifold welded to the top of the injector body. There are three injector feed passages per baffle compartment. The oxidizer strips are fed by slots in a manner similar to the fuel strips.

(C) A transient conduction heat transfer analysis was made of the injector body during a pretest chilldown and mainstage test. This information is necessary for the determination of injector thermal stresses. Isotherms, after a 5-second hydrogen chilldown period and after 10 seconds of mainstage operation, are illustrated in Fig. 44 and 45. It is of interest to note that the average injector body temperature changes only approximately 50 R (380 to 430 R) and the average chamber body remains essentially constant (510 R) at these two conditions.

Injector Average Body Temperature ~ 380 R
Chamber Average Body Temperature ~ 510 R

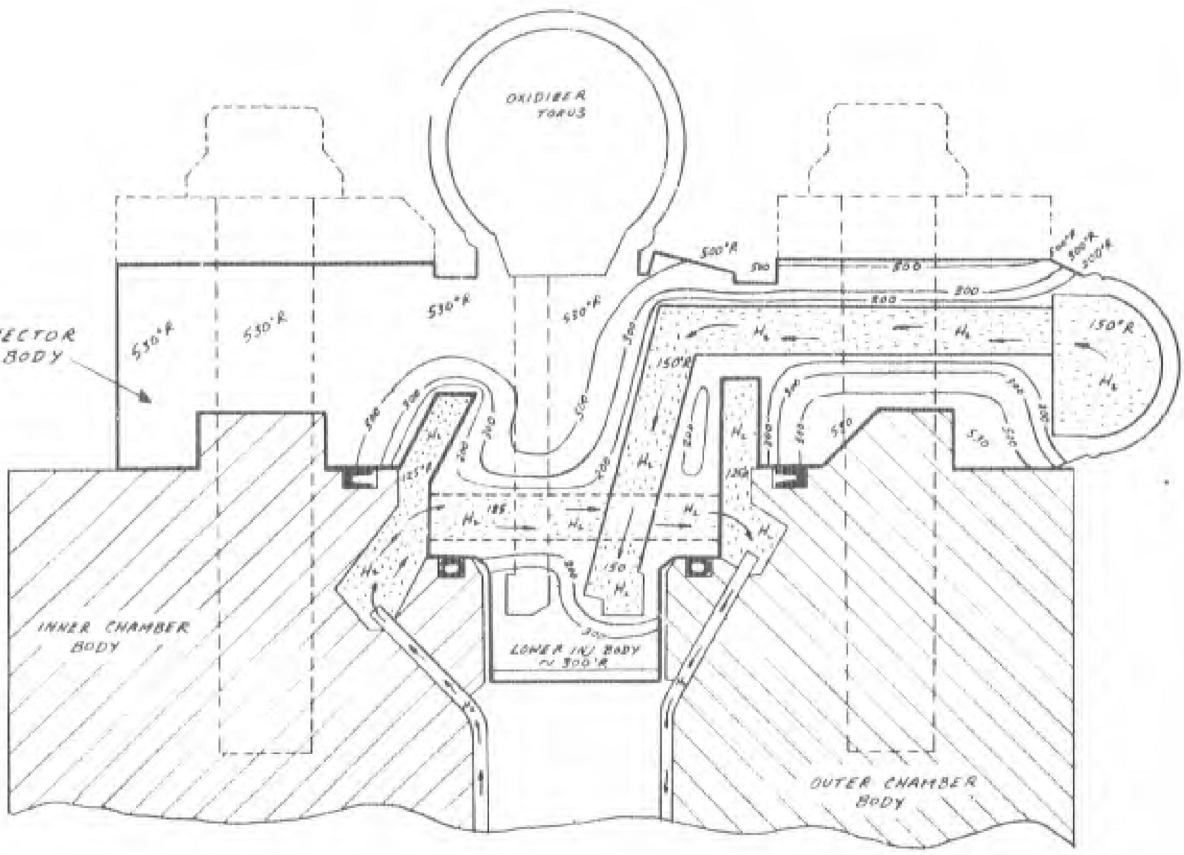

Figure 44. Approximate Injector Body Isotherm Distribution After a 5-Second Hydrogen Childown

Injector Average Body Temperature~430 R
Chamber Average Body Temperature~510 R

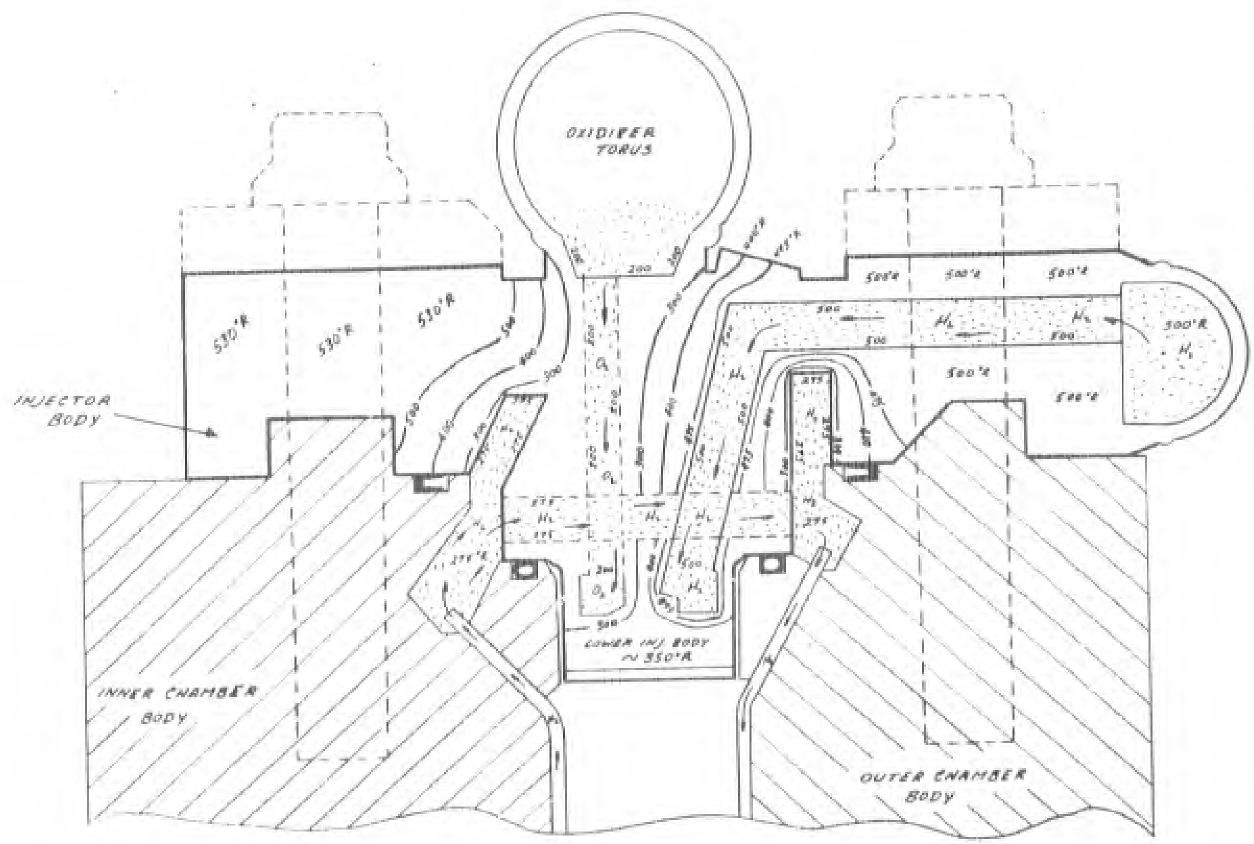

Figure 45. Approximate Injector Body Isotherm Distribution After a 10-Second Mainstage Test

(C) Oxidizer Manifold. The selected oxidizer manifold configuration consists of four equally tapered segments with four tangential (to top of manifold) inlets similar to that shown in Fig. 46. The inlets are fed from a diffuser plenum chamber assembly centrally located on the axis of the experimental chamber. The selections have a 20-percent carryover of the propellant from one sector to the next. This design provides for control of flow and pressure distribution.

(U) Design of the oxidizer manifold was finalized during the quarter and detailing is nearing completion. Drawings of the plenum chamber, diffuser, and feed line assembly are approximately 50 percent complete. Design layout of a flow test manifold support structure (for assembly and test stand) is approximately 90 percent complete.

(U) Fuel Manifold System. The fuel manifold system is being designed to provide balanced distribution to the thrust chamber tubes, baffles, and injector annulus for all operating conditions of the aerospike engine. The fuel inlet manifold configuration has been selected, and design and stress analysis of this configuration is proceeding. Configurations for the fuel system between the shroud coolant tubes and injector body and potential baffle coolant circuits have been investigated. Effort is continuing to define these systems.

(C) A study consideration of the fuel inlet manifold was conducted to include constant area vs a tapered manifold, the type of inlet, and the manifold-to-tube inlet configuration. A manifold tapered such that the static pressure is constant throughout the manifold provides uniform distribution. However, equally good distribution may be obtained with a low velocity head constant area manifold. A constant area manifold was recommended and this manifold will have a maximum variation in flow of less than 1.0 percent at the 1500-psia flow conditions. Two tee inlets are used to feed the manifold. The manifold-to-tube configuration was selected to eliminate tube-to-tube flow variations. Detailed design and stress analysis of this manifold will be completed during the next report period.

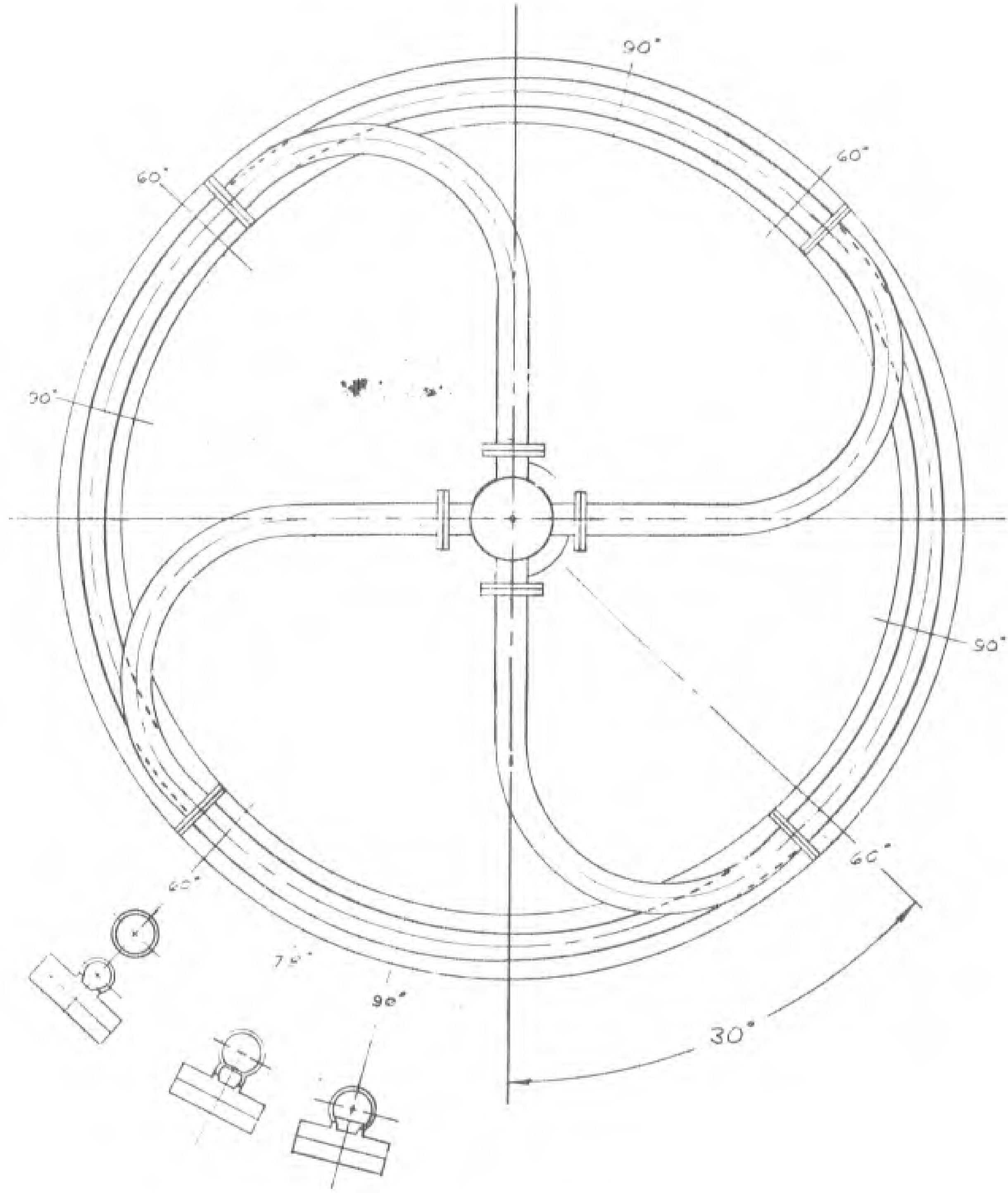

Figure 46. Oxidizer Manifold Cold Flow